

AD

Award Number: DAMD17-02-1-0211

TITLE: Characterization of Plasmodium falciparum Choline Transporters

PRINCIPAL INVESTIGATOR: Choukri Ben Mamoun, Ph.D.

CONTRACTING ORGANIZATION: University of Connecticut Health Center
Farmington, Connecticut 06030-2806

REPORT DATE: April 2005

TYPE OF REPORT: Final

20060307 078

PREPARED FOR: U.S. Army Medical Research and Materiel Command
Fort Detrick, Maryland 21702-5012

DISTRIBUTION STATEMENT: Approved for Public Release;
Distribution Unlimited

The views, opinions and/or findings contained in this report are those of the author(s) and should not be construed as an official Department of the Army position, policy or decision unless so designated by other documentation.

REPORT DOCUMENTATION PAGE

*Form Approved
OMB No. 074-0188*

Public reporting burden for this collection of information is estimated to average 1 hour per response, including the time for reviewing instructions, searching existing data sources, gathering and maintaining the data needed, and completing and reviewing this collection of information. Send comments regarding this burden estimate or any other aspect of this collection of information, including suggestions for reducing this burden to Washington Headquarters Services, Directorate for Information Operations and Reports, 1215 Jefferson Davis Highway, Suite 1204, Arlington, VA 22202-4302, and to the Office of Management and Budget, Paperwork Reduction Project (0704-0188), Washington, DC 20503

1. AGENCY USE ONLY (Leave blank)			2. REPORT DATE April 2005		3. REPORT TYPE AND DATES COVERED Final (1 Apr 02 - 31 Mar 05)	
4. TITLE AND SUBTITLE Characterization of Plasmodium falciparum Choline Transporters			5. FUNDING NUMBERS DAMD17-02-1-0211			
6. AUTHOR(S) Choukri Ben Mamoun, Ph.D.						
7. PERFORMING ORGANIZATION NAME(S) AND ADDRESS(ES) University of Connecticut Health Center Farmington, Connecticut 06030-2806 E-Mail: choukri@up.uchc.edu			8. PERFORMING ORGANIZATION REPORT NUMBER			
9. SPONSORING / MONITORING AGENCY NAME(S) AND ADDRESS(ES) U.S. Army Medical Research and Materiel Command Fort Detrick, Maryland 21702-5012			10. SPONSORING / MONITORING AGENCY REPORT NUMBER			
11. SUPPLEMENTARY NOTES						
12a. DISTRIBUTION / AVAILABILITY STATEMENT Approved for Public Release; Distribution Unlimited					12b. DISTRIBUTION CODE	
13. ABSTRACT (Maximum 200 Words) <i>Plasmodium falciparum</i> is the causative agent of severe human malaria. The rapid multiplication of the parasite within human red blood cells requires an active synthesis of new membranes. Choline analogs are potent antimalarial drugs. Although choline transport has been suggested to be the target of these compounds, their exact mode of action is unknown. We identified two genes <i>PfGAT</i> and <i>PfCTL1</i> as potential targets of these compounds. Here we report evidence that <i>PfGAT</i> encodes a Glycerol-3-phosphate acyltransferase enzyme responsible for the initial step of synthesis of <i>P. falciparum</i> membranes. Genetic data suggest that this pathway is essential for parasite survival and is a good target for development of new antimalarial drugs. We have also initiated a thorough genetic and biochemical characterization of <i>PfCTL</i> . Our data suggest that membrane proteins of the CTL family are not choline transporters. We generated transgenic parasites lacking <i>PfCTL1</i> , and showed that <i>PfCTL</i> is not essential for parasite intraerythrocytic development and survival. Finally we provide biochemical and genetic data suggesting that choline analogs act by specifically inhibiting phospholipid metabolism and the ability of the parasite to generate new membranes.						
14. SUBJECT TERMS Choline, phospholipid, analogs, chemotherapy, yeast					15. NUMBER OF PAGES 54	
					16. PRICE CODE	
17. SECURITY CLASSIFICATION OF REPORT Unclassified	18. SECURITY CLASSIFICATION OF THIS PAGE Unclassified	19. SECURITY CLASSIFICATION OF ABSTRACT Unclassified	20. LIMITATION OF ABSTRACT Unlimited			

NSN 7540-01-280-5500

Standard Form 298 (Rev. 2-89)
Prescribed by ANSI Std. Z39-18
298-102

Table of Contents

Cover.....	1
SF 298.....	2
Table of Contents.....	3
Introduction.....	4
Body.....	5
Key Research Accomplishments.....	20
Reportable Outcomes.....	21
Conclusions.....	22
References.....	23
Appendices.....	24

Physiological roles of *PfGAT* (*PfSCT1*) and *PfCTL1* in *Plasmodium falciparum*

INTRODUCTION:

Plasmodium falciparum is an important intraerythrocytic protozoan pathogen responsible for the most severe form of human malaria. The rapid spread of drug-resistant parasites and lack of an effective malaria vaccine result in an urgent need for alternative approaches to prevent malaria infection and pathogenesis. By 48 hours after invasion of human red blood cells, a single *P. falciparum* grows to many times its original size, and then divides asexually to produce up to 36 new parasites. This high rate of growth and multiplication of the parasite correlates with an active synthesis of phospholipids to generate new membranes. Accordingly, quaternary ammonium choline analogs, which interfere specifically with parasite membrane biogenesis inhibit the growth of the parasite *in vitro*, are non-toxic to human cell lines, impair the infectivity of developing gametocytes, reduce sporogony, and clear malaria infection in mice and monkeys (Wengelnik *et al.*, Science 2002, 295:1311-4) (1). Although, the lead compound, G25 [1,16-hexamethylenebis(N-methylpyrrolidinium] and its prodrug derivatives are now undergoing preclinical trials and show excellent clinical signs with little or no toxicity, their mode of internalization, intracellular target(s) and specificity remain unknown. Although choline transport has been proposed to be the main target of these compounds, the identity of the malarial choline transporters is not known. Genetic studies in yeast revealed three genes, *HNM1*, *SCT1* and *tCTL1* whose function is linked to choline transport. Our studies revealed that *P. falciparum* lacks homologs of *Hnm1* or human high affinity choline transporters, but instead expresses two homologs of *SCT1* and *tCTL1* that we named *PfGAT* and *PfCTL1*. This report summarizes the efforts made during our funding period to characterized their physiological role in *P. falciparum* development and survival.

PfGAT

Our studies revealed that *PfGAT* encodes a glycerol-3-phosphate acyltransferase involved in the initial step of synthesis of glycerolipids in the endoplasmic reticulum but not involved in choline transport (Reprint I). Our genetic studies revealed that despite the presence of a second putative GPAT activity in the apicoplast of the parasite, PfGat activity is essential for parasite development and survival and is a good target for development of new antimalarial drugs. A yeast model system in which *PfGAT* expression is required for survival was developed in our laboratory. This yeast genetic system will allow future studies to directly screen for PfGat-specific inhibitors.

PfCTL1

Because of the presence of several introns in *PfCTL1* gene, we performed various RT-PCR reactions in an attempt to construct a full-length cDNA that could be used for biochemical analysis in yeast and *Xenopus laevis* oocytes.

In this final progress report we provide the following:

- (i) Genetic evidence for disruption of the *P. falciparum PfCTL1* gene: We have generated a gene disruption of the *PfCTL1* by single cross-over genetic strategy.
- (ii) Biochemical and genetic evidence using yeast as a model system indicating that CTL proteins are not choline transporters. This specific portion of our study has been published in the journal "Neurochemical Research" (**Reprint II**) (2).

Of great importance to our research tasks, our laboratory has identified a new pathway for phosphatidylcholine biosynthesis in *P. falciparum*, which links hemoglobin catabolism to phospholipid metabolism (**Appendix. I**) (3). The identification of this novel pathway suggests that the initial steps of the CDP-choline pathway (choline uptake and phosphorylation) are not critical for *P. falciparum* survival, whereas the later steps of the CDP-choline pathway catalyzed by phosphocholine cytidyltransferase and CDP-choline phosphotransferase enzymes might be essential. Therefore bisquaternary ammonium choline analogs must exert their antimalarial activity by inhibiting not only choline transport, but also additional enzymes important for the synthesis of the major phospholipids. Accordingly, our laboratory has shown that the choline analog G25 inhibits choline incorporation into phosphatidylcholine, decarboxylation of phosphatidylserine into phosphatidylethanolamine (**Reprint III**), as well as the three-step methylation of phosphoethanolamine into phosphocholine.

Collectively, our data supported by the USAMRMC provide a much better understanding of membrane biogenesis in *P. falciparum* and provide strong support for lipid-based therapies to fight this disease.

BODY

The establishment of an effective parasite-specific therapeutic regimen for the treatment of malaria, or for that matter any parasitic disease, depends upon fundamental metabolic differences between parasite and host. Building upon this philosophy, our laboratory has been focusing on the transport and metabolism of nucleosides and choline which reflect striking disparities between parasites and their human host. The driving force for our work was the idea that, because *P. falciparum* relies on its host to acquire nutrients to fuel its rapid

multiplication and to synthesize new membranes, the machinery involved in this transport and the enzymes involved in the metabolism of the transported substrates should be regarded as potential targets for a rational approach to design inhibitors and fight this devastating disease.

The primary goal of our research project is to characterize the role of the *PfSCT1* (now renamed *PfGAT*) and *PfCTL1* genes of the human malaria pathogen *Plasmodium falciparum* in membrane biogenesis.

These studies, are part of a large program in our laboratory to dissect the molecular determinants of phosphatidylcholine biosynthesis in *P. falciparum*, identify the genes involved in positive regulation of phosphatidylcholine biosynthesis and understand the mechanism of action of the antimalarial choline analogs. Therefore we decided to divide the present Progress Report into two sections that detail our progress in understanding the physiological functions of PfGat and PfCTL.

The first section focuses on our genetic and biochemical characterization of *PfGAT* and its homolog PfPlsB. The biochemical and genetic characterization of *PfGAT* in *P. falciparum* and yeast is described in detail in **Reprint I**. Other unpublished data, which will be described in this report, include genetic evidence that *PfGAT* is an essential gene, and the initial characterization of PfGat homolog, PfPlsB.

In the second section of this report, we describe our isolation of *P. falciparum* *Δpfctl* strain lacking *PfCTL1* and the initial characterization of its cellular defects. In our attempts to understand the physiological function of PfCtl we have used yeast as a model system. Our studies revealed that membrane proteins of the CTL family are not involved in choline transport. These findings are described in detail in **Reprint II**.

Our biochemical and genetic analyses in yeast have allowed us to determine the mode of inhibition of phospholipid metabolism by the antimalarial choline analog G25. These studies are described in detail in **Reprint III**.

SECTION ONE:

PfGAT encodes an endoplasmic reticulum membrane protein involved in the initial step of glycerolipid metabolism.

Our analysis of PfGat sequence and initial biochemical characterization indicated that this protein is not involved in choline transport, but instead plays a role in the initial step of glycerolipid metabolism by catalyzing the acylation of glycerol-3-phosphate to form 1-acyl-glycerol-3-phosphate (GPAT activity). The product of this reaction serves as a precursor for the synthesis of DAG and CDP-DAG, which are incorporated into the major malarial phospholipids (**Reprint I**).

PfGAT1 is an essential gene of *P. falciparum* and a valid target for anti-malarial chemotherapy. We have initiated a genetic approach to generate a gene disruption of the *PfGAT1* ORF by homologous recombination (**Appendix 2**). *P. falciparum* parasites harboring a targeting vector have been obtained after selection on pyrimethamine. These parasites were grown on increasing concentrations of pyrimethamine (0.1, 0.5 and 1 µM) followed by removal of the drug for 4 weeks to select for integration of the targeting vector into *PfGAT1* chromosomal locus. PCR and Southern analyses on genomic DNA isolated from these parasites indicated that no integration events could be detected into *PfGAT1* chromosomal locus (**Appendix 2**). However, Southern analysis revealed integration of the targeting vector into other chromosomal loci (probably *CAM* promoter or HrpII terminator chromosomal regions) (**Appendix 2**). These data suggest that *PfGAT1* is an essential gene.

Identification of a second GPAT enzyme, PfPLSB, of *P. falciparum* and the implication of this finding on the physiological function of PfGat

We have identified a second putative GPAT gene, *PfPLSB*, in the *P. falciparum* genome (**Appendix 3. A**). This gene contains a signal peptide (SP) and a transit peptide (TP) upstream of the mature polypeptide (M) (**Appendix 3. B**). This structure is characteristic of proteins targeted to the parasite apicoplast. To confirm the localization of PfPlsB to the apicoplast and determine the importance of the signal (SP) and targeting (TP) peptides in this localization, we have cloned the sequences corresponding to SP, TP, SP+TP, SP+TP+M and M under the control of the *CAM1* promoter and upstream of the open reading frame of green fluorescence protein (GFP) in the pHCl vector (**Appendix 3. C**). Initial transfection attempts failed and we are currently repeating these studies to select for positive transfecants. To examine whether *PfPLSB* encodes an active GPAT enzyme, we expressed full-length and mature forms of PfPlsB in *E. coli* as fusion proteins with various epitope tags and targeted the protein to both the cytoplasm and periplasm. Unfortunately, all attempts to obtain a soluble and active PfPlsB have failed. We have generated a codon-optimized version of PfPlsB and expressed it in a yeast mutant lacking GPAT activity. However the codon-optimized version of this gene could not complement the lethality of the yeast mutant lacking GPAT activity. It is possible that our failure to detect PfPlsB activity *in vitro* might be due to its high specificity for acyl-ACP, for all our studies were performed with acyl-CoA substrates.

Collectively, our analysis suggests that PfGat1 and possibly PfPlsB are the only GPAT activities of *P. falciparum*. Our genetic studies suggest an essential role for PfGat. Therefore PfPlsB cannot compensate for the lack of PfGat, suggesting that unlike in yeast and humans, the GPAT function in *P. falciparum* is not redundant.

Phosphatidic acid formed in the ER and the apicoplast might be structurally different (different fatty acid chain lengths) and could contribute to distinct phospholipid pools of the parasite. Such properties make these pathways attractive targets for chemotherapy, since GPAT inhibitors that interfere with either enzyme would kill the parasite.

PfGat activity is inhibited by choline and phosphocholine analogs

To identify possible inhibitors of PfGat activity that could be optimized for their enzyme and antimalarial activities, we tested three analogs of dihydroxyacetone phosphate that were provided to us by Dr. Burton Tropp (Queens College, NY). Compound A: $\text{Li}_2\text{O}_3\text{PCH}_2\text{CH}_2\text{CHOHCH}(\text{OCH}_2\text{CH}_3)_2$, Compound B: $\text{CH}_2\text{OHCHOHCH}_2\text{CH}_2\text{PO}_3\text{Li}_2$ and Compound C: $\text{NaHO}_3\text{PCH}_2\text{CH}_2\text{COCH}_2\text{OH}$. *In vitro* inhibition assay was performed in the presence of glycerol-3-phosphate, 50-fold excess of each compound and using C16:1-CoA as a fatty acyl-CoA donor (**Appendix 4. A**). Under these conditions none of the compounds was found to inhibit PfGat activity. Furthermore, we tested these compounds at concentrations of 100 nM and 1 μM against asynchronous and synchronous culture of *P. falciparum* using a hypoxanthine proliferation assay (**Appendix 4. B**). None of the compounds had any effect on *P. falciparum* growth. As a control, chloroquine was used at concentrations of 1 and 10 nM and found to inhibit *P. falciparum* proliferation by more than 90%. These findings support our *in vitro* studies, which indicated that PfGat does not acylate a dihydroxyacetone phosphate substrate. Interestingly, we found that 10-fold and 50-fold excesses of the bisquaternary ammonium choline analog G25 and the phosphocholine analog miltefosine resulted in complete inhibition of *PfGat* activity *in vitro* (**Appendix 4. A**). Both compounds possess antimalarial activity, suggesting that inhibition of PfGat activity *in vivo* might be one of their primary mode of action.

SECTION TWO:

Characterization of *PfCTL*

Sequence and predicted topology. *PfCTL* was identified on chromosome 14 after searching the TIGR *P. falciparum* genomic DNA database with tCtl1p and rCtlp protein sequences. To identify the full-length *PfCTL* cDNA, total RNA was isolated from an asynchronous culture of 3D7 and cDNA was synthesized using random primers. Fragments of the *PfCTL* cDNA were amplified using one forward primer (PfCTL KO-172nX) near the predicted ATG start site of the *PfCTL* gene and several reverse primers that correspond to sequences in predicted *PfCTL* exons (Fig. 19, A and B). Sequencing of the PCR fragment obtained when the primer pair

PfCTL KO-172nX/PfCTL primer 3204- was used revealed that the *PfCTL* gene contains at least 10 exons (Fig. 1A and Fig. 2A), encoding a polypeptide that contains 735 amino acids (Fig. 2B) and shares 19% amino acid identity and 15% similarity with tCtlp and 12% identity and 13% similarity with Pns1p (**Reprint II**). PCR analyses of the 3' and 5' ends of the cDNA showed that the 5'end extends until at least 164 bp, but not 300 bp, upstream of the ATG start site and that the 3' end extends until at least about 27 bp, but not 239 bp, downstream of the predicted termination site (data not shown). Although the nucleotide sequence of the cDNA ends needs further confirmation by sequencing, no additional introns can be detected in both 5' and 3' ends based on the size of PCR fragments when the ends were amplified (data not shown). The polypeptide encoded by the predicted full-length cDNA was analyzed for its hydrophobic character by using the TMHMM program. Like tCtl1p, PfCtlp has 10 predicted transmembrane domains, a large extracellular loop between the first and second transmembrane domains, and N- and C-terminal tails extending towards the intracellular space (Fig. 3A and Reprint II). The amino acid residues that are highly conserved among Ctlp proteins are also present in the PfCtlp sequence (Y498, P506, Y521, G524, A585 and Y586) (Fig. 2B and Fig. 3A) and have similar locations as in the other Ctlp proteins. The clones that we sequenced revealed polymorphisms from the published 3D7 sequence: the adenine nucleotide at position 599 is replaced by a thymine, and 6 additional nucleotides (AATAAT) are present in our clones. These changes in nucleotide sequence result in the replacement of a lysine residue at amino acid position 200 by an asparagine, and in the insertion of 2 additional asparagine residues (Fig. 1A and Fig. 2B).

Unexpectedly, we found that the *PfCTL* mRNA undergoes alternative splicing. When the same PCR product (obtained from primer pair PfCTL KO-172nX/PfCTL primer 3204-) was cloned and sequenced in a TA vector (Invitrogen), the cDNA sequence of that clone was missing the 8th exon, yielding a second smaller isoform product that has only 9 predicted transmembrane domains and whose C-terminus is predicted to extend towards the extracellular space (Fig. 3B).

A ATGAAATTACATCGAGATGGAAAGAACGTGAATATAACCACCTTATAGAAGAAGTGGATAATGGAAACAATATTATAAATAACAAAGGAATATTATAACATGATGAA
AACAAATAATATAAATAATGATAATATTAAATTCATGAACGTGTACCTCTAGAACACCTTTAACGTATATCTCTGGTAATCTGGATTATATAACACATAG
ATATGTATAACGTTGAAGAGGAAAAAAAAGGGAAAAAAAGATTAGCAACAGATAAATAATTTAACTACTTTGFACTTTATGATTCTTAAATT
ATTATAATTATTATTATGGAAATATACTCGTATTTATGTTAAATTACAAATGGGAAATATGTGAAAGCATTACATAAAATCCATA
TTTATACCTCCCTCTACTCTAAACCTGAAATATTAAAGTACKTATGCTAAATGCCAGAGTCTCTGTCATCATCTAAATTGTGCAAAG
ATATAGCAGATTAAATAAAGATAAAATAAGATAAAGAAATAATTTGTTGAATCTTATTCTTCTTAAATAAATAAATAAATAAATAAAT
ATAGTTATTGATAAAAGAGGAAATAGTGAACAAATATAGTATATAGTATTACAAAAAGGCCGAATAATAATTGTATGTTGAATATTCTTAAATC
TCCATATTATGATACTGTAAATATTATGAAATATGTAACCTAAAGATAAATTATAAGAGAAAAAGTGTCAAAATTATTTACAGACAGATAAATAA
CATTGITAATTTATCTTCTTACAACCTTAAATTCTTATTTATTTGTTTAACTACTATAGTATTATGTTCCITTATTTACTTTCTTATATA
TCATCAACTCCAACCTTCAATTATTTAATATCCTTGTCTTGTGATTTCTTACCCATTATTATCATAAAACATTATGATATATAATC
CTGTCAGACATCCCTTTCTTCAATTATTTCAATTATGTTATGTCATCATATTATTCAATCCTTCTTCTGTCATATTCTTATATA
TAAAAGTACCTACAAGTACACATCTCAGATAATAGGAATTACCTGAAATTCTATCTAAATAATGACAAATAATTACTCCCCATTATGTGTCAGTA
TATCATTTGCTGGTTTCTGTTGTTATATTTATATTGATAATGACAGCTGGAGGGGTGACGAAAAAAAGGGTAAGTTTTTTATGTAATATA
GCCAAATGAAATAAATGAGAAAATAAAGAAAAAGCTAGCTGTCAGAATTTTTAACTTTTTTTAATTAAATTAAATTAAATAACAAATT
TGGCTAGTTATTGATAATATAACCGAATAATCTATAAAATAAATAATATATATTCTTCTTGTGTCGTTICATTGTTAGTGCAGATGGAATT
GATTCGAATGGTTTATGAAATAATGCCCTTCAAAATTCTTATCTAAAGCTCTICATTCTTCTATGTAACATAAAATAAATAAATCAA
AATAAAGAAACAAAATAATTGATCACTTATATATATATTTAATAACATTTCAGATTGGGTGATTCTTATTCTTATTGTAATATT
ACAAAGCTTAAATCAGTTACTATAAAATTGGTAAATACACAATTCTGTTTATATAAATAATTCTTATATAAGAAATGTATATAACGAACATATA
ATATATATGTATATATTATGTTATCTTAAATTGAAAGGCTACTGTTGTTATCTTCTTCTATGTAACATCTGAAATTCTTCAAAACAAAATAAATGTCGGA
AGGTTATGAGTAATTAACTATATAAAATGACGAATTGAAAGATAAAATAAATTATTGTAATAAGAAAAAGAAATCTCTATATAATATTG
TAACCTTTTTTTTTAGAAACAATAAAATTATCATTTGGAAAGTGTGTTTATCAAGTTTATTAAATTGTTGTTTAAGCTTACAGT
TTATTTCTTGGACAATGCACTTATCTCTTCTTATAATCATATTATAAGATAAAAGATAAAATTGTAACAGAGAAAAATAAA
AAATGAAAGATAACAATGCACTATATAATATATATATATATGTCAGTGTGAAAGATAAAACTAATATTATATAATTCTTCTTCTTCTT
ACAGATATTCTTAAAGCTTATCTAAAGATAATGATCTTACATCAGCTGTCATATTGTGAAGTATGTTCTTGTAAATTAAATTAAATAA
AAAAAATAATATTAAAGGGAAATATAAAT
TTATTATTTATATAGATGTCATATCTCTATATAATTATGTTGTTGTCATGTGATACGTCCTGTAAAAACATAAAATTCAACATCTCTGCGGCTGCG
TTACATGGAGTAACAAAGAAATACCTTAAAGAAAGAAAAAGAAAAAGAAACATAACAAAGTATATGTCATATATAATATATATATATGTGAGCAT
ATTTCTTCTTGAGTAACCTATATATGAAATAATTCTGTTFACTACCTCTCATATTACCTTGTGTCATTAATGTAATATGATAAAA
TGGTTATTATGATATGTCATTGAAAGATAATTAAAGAACCAAGTCTTGATAAAATTAGAACATAATCATATTATAATATATATATATATAT
TTTTTTCTTCTTATATAGATTAAATAATTCTCAAAAGATAATGTTGATTCTCATTAATTCTGAAACCCCTTTCTGCTCCCTGTAACCTT
AGAAATTCAAATAAAATATATATATATATATTAAATAATATTATTTCTTCTTCTGAAAGATAATTGTCACATTATGCGGAATTCTCTG
CITATTATACCTCTTATCATCTCTGTCATTGTCATATTATGTTGTTGTTGTAATGTTATAAAACAAATGATTGATGAAAGATCTATGAGAAATATA
TTTACACCTCTTATGTTAAGAAATTCTTATGTTGAAATATGATGATATAACTGCAATTGTC

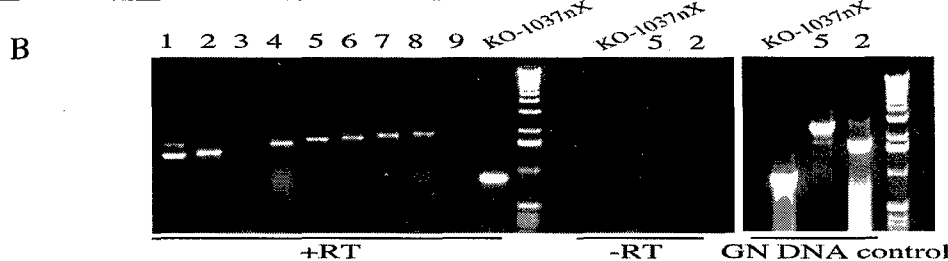
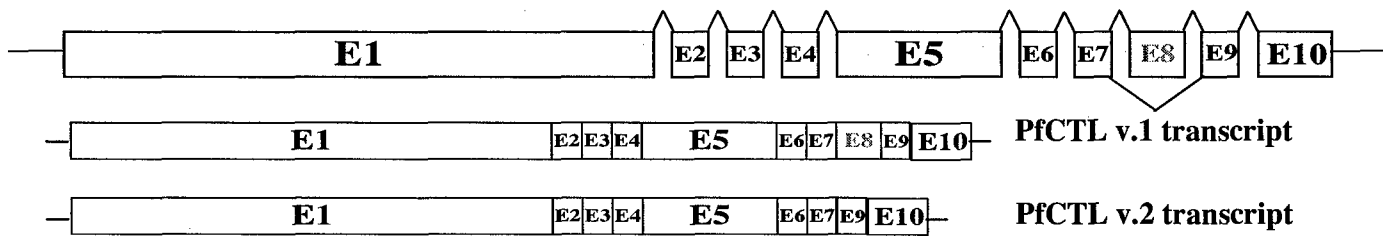


Fig. 1. *PfCTL* gene and cDNA. A, Nucleotide sequence of the *PfCTL* gene according to the published 3D7 sequence. Underlined sequences indicate exons. Unconfirmed predicted exon sequences are italicized. Arrows indicate oligonucleotides used for the identification of the full-length cDNA as described in “Experimental Procedures”. * indicates the region where nucleotide polymorphisms were detected between the cDNA of our laboratory strain and the sequenced 3D7 strain. Boxed sequence indicates alternatively spliced exon. B, Amplification of cDNA fragments using forward primer PfCTL KO-172nX and reverse primers 1-8 (shown in A) and primer 9 (~200bp downstream of the predicted stop codon) as described in Table II.

A

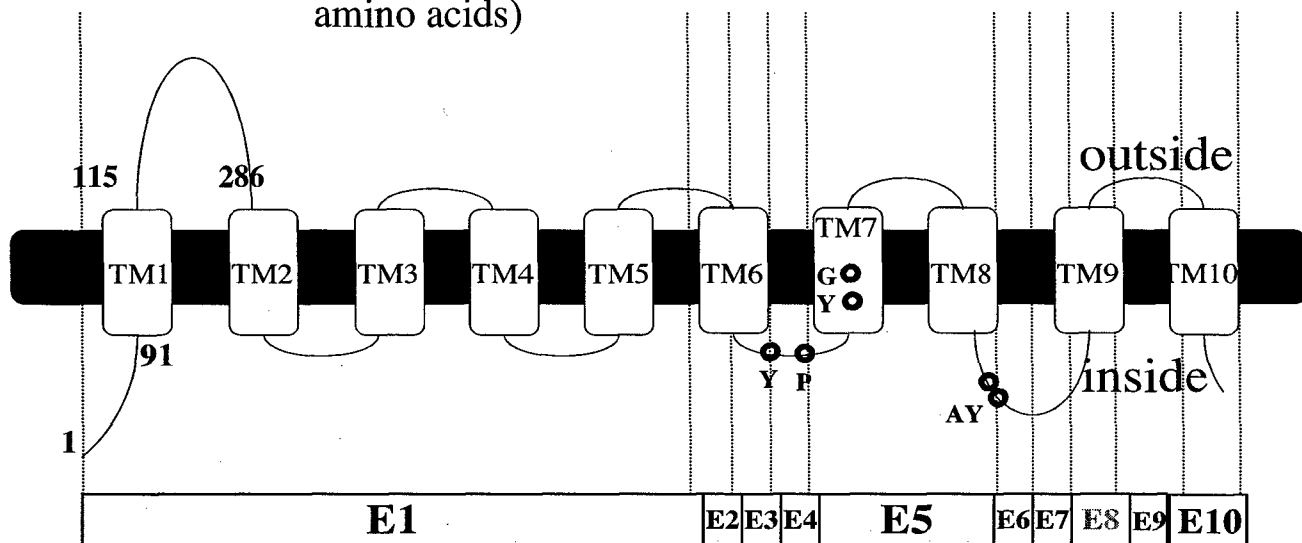


B

1/1	31/11	61/21	91/31
ATG AAT TAC ATC GAG ATG GAA GAA CGT GAA TAT AAA CCA CTT ATA GAA GAA GTG GAT AAT	GGA AAC AAT ATT ATA ATA AAT AAC AAG GAA TAT TAT AAC ATG TAT GAA AAC AAT AAT ATA		
M N Y I E M E E R E Y K P L I E E V D N G N N N I I I N N K E Y Y N M Y E N N N I			
121/41	151/51	181/61	211/71
AAT AAT GAT AAT ATT AAT ATT CAT GAA CGT GTA CCT CTA GGA ACA CCT TTA ACG TAT ATC	TCT GGT AAT CCT GGG GAT TAT ATA CAA CAC ATA GAT ATG TAT AAC GTT GAA GAG GAA AAA		
N N D N I N I H E R V P L G T P L T Y I S G N P G D Y I Q H I D M Y N V E E E K			
241/81	271/91	301/101	331/111
AAA CGG AAA AAA AGA TTA GCA ACA GAT ATA TAT TTT AAC TAC TTT GGT ACT TAT TTT	ATG ATT TCA TTA ATT ATT ATA TTT TAT TAT TTT TAT TAT GGT AAA TAT AGT CGT ATA TTA		
K G K K R L A T D I K Y F N Y F V T Y F M I S L I I I F Y Y F Y Y G K Y S R I L			
361/121	391/131	421/141	451/151
TAT GGT ATA AAT TAC AAT GGG AAA ATA TGT GGA AAG GAT CTA CAT AAA TAT CCA TAT TTA TAC TTC CCT CTT ACT CCT AAA AAT CCT AAA CCT GAA ATA TTA AGT ACC TAT GCT AAA TGC			
Y G I N Y N G K I C G K D L H K Y P Y L Y F P L T P K N P K P E I L S T Y A K C			
481/161	511/171	541/181	571/191
CTA GAG TCT TGT CCA TCA TCT AAT ATT GTT TCA AAA GAC ATA GCA GAT TTA AAT AAA GAT	AAA AAT AAA GAT AAG ATA GAT AAA TAT TTT GTG GAA TCT TAT TTT TTT TCT TAT AAA AAA		
L E S C P S S N I V S K D I A D L N K D K N K D K N K Y F V E S Y F F S Y K K N			
601/201	631/211	661/221	691/231
AAT AAT AAT AAT AAT AAT ATA GTT ATT GAT AAA AGA GGA AAT AGT GCA ACA AAT ATA GIA TAT AGT GAT TAT ACA AAA AGC CGG	AAT AAT AAT TTG TAT GTT GAA TAT TGT TTA		
N N N N N N I V I D K R G N S A T N I V Y S D Y T K S P N N N L Y V E Y S L			
721/241	751/251	781/261	811/271
ATT TCT CCA TAT TAT GAT ACT GTA AAT ATT ATG AAT ATA TGT TAC CCT AAA GAT AAA TTA TTA AGA GAA AAA GTT GCA AAA ATT ATA TTT	ACA GAC AGA TAT AAA ACA TTT GTT ATT TTA		
N S P Y Y D T V N I C Y P K D K L L R E K V A K I I F T D R Y K T F V N L			
841/281	871/291	901/301	931/311
TTT TCT CTT CAC AAC TCT TTT ATT TTT ATA TTT CCT TTT GTT TTT ACT ACT ATA GIA TTA TGT TTC CTT TAT TTA CCT TTC TTA TAT ATA	TCA TCA ACT CCA ACT TTT CAT TTA TTT TTA		
F S L H N S F I F I F L F V F T T I V L C F L Y L L F L Y I S S T P T F H L F L			
961/321	991/331	1021/341	1051/351
ATA TCC TTT GTT TCT TTG ATG TTT TTC TTA CCC ATT TAT TTT ATT CAT AAA CAT TTA TAT ATG ATA TAT AAT CCT GTC AAG ACA TCC	CAT CAA TAT TTT ATT TCC ATA TTT		
I S F V S L M F F L P I Y F I H K H L Y M I Y N P V K T S L F S H Q Y F I S I F			
1081/361	1111/371	1141/381	1171/391
ATA TGT ATC ATC ATA TTT ATT CAA TCC TTT TTT TTT CTG TCT ATT TTT ATA TAT AAA AGT ACC TAC AAG TAC ACA TCT CAG ATA ATA	GGA ATT ACC TTG AAT TTT ATC TAT AAA ATG		
I C I I I F I Q S F F F L S I F F I Y K S T Y K Y T S Q I I G I T L N F I Y K M			
1201/401	1231/411	1261/421	1291/431
ACA AAT ATA ATT TAC TCC CCC ATT ATT GTG TCA AGT ATA TCA TTT GTC TGG TTT TTC GTT TGG TTA TAT ATT TAT ATT ATG ATA ATG ACA	GCT GGA GGG GTG CAC GAA AAA AGG TTG CGA		
T N I I Y S P I I V S S I S F V W F V W L Y I Y I M I M T A G G V H E K R L R			
1321/441	1351/451	1381/461	1411/471
ATG GAA TTA GAT TCG AAT GGT TTT AGT GAA ATA ATG CCC CTT CAA AAA TTT TAT TAT TTC AAA AGC TCT TCA TTT TTT TCT ATA TTA	TGG GTG TAT TCC TAT TTT TTT ATT TGT GAA		
M E L D S N G F S E I M P L Q K F F Y Y F K S S S F F S I L W V Y S Y F F I C E			
1441/481	1471/491	1501/501	1531/511
ATA TTA CAA AGC TTA AAT CAG TTT ACT ATA ATT TAT TTG GGC ACT GIA TGG TAT TTT AGT GAT AAA TCG AAT TTT CCA AAA CAA AAT ATA	GTC TGG AGG GTT ATG AAA ACA ATA ATA AAT		
I L Q S L N Q F T I N Y L G T V W Y F S D K S N F P K Q N N V W K V M K T I I N			
1561/521	1591/531	1621/541	1651/551
TAT CAT TTG GGA AGT TTG GTT TTA TCA AGT TTT ATT ATT TTG TTG TTT AAG CCT TTA CGT GTT ATT TTC TTT TGG ACA AAT AGC ACT	TTA TCT CTT CCT TTT TAT ATT CAT ATT ATA		
Y H L G S L V L S S F I N L L F K P L R V I F F W T N S T L S L P F F Y N H I I			
1681/561	1711/571	1741/581	1771/591
CAT AAG ATA AGG CAT ATT TTT ATT TAT ATT TTA AAG CCT ATT TCT AAG ATA ATC GAT TCT TAT ACA TCA GCT GCA TAT TGT GAA ATG TCT	ATA TCT TCA TAT ATT TAT TTG TTT GCA TGT		
H K I K H N F Y I F L K P I S K I I D S Y T S A A O Y C E M S I S S Y N Y L F A C			
1801/601	1831/611	1861/621	1891/631
GAT ACG TCC TGT AAA AAA CTA ATA AAT TCA ACA TCC CCT GCG GCT GCG TTA CAT GGA	ATA ACC TAT ATA TTG AAT ATA ATA TTT CCA TGT TTT ACT ACC CTC ATT ATT ACC TTT TTG TCA		
D T S C K K L I N S T S P A A A L R G I T Y I L N I I F P C E T T L I I T F L S			
1921/641	1951/651	1981/661	2011/671
TTT AAT ATT TTT ATT AAT TTT CAA AGA TAT AAT GAT TTG TAT TCA TCT ATT TTT ATT CCT AAC CCC TTT TTT GCT TCC ATA ATT GGT	ACA TTA TGC GGA ATT ATT TCG TCT TAT TTT		
F N I F N N F Q R Y N D L Y S S N F I P N P F F A S L I I G T L C G I I S S Y F			
2041/681	2071/691	2101/701	2131/711
ATT ACC CTT ATA TCA TCT CTG TCT GAT TGC ATA TTA TAT TGT TTT GTT TGT GAA TGT TAT AAA AAC CAA ATG ATT GAT GAA GAT CCT ATG AGA	ATA CCT CCT ATG TTA AGA AAT ATA TTT ACA CCT CCT ATG TTA AGA		
I T L I S S L S D C I L Y C F V C E C Y K N Q M I D E D P M R N I F T P P M L R			
2161/721	2191/731		
AT TTT ATA TTG GAA ATA TAT GAT GAA TAT AAC TCG AAT TTG TGA			
N F I L E I Y D E Y N S N L *			

Fig. 2. Alternative splicing of PfCTL. A, Schematic of the gene structure and splicing patterns of PfCTL. The PfCTL v.1 mature transcript consists of all 10 exons (E1 to E10), whereas that of the alternative splice variant PfCTL v.2 consists of only 9 exons, as a result of the exclusion of Exon 8 that is part of an alternative intron represented here as (V). B, The deduced protein sequence of PfCTL v.1. The amino acid sequence of Exon 8 is boxed in red. The highly conserved Ctp amino acid residues described in Chapter II are encircled. The amino acids resulting from polymorphisms are boxed in black.

A PfCt1p v.1 protein (735 amino acids)



B PfCt1p v.2 protein (712 amino acids)

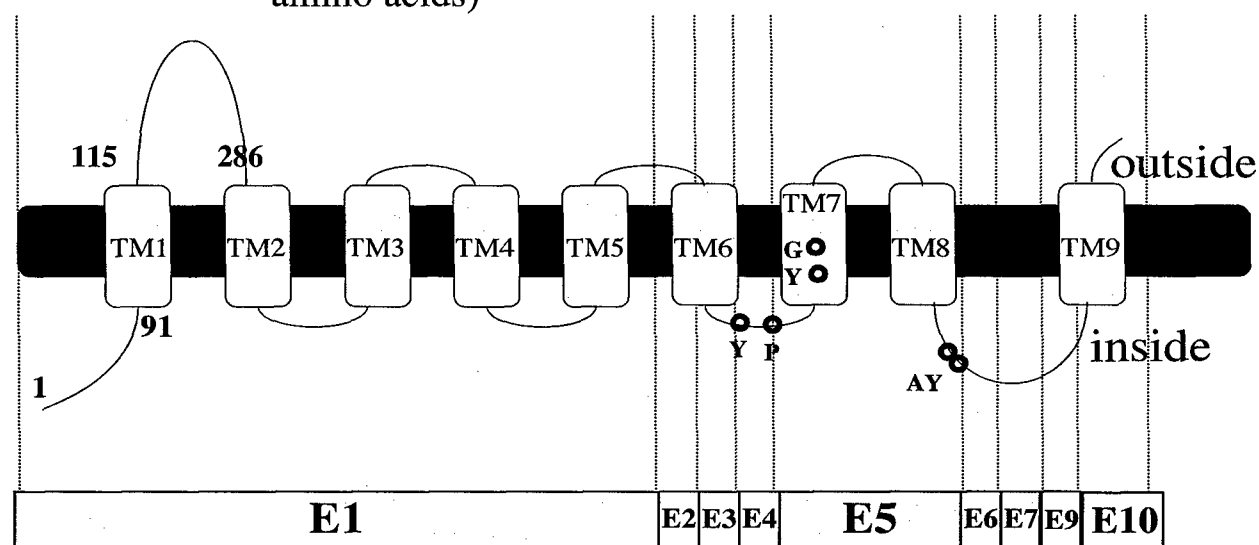


Fig. 3. PfCt1p predicted topology. Standard hydropathy algorithms were used to predict the topologies of PfCt1p v.1 (A) and PfCt1p v.2 (B) and include 10 and 9 transmembrane domains (TMs), respectively, a long N-terminal tail (residues 1-91) and a large extracellular loop between the TM1 and TM2 (residues 115-286). The highly conserved C-terminal residues and the relationship of the predicted topology with the corresponding exonic sequences are shown.

PfCTL is not essential for *P. falciparum* intraerythrocytic development. In order to determine the importance of *PfCTL* in parasite survival and development, we disrupted the *PfCTL* locus by interrupting the *PfCTL* open reading frame with a drug resistance cassette (Fig. 4) using pHc1 (5), a vector which encodes the pyrimethamine-resistant *T. gondii* dihydrofolate reductase-thymidylate synthase (*DHFR-TS*). In this vector, *DHFR-TS* is under the control of the *P. chabaudi* DHFR-TS *PcDT* promoter and *P. falciparum* *HrpII* terminator and enables selection of transfectants 3 to 4 weeks after transfection in 100 nM pyrimethamine, a potent inhibitor of the malarial DHFR-TS. To construct the targeting vector, a ~1 kb fragment of *PfCTL1* that lacks the coding sequences for the N-terminus and critical C-terminal domains into the unique *XhoI* site of pHc1 that is located upstream from the *P. falciparum* calmodulin *CAM* promoter. A single cross-over event in the region of homology would result in the insertion of DHFR-TS with the interruption of the *PfCTL* gene (Fig. 4). The targeting vector was then transfected into the 3D7 clone of *P. falciparum* and transfectants were detected 3 weeks post-transfection. Plasmid integration into the genome of *P. falciparum* was performed by culturing the parasites on increasing pyrimethamine concentrations (500 nM, 1 μM and 2 μM) until parasites were observed. These parasites were then grown on pyrimethamine-free medium for four weeks to induce loss of the episomes, followed by growth on 100 nM pyrimethamine. Once drug-resistant parasites were detected, the genomic DNA was isolated from the pool of parasites and screened for *PfCTL1* disruption by PCR. To confirm the occurrence of integration in the *PfCTL* locus, PCR was performed on the genomic DNA obtained from this pool of parasites. Using *PfCTL*-specific forward primer (*PfCTL med-5'*) that lies upstream of the region of homology and a reverse primer within the vector backbone (Camseq2), a PCR fragment was obtained that has the expected size if homologous recombination had occurred (PCR product 3 of Fig. 5). Sequencing of this fragment confirmed the integration event (data not shown). Using a set of *PfCTL*-specific primers that would anneal to sequences upstream (*PfCTL med-5'*) and downstream (*PfCTL primer 1775-*) of the region of homology, a PCR product was obtained corresponding to the wild-type *PfCTL* allele (PCR product 4 of Fig. 5). This suggests that at least some parasites in the pool have intact *PfCTL*, and that these parasites might be possibly relying on the presence of the episome for resistance to pyrimethamine. To promote the loss of the episome from the pyrimethamine-resistant parasites, and enrich the population of parasites in which homologous recombination had occurred, pyrimethamine was removed from the medium and the parasites were maintained in pyrimethamine-free RP complete medium for 4 weeks. After four weeks without drug, pyrimethamine was re-added to the medium that killed a large number of parasites in the population. After about a week of exposure to the drug, some pyrimethamine-resistant parasites had recovered to moderate parasitemia. To isolate individual

clones from this pool, the culture was diluted in 96-well plates to dilutions of 0.25 and 0.5 infected red blood cells (IRBC) per well. Two clones, that we named *PfctlΔ* clones 1 and 2, were obtained 4 weeks after dilution. To test the disruption of the *PfCTL* locus in these clones, PCR was performed on genomic DNA obtained from each clone. To our delight, both clones lacked the *PfCTL* wild-type copy (Fig. 5). As further tests, southern blot analyses were performed using pHC1- or *PfCTL*-specific probes. Accordingly, the 6.3-kb fragment that should result from digestion of the integrant DNA with *Bgl*II and *Bcl*II was detected in *PfctlΔ* clones 1 and 2 using a pHC1-specific probe (Fig. 6). Expectedly, no bands were detected in the wild-type control (Fig. 6). Using a *PfCTL*-specific probe, the 11.9-kb fragment that should result from digestion of the integrant DNA with *Cla*I was detected in *PfctlΔ* clones 1 and 2 but not in the wild-type control (Fig. 7). Unexpectedly, however, the 3.8-kb fragment that should result from digestion of the integrant DNA with *Cla*I and *Sap*I was not detected in *PfctlΔ* clones 1 and 2 (Fig. 7). Instead, a fragment of about 9 kb was detected, suggesting that the expected *Sap*I site in the plasmid backbone was absent, and that our strain contains a *Sap*I site in the *PfCTL* gene. The presence of this *Sap*I site is supported by the detection of a smaller (~3 kb) band in the wild-type control when it was digested with *Cla*I and *Sap*I (Fig. 7). This data suggests the existence of a polymorphism between the fully sequenced 3D7 clone and our lab strain. Nevertheless, it is clear that we have obtained two clones in which the *PfCTL* locus was disrupted. To confirm that the *PfCTL* transcript is not expressed in the *PfctlΔ* clones, total RNA was extracted from these clones and RT-PCR was performed using *PfCTL*-specific primers. Figure 8 shows that the *PfCTL* cDNA was detected in the wild-type strain, barely detected in the parasite pool and undetected in *PfctlΔ* clones 1 and 2, suggesting that the transcript is not expressed in the *PfctlΔ* clones. As a control, the cDNA of *PfGAT* was PCR-amplified in the wild-type strain, pool and in *PfctlΔ* clones 1 and 2 and a PCR product of the expected size was detected in all strains (Fig. 8). These data suggest that we have isolated a viable *PfCTL* knockout strain, indicating that *PfCTL* is not an essential gene.

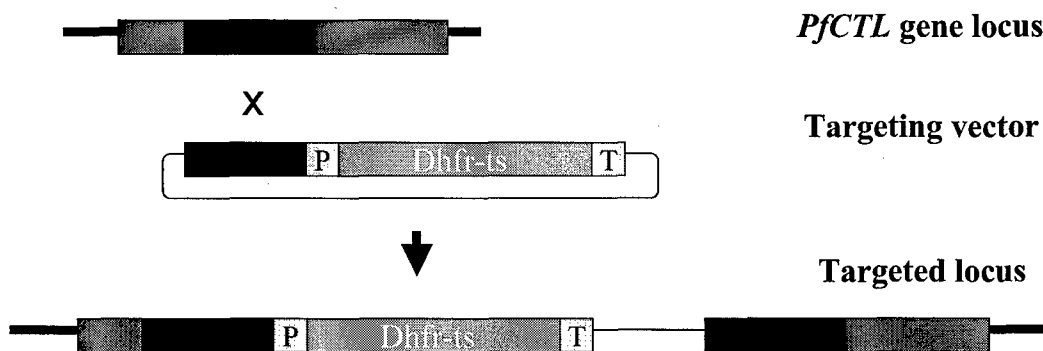
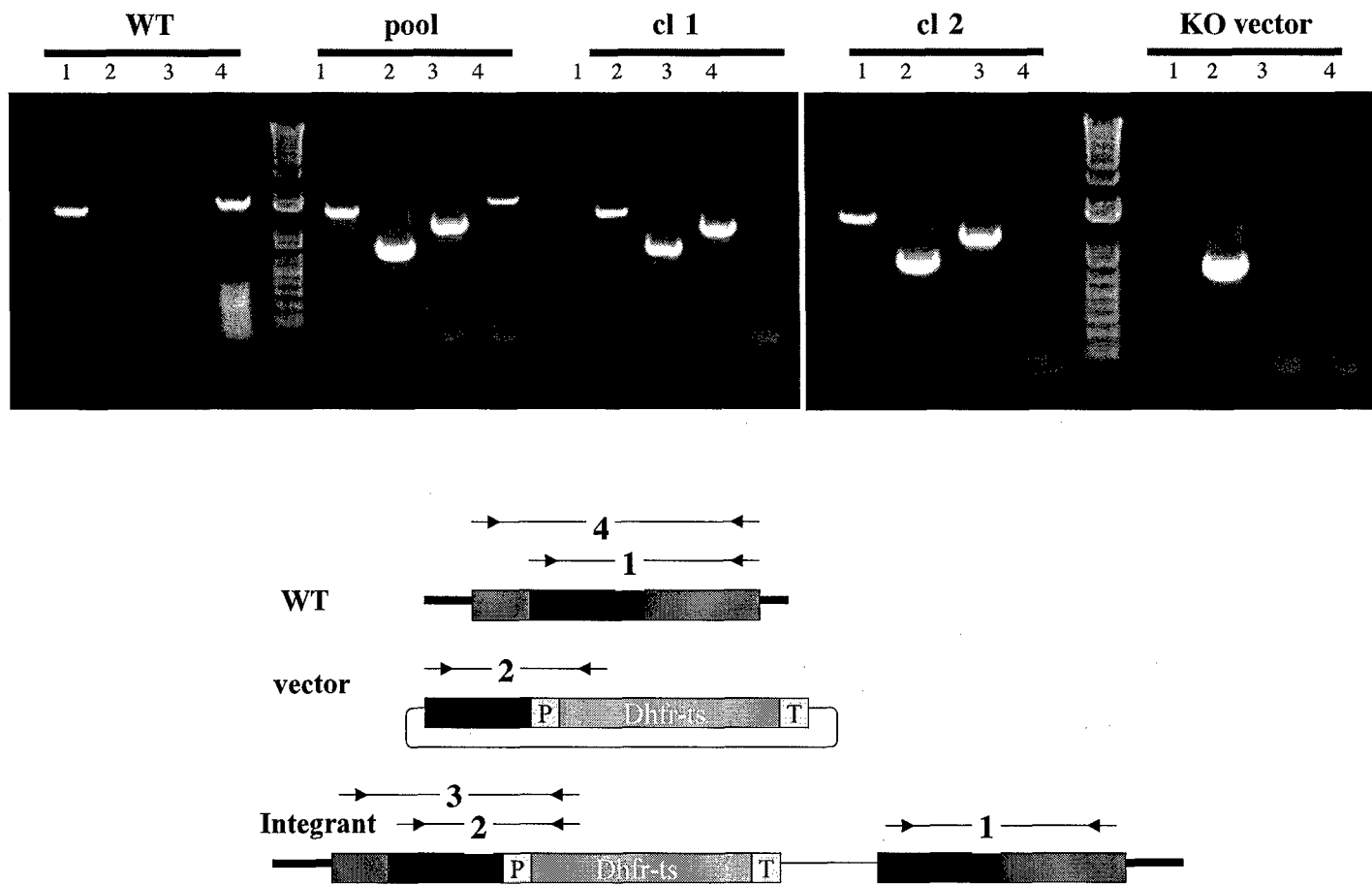


Fig. 4. Disruption of the *PfCTL* locus by homologous recombination mediated by a single cross-over event. The targeting vector, [*pHC1-PfCTL*], constructed as described in "Experimental Procedures", includes a the *T. gondii* dihydrofolate reductase-thymidylate (DHFR-TS) gene flanked by a 500-bp fragment of *PfCTL* gene (black rectangle). DHFR-TS, under the control of the *P. chabaudi* dihydrofolate reductase-thymidylate synthase promoter (P) and *P. falciparum* HrpII terminator (T), confers resistance to the drug pyrimethamine for positive selection of cells that have undergone the homologous recombination.



PCR	Forward Primer	Reverse Primer
1	PfCTL NtAb 127aaX	PfCTL primer 1775-
2	PfCTL NtAb 127aaX	Cam-seq1
3	PfCTLmed5'	Cam-seq1
4	PfCTLmed5'	PfCTL primer 1775-

Fig. 5. Testing the disruption of the *PfCTL* locus by PCR. Testing the disruption of *PfCTL* locus in the genomic DNA of the transformant pool (*pool*) and of the $\Delta Pfc\text{tl}$ clones (*cl 1* and *cl 2*) by PCR as described in "Experimental Procedures". The primers used and expected PCR products are shown. Genomic DNA from the wild-type strain (WT) and pHG1-PfCTL DNA (*KO vector*) were used as controls.

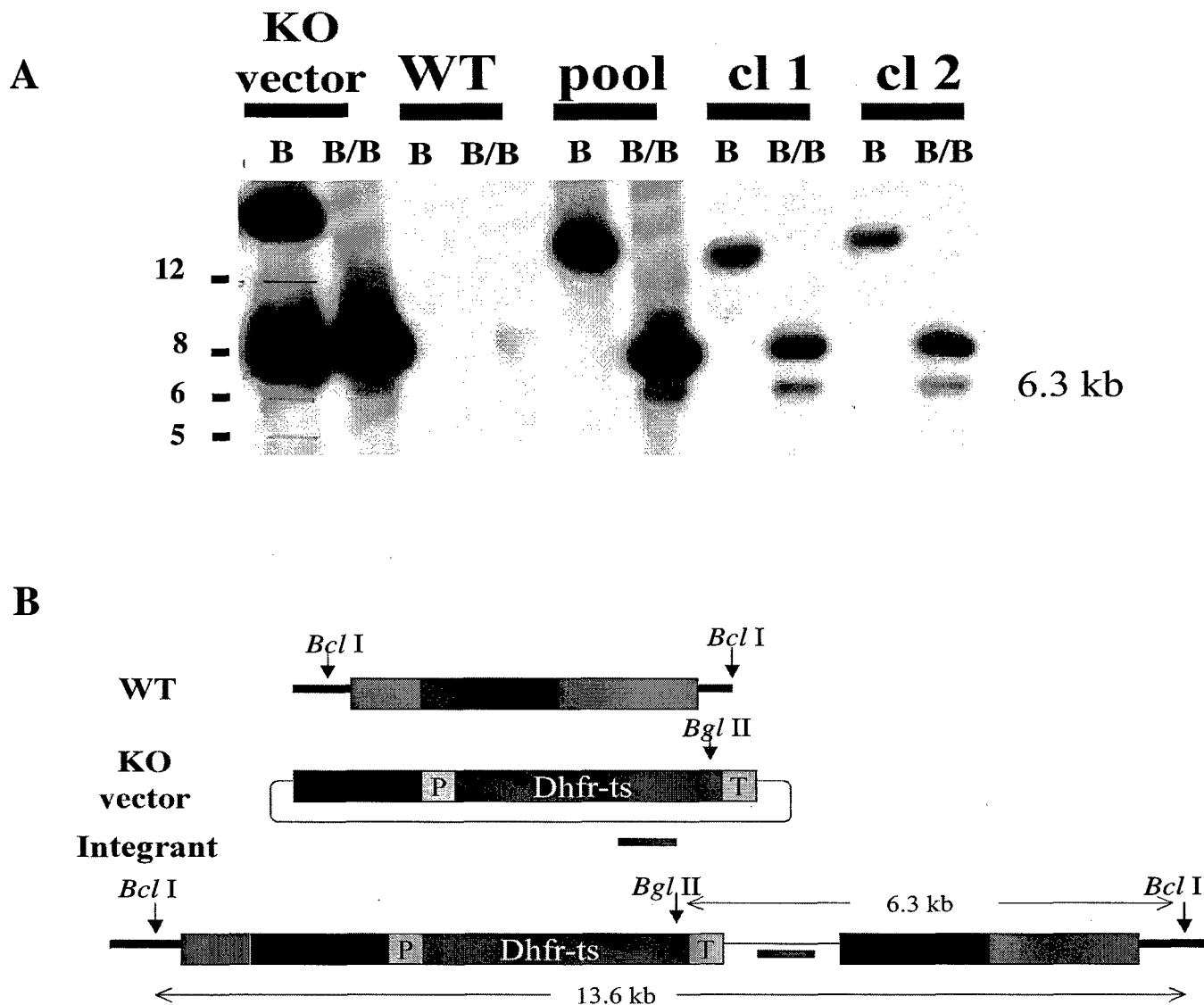


Fig. 6. Testing the disruption of the *PfCTL* locus by Southern blot analysis using a pHC1-specific probe. A, Genomic DNA isolated from the transformant pool (*pool*), and Δ *Pfctl* clones (*cl 1* and *cl 2*) were digested with *Bcl*II (*B*) or *Bcl*II/*Bgl*II (*B/B*). Ten micrograms of digested DNA/lane were loaded in a gel and analyzed by southern blot analysis using 32 P-labeled pGEM DNA (plasmid containing the backbone sequence of pHC1) as probe. DNA from the pHC1-PfCTL targeting vector (*KO vector*) and genomic DNA from the wild-type strain (*WT*) were used as controls. B, Map of *Bcl*II and *Bgl*III restriction sites in the *PfCTL* locus (*WT*), pHC1-PfCTL vector (*KO vector*) and the targeted locus (*Integrant*).

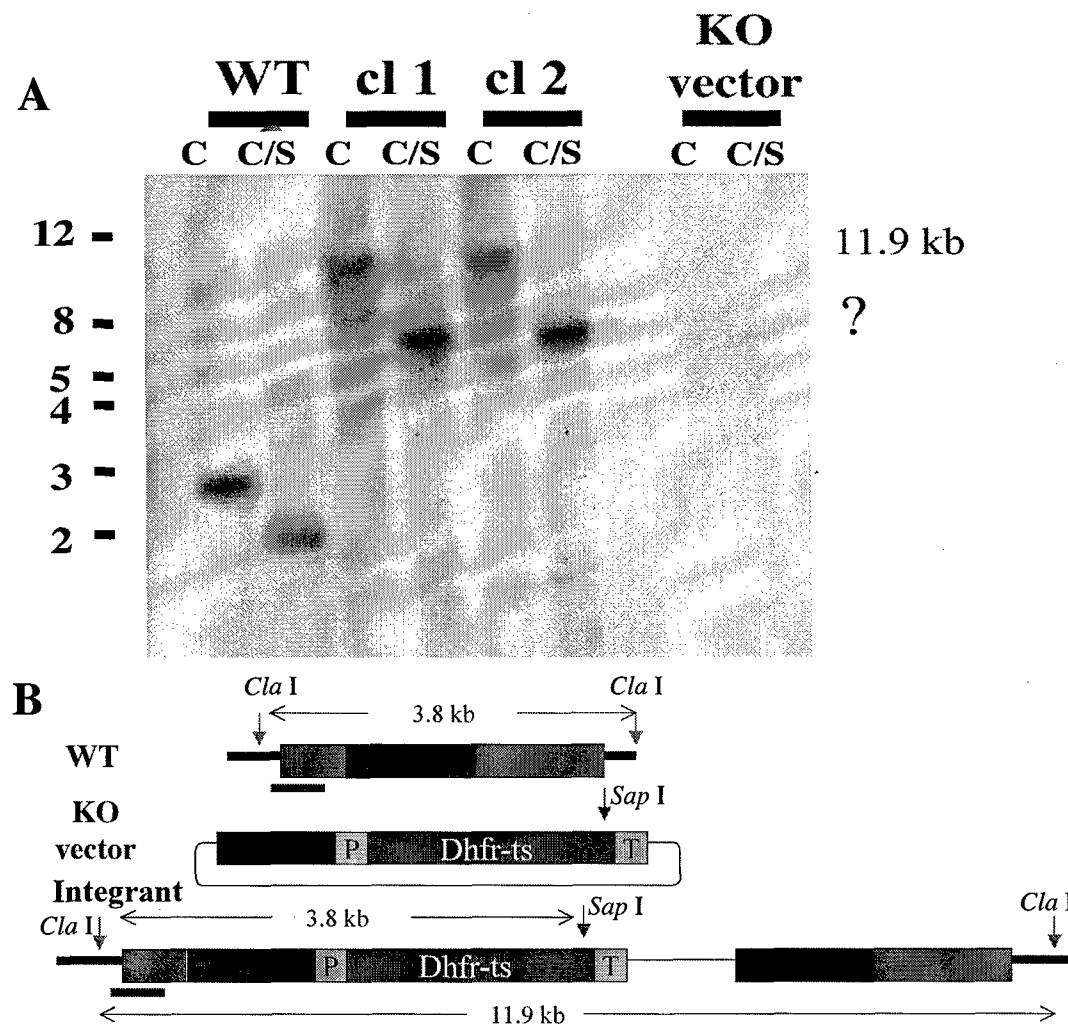
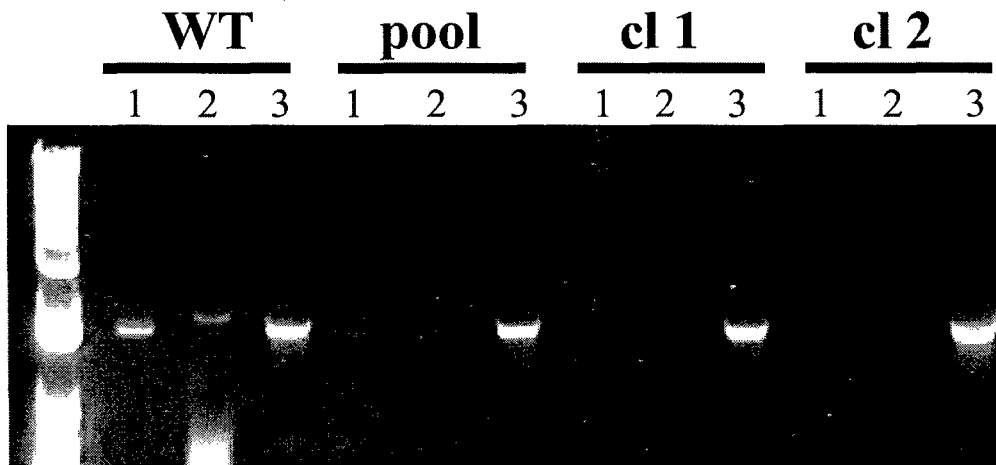


Fig. 7. Testing the disrupton of the *PfCTL* locus by Southern blot analysis using a *PfCTL*-specific probe. B, Genomic DNA isolated from the ΔPfc l clones (*cl 1* and *cl 2*) were digested with *Cla*I (C) or *Cla*I/*Sap*I (C/S). Ten micrograms of the digested DNA/lane were loaded in a gel and analyzed by southern blot analysis using a 32 P-labeled *PfCTL* fragment as probe, which was prepared as described under "Experimental Procedures". DNA from the pHG1-PfCTL targeting vector (KO vector) and genomic DNA from the wild-type strain (WT) were used as controls. (?) denotes the unexpected band obtained from the digestion of the genomic DNA of ΔPfc l clones with *Cla*I/*Sap*I. B, Map of *Cla*I/*Sap*I restriction sites in the *PfCTL* locus (WT), pHG1-PfCTL vector (KO vector) and the targeted locus (Integrand).



		Forward Primer	Reverse Primer
1	PfCTL cDNA	1.6 kb	PfCTLmed5' PfCTL primer 2415-
2	PfCTL cDNA	2 kb	PfCTLmed5' PfCTL primer 3204
3	PfGAT cDNA	1.75 kb	ScBPfCTR PfCTRhind3

Fig. 8. Testing the disruption of the *PfCTL* locus by RT-PCR. Testing the expression of the *PfCTL* transcript by RT-PCR as described in "Experimental Procedures". The expression of the *PfCTL* transcript was tested using total RNA isolated from asynchronous cultures of the wild-type (WT), transformant pool (*pool*), and Δ *Pfctl* clones (*cl 1* and *cl 2*). The PCR primers used and expected PCR products are shown. The *PfGAT* gene was used as a control.

Hypoxanthine incorporation assay

We have initiated studies to analyze the possible morphological and physiological defects in *pfctl1Δ* and *pfctl2Δ* clones, lacking *PfCTL1* gene. As a first step in our analysis, we have compared the sensitivity of 3D7, *pfctl1Δ* and *pfctl2Δ* clones to the lipid inhibitor and phosphocholine analog, miltefosine using a hypoxanthine incorporation assay. *pfctl1Δ*, *pfctl2Δ* and 3D7 strains were synchronized and diluted to 0.5 % in hypoxanthine-free medium when they reached 10 % rings. 990 µl of diluted parasite culture (at 2% hematocrit) was incubated with 10 µl of miltefosine (Cayman Chemical, prepared in PBS) to a final concentration of 15-180 µM miltefosine in 24-well plates. The plates were incubated at 37 °C for 24 hr. Then, 200 µl of culture was added to 0.5 µCi of ³H hypoxanthine (25 µl, prepared in hypoxanthine-free) in 96-well plates and incubated at 37 °C for another 24 hr. Triplicates were prepared for each miltefosine concentration. The cells were harvested in 96-well microplates using a Packard Filtermate Harvester. Scintillation fluid was added into each well and the radioactivity was measured using a scintillation counter. No growth differences between *pfctl1Δ* and *pfctl2Δ*, and 3D7 could be detected. Our next step in drug sensitivity will be to compare the sensitivity of all those clones to the bisquaternary ammonium choline analogs. Other future studies will include examining the ability of the mutants to differentiate into gametocytes or to undergo normal sexual development in the mosquito.

Membrane proteins of the CTL family are not involved in choline transport.

PfCTL is a member of a large family of membrane proteins with a ten transmembrane helical model named CTL (Choline Transporter-Like) family. Our interest in PfCTL was motivated by a report by O'Regan and colleagues (O'Regan et al., *Proc Natl Acad Sci U S A.* 2000 97:1835-40) that indicated that members of this family are involved in choline transport. This observation was made using a genetic complementation assay in yeast. Our thorough genetic and biochemical characterization of CTL proteins indicated that they are not choline transporters. A detailed description of this work is in **Reprint II** (2).

KEY RESEARCH ACCOMPLISHMENTS:

1. We have determined the molecular routes of membrane biogenesis in *P. falciparum* and identified the genes that play an essential role in parasite development and survival.
2. We have demonstrated through extensive biochemical and genetic studies that neither PfGat nor PfCTL proteins are choline transporters.

3. We demonstrated that *PfGAT* encodes a membrane protein of the endoplasmic reticulum that catalyzes the first acylation step of glycerol-3-phosphate at the sn-1 position. PfGat is the first protozoan GPAT enzyme to be identified. It exists as a multimeric complex in the ER membrane and plays an essential role in parasite development and survival by controlling the synthesis of phosphatidylcholine, the major phospholipid of the parasite membranes.
4. We have created a yeast strain that relies on the malarial *PfGAT* gene for survival. This strain will be used in future pharmacological studies to identify new antimalarial drugs that target the initial steps of malarial glycerolipid metabolism.
5. We have obtained two clones of *P. falciparum*, *pfctlΔ1* and *PfctlΔ2*, which lack the *PfCTL1* gene, and confirmed the gene disruption by PCR and Southern blot analyses, and lack of *PfCTL* mRNA by RT-PCR. Loss of *PfCTL* does not affect the intraerythrocytic development of *P. falciparum*.

REPORTABLE OUTCOMES:

I. Our laboratory published the following research papers related to the studies described in this report:

1. Rachel ZUFFEREY and **Choukri BEN MAMOUN**. The Initial Step of Glycerolipid Metabolism in *Leishmania major* Promastigotes Involves a Single Glycerol-3-Phosphate Acyltransferase Enzyme Important for the Synthesis of Triacylglycerol but not Essential for Virulence. (2005) *Molecular Microbiology*. **56**, 800 - 810.
2. Henri J. VIAL and **Choukri BEN MAMOUN**. *Plasmodium* lipids: Metabolism and Function. In I. W. Sherman (ed.), *Malaria: Parasite Biology, Pathogenesis, and Protection*. American Society for Microbiology, Washington, D. C. (2005). *In Press*.
3. Rodolphe ROGGERO, Rachel ZUFFEREY, Mihaela MINCA, Eric RICHIER, Michele CALAS, Henri VIAL and **Choukri BEN MAMOUN**. Unraveling the Mode of Action of the Anti-Malarial Choline Analog G25 in *Plasmodium* and Yeast. *Antimicrob. Agents Chemother.* (2004) **48**, 2816 – 2824.
4. Teresa C. SANTIAGO, Rachel ZUFFEREY, Rajendra S. MEHRA, Rosalind, A. COLEMAN and **Choukri BEN MAMOUN**. The *Plasmodium falciparum* PfGatp is an Endoplasmic Reticulum

Membrane Protein Important for the Initial Step of Malarial Glycerolipid Synthesis. *J. Biol. Chem.* (2004) 279, 9222-9232.

II. Our findings have been presented at the following research conferences:

- Molecular and Biochemical Parasitology Meeting XV (2004)
- Molecular, Microbial and Structural Biology Retreat (2004).
- Gordon Research Conference (2003). Molecular Biology of Lipids
- Molecular and Biochemical Parasitology Meeting XIV (2003)
- Keystone Symposium (2002): Malaria's Challenge: From Infants to Genomics to Vaccines. Drugs Against Tropical Protozoan Parasites: Target Selection, Structural Biology, and Rational Medicinal Chemistry.
- Molecular and Biochemical Parasitology Meeting XIII (2002)

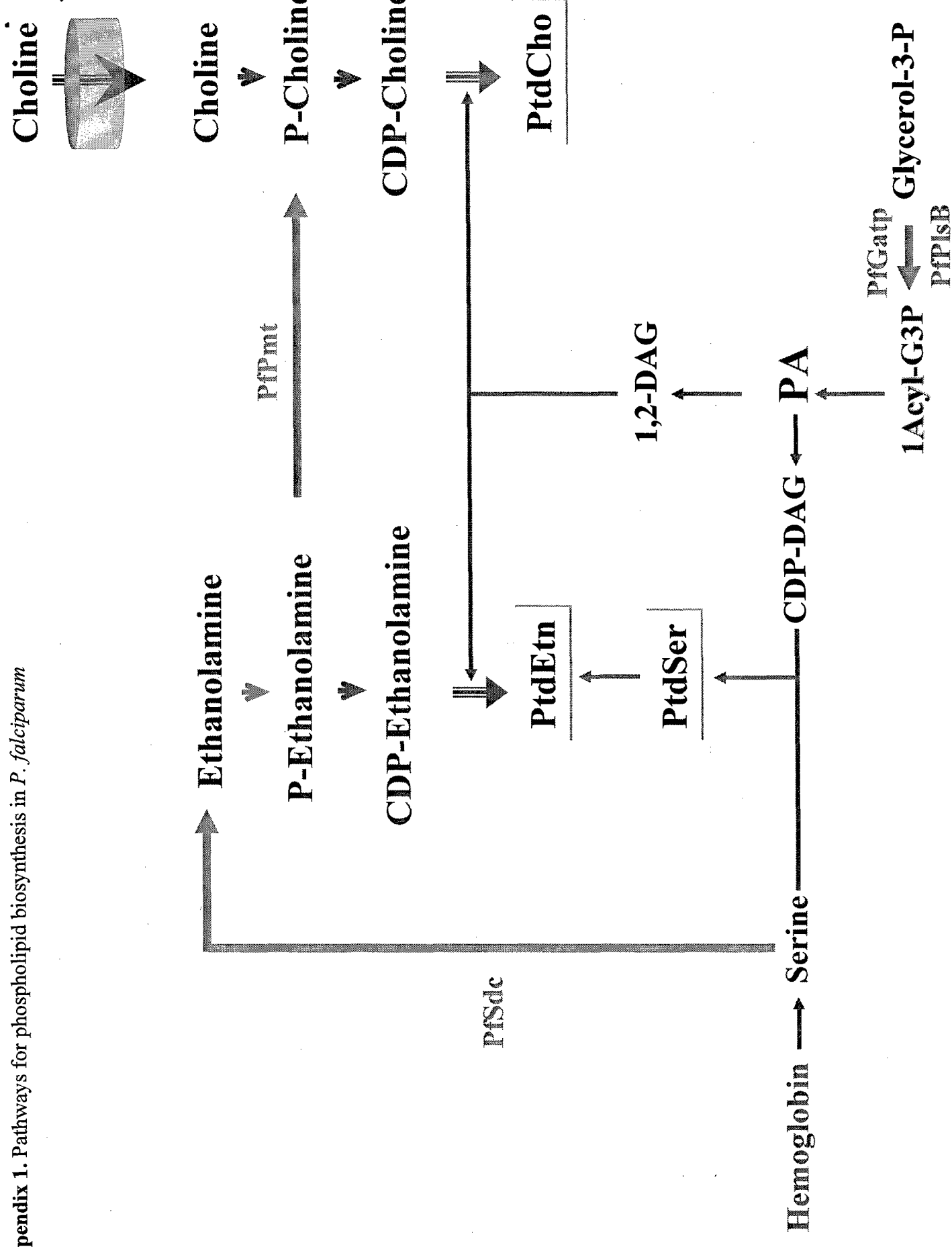
CONCLUSIONS:

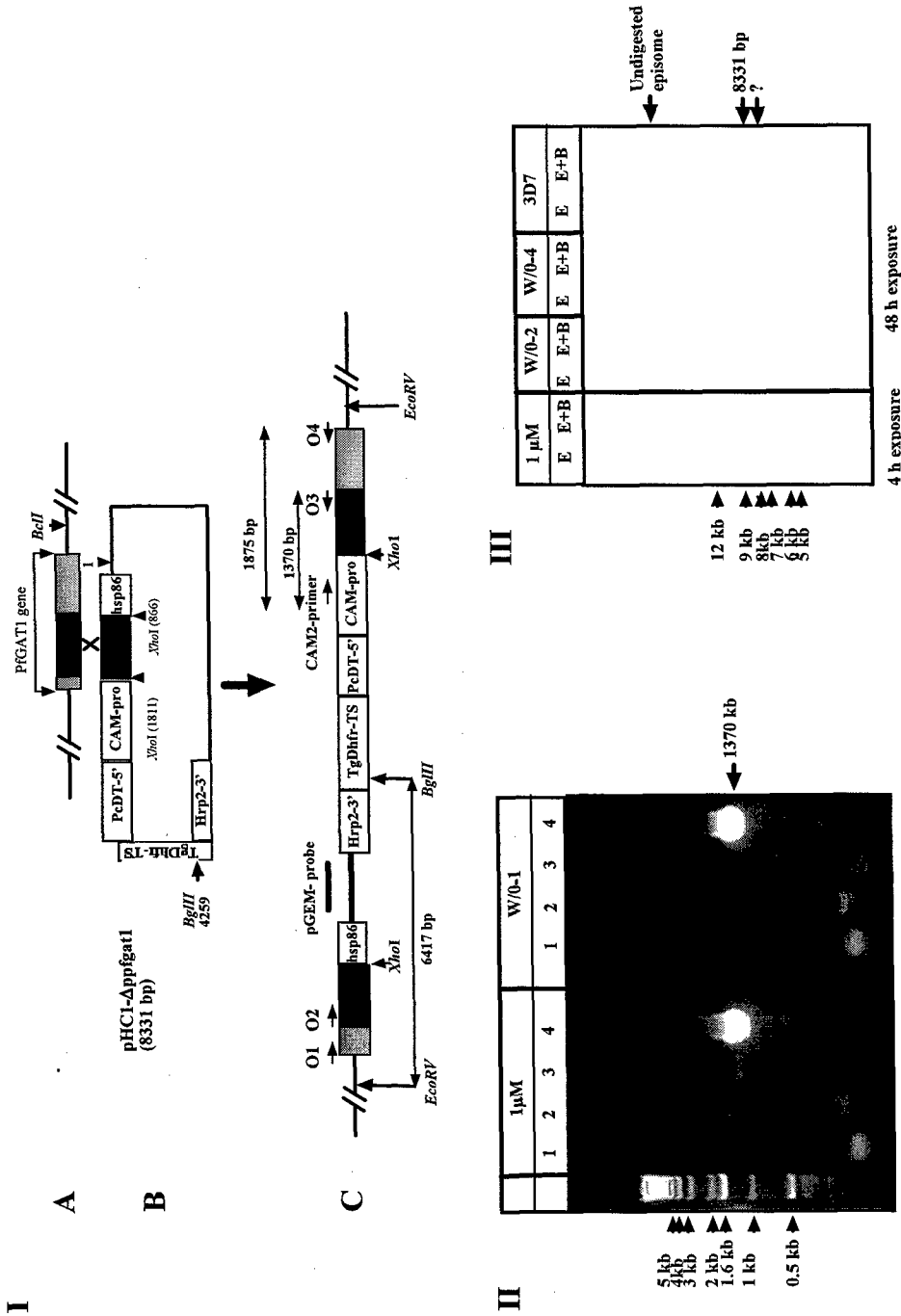
During this funding period we have made several key findings that allow us to determine the biological function and examine the importance of *PfSCT1* (*PfGAT*) and *PfCTL1* in phospholipid metabolism and parasite physiology. Our future studies will include testing various compounds for their ability to inhibit PfGat function, and determine the primary function of PfCtl in parasite physiology, in general, and phosphatidylcholine biosynthesis, in particular. Our thorough characterization of GAT and CTL proteins has allowed us to conclude that members of these two family of membrane proteins do not function as choline transporters. Bioinformatics analysis of *P. falciparum* genome revealed the presence of three genes encoding putative membrane proteins of the amino acid/auxin permease family. Our prediction is that one of these proteins is the primary choline transporter of the parasite. Our future studies will utilize the tools and strains developed during the funding period of this grant to determine the function of these proteins in choline uptake into the parasite.

References

1. Wengelnik, K., Vidal, V., Ancelin, M. L., Cathiard, A. M., Morgat, J. L., Kocken, C. H., Calas, M., Herrera, S., Thomas, A. W., and Vial, H. J. (2002) *Science* 295(5558), 1311-1314.
2. Zufferey, R., Santiago, T. C., Brachet, V., and Ben Mamoun, C. (2004) *Neurochem Res* 29
3. Pessi, G., Kociubinski, G., and Mamoun, C. B. (2004) *Proc Natl Acad Sci U S A* 101, 6206 - 6211
4. O'Regan, S., Traiffort, E., Ruat, M., Cha, N., Compaore, D., and Meunier, F. M. (2000) *Proc Natl Acad Sci U S A* 97(4), 1835-1840.
5. Crabb, B. S., Triglia, T., Waterkeyn, J. G., and Cowman, A. F. (1997) *Mol Biochem Parasitol* 90(1), 131-144.

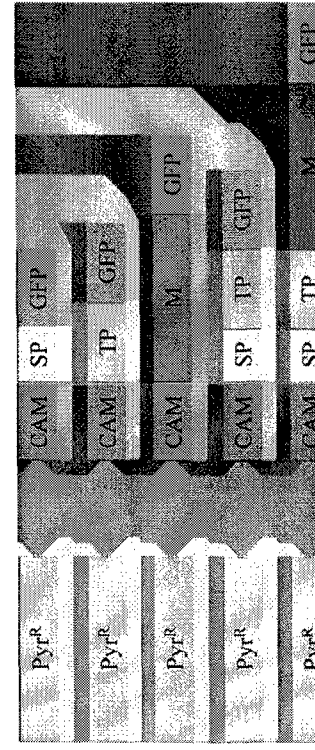
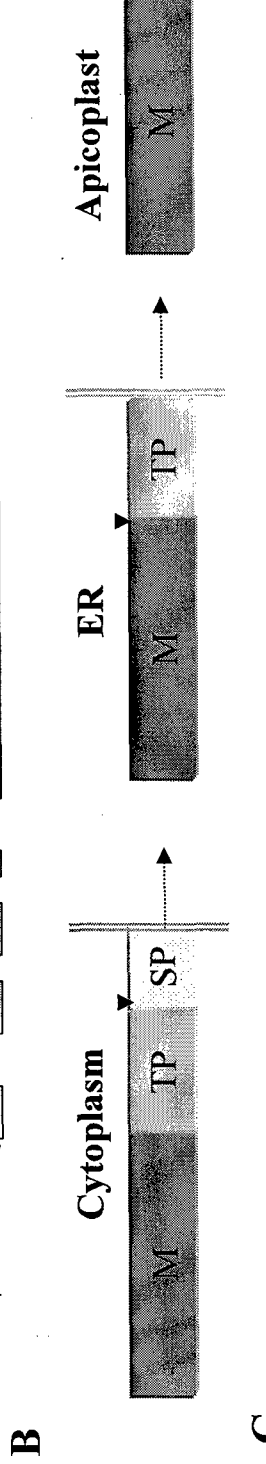
Appendix 1. Pathways for phospholipid biosynthesis in *P. falciparum*



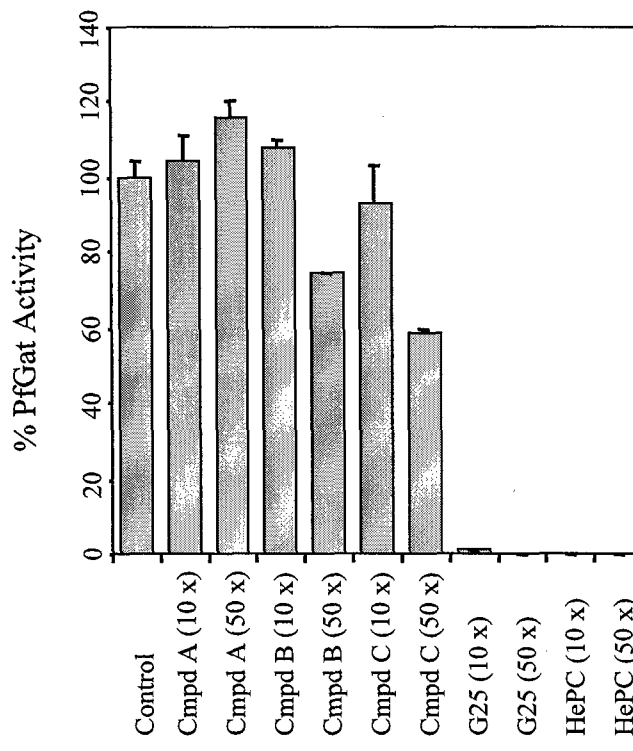
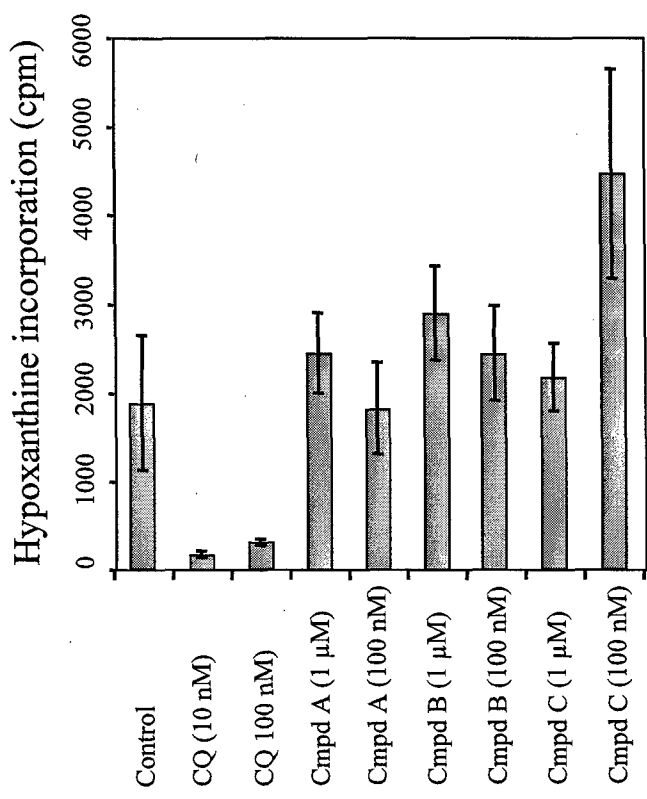


Appendix 2. (I) Schematic representation of the structure of the *PfGAT1* chromosomal locus (A), the plasmid vector pHCI-Δpfagt1 used for stable transformation of *P. falciparum* (B) and the proposed model of integration of the plasmid pHCI-Δpfagt1 by single crossing-over into the *PfGAT1* chromosomal locus (C). CAM-pro: promoter region of the calmodulin gene. TgDhf-TS: *Toxoplasma gondii* DHFR-TS gene mutated to confer pyrimethamine resistance to parasites. Hrp2-3': 3'-untranslated region of the histidine-rich protein II gene. PcDT-5': promoter region of the *P. chabaudi* DHFR-TS gene. 2C3-5' and CAM2 primers were used to confirm the integration of pHCI-1-Δpfagt1 into *PfGAT1* locus by PCR. 1: O1 + CAM2; 2: O2 + CAM2; 3: O2 + CAM2; 4: O3 + CAM2. 3D7 parasites harboring pHCI-Δpfagt1 plasmid, were grown on increasing concentrations of pyrimethamine (0.1, 0.5, 1 μM) followed by removal of the drug for 4 weeks. Genomic DNA was extracted from parasites growing on 1 μM pyrimethamine (1 week (W/O-1), 2 weeks (W/O-2) and 4 weeks (W/O-4)). (II) DNA from W/O-1 was used in PCR analysis using O1, O2, (1 μM) and every week after removal of the drug (1 week (W/O-1), 2 weeks (W/O-2) and 4 weeks (W/O-4)). (III) DNA from 3D7, 1 μM, W/O-2 and W/O-4 parasites was digested with EcoRV (E) and EcoRV+BglII (E+B) and probed with pGEM (see panel I/C). No episome could be detected after 4 weeks of removal of pyrimethamine (see EcoRV digestion in W/O-4). However, digestion with EcoRV+BglII revealed two new bands smaller than 8.2 kb (size of the linearized episome) and higher than 6.4 kb (the size of the predicted fragment EcoRV+BglII if integration into *PfGAT1* locus occurred). These two bands are likely to be integrations into CAM2 and/or Hrp2 chromosomal loci. Further analysis is being performed using different probes to assess the validity of this hypothesis.

A	PfPlsB.mv	L Y E T I K K H K S C S S Q D F L N - N F L I Y I D T F K K Y Q N - - Y E F P N I H - - R Y D Q T L
	OsPlsB.mv	K D A V M Q S R D N A H D I V S N N V A L F D C V I L D V E N P F T F P P Y H K A V R E P F D Y
	EGPlsB.mv	R N A V L Q S G D P R A N K I I L S N N A V A F D R I I L D V E D P F T F S P H H Q A I R E P F D Y
	CucosPlsB.mv	K N A V F E S G N P K A D E I V L S N M T V A L D R I I I D V E D P F M F S P H H K A I R E P F D Y
	CpPlsB.mv	I D A A T K K A A A D Q A E V L C - - - L Q W V K V I I E D L K N P F I F P P Y I K K L R A P I D L
	PfPlsB.mv	Y E W S L K F W S E I I D K K N S K F L G I S N I K K I E E W R D K G H N I I F S N H H I E A D A
	OsPlsB.mv	Y M F G Q N Y I R P I V D Y R N S Y V G N I S I F Q D M E Q K T Q Q C H N V Y L M S N H Q I E A D P
	EGPlsB.mv	Y M F G Q N Y I R P I I D F R R S Y I G N I S I F S D M E E K L Q Q G H N I V L M S N H Q T E A D P
	CucosPlsB.mv	Y T F G Q N Y V R F L I D F E N S F V G N I S L S L F K D I E E K L H Q G H N V V L I S N H Q T E A D P
	CpPlsB.mv	F R L S I D F F S L V I B D K N S R I L N L H R L K E I E E Y I A R G D N V V L L A N H Q T E C D P
	PfPlsB.mv	N I I K Y F F H I Q D S E Q S R N I I F T G G H K I R V D P I S R P F S V T A N I I C I Y S K K Y
	OsPlsB.mv	A I I A E L L E R S N P - W I S F N I V Y V A G D R V V T D P I L C K P F S M G R N I I C V Y S K K H
	EGPlsB.mv	A I I A E L L E R S N P - H I A E T M V F V A G D R V L T D P I L C K P F S M G R N I I C V Y S K K H
	CucosPlsB.mv	A I I S L L L E K T N P - Y I A E T N M I Y V A G D R V I A D P L C K K P F S I G R N L I I C V Y S K K H
	CpPlsB.mv	Q L M Y Y A L G K T H P - E L M E N M I F V A G D R V T S D P I A R P F S M G C D I L E C I Y S K R H



Appendix 3. (A) PfPlsB sequence alignment. Alignment of the putative catalytic domains of PfPlsB and its homologs from *Oryza sativa* (OsPlsB.mv), *Elaeis guineensis* (EGPlsB.mv), *Cucurbita Moschata* (CucsPlsB.mv) and *Chlamydomonas pneumoniae* (CpPlsB.mv). Identical (gray) residues and similar (light gray) residues are outlined. (B) Proposed mechanism of trafficking of PfPlsB to the parasite apicoplast. M: mature enzyme, TP: targeting peptide, SP: signal peptide. (C) PfPlsB-GFP constructs made to confirm the apicoplast localization of PfPlsB. PyrR: pyrimethamine-resistance cassette used to select for transgenic parasites. CAM: calmodulin promoter driving the expression of the fusion proteins.

A**B**

Appendix 4. (A) Inhibition of PfGat activity. PfGat activity was assayed in the presence of 10- or 50-fold excess of compound A: $\text{Li}_2\text{O}_3\text{PCH}_2\text{CH}_2\text{CHOHCH}(\text{OCH}_2\text{CH}_3)_2\text{PO}_3\text{Li}_2$, compound B: $\text{CH}_2\text{OHCHOHCH}_2\text{CH}_2\text{PO}_3\text{Li}$, compound C: $\text{NaHO}_3\text{PCH}_2\text{CH}_2\text{COCH}_2\text{OH}$, choline analog G25 and phosphocholine analog (miltefosine (HePC)). (B) Inhibition of *P. falciparum* proliferation. Hypoxanthine uptake into *P. falciparum* was measured in the absence and presence of 10 nM or 100 nM of chloroquine (CQ) or compounds A, B and C.

The *Plasmodium falciparum* PfGatp is an Endoplasmic Reticulum Membrane Protein Important for the Initial Step of Malarial Glycerolipid Synthesis*

Received for publication, September 23, 2003, and in revised form, December 9, 2003
Published, JBC Papers in Press, December 10, 2003, DOI 10.1074/jbc.M310502200

Teresa C. Santiago†\$¶, Rachel Zufferey‡||, Rajendra S. Mehra†\$, Rosalind A. Coleman***‡, and Choukri Ben Mamoun†\$ ¶\$

From the †Center for Microbial Pathogenesis, the §Department of Genetics and Developmental Biology, and the ||Department of Pathology, University of Connecticut Health Center, Farmington, Connecticut 06030-3710, and the **Department of Nutrition, University of North Carolina, Chapel Hill, North Carolina 27599

During its 48-h asexual life cycle within human erythrocytes, *Plasmodium falciparum* grows to many times its own size and divides to produce 16–32 new parasites. This rapid multiplication requires active synthesis of new membranes and is fueled by phospholipid precursors and fatty acids that are scavenged from the human host. *Plasmodium* membrane biogenesis relies heavily on the expression of parasite enzymes that incorporate these precursors into phospholipids. However, little is known about the genes involved in membrane biogenesis or where this process takes place within the parasite. Here, we describe the analysis in *P. falciparum* of the first step of phospholipid biosynthesis that controls acylation of glycerol 3-phosphate (GPAT) at the *sn*-1 position. We show that this activity is of parasite origin and is specific for glycerol 3-phosphate substrate. We have identified the gene, *PfGAT*, encoding this activity in *P. falciparum* and reconstituted its codon composition for optimal expression in the yeast *Saccharomyces cerevisiae*. *PfGAT* complements the lethality of a yeast double mutant *gat1Δgat2Δ*, lacking GPAT activity. Biochemical analysis revealed that PfGatp is a low affinity GPAT enzyme with a high specificity for C16:0 and C16:1 substrates. PfGatp is an integral membrane protein of the endoplasmic reticulum expressed throughout the intraerythrocytic life cycle of the parasite but induced mainly at the trophozoite stage. This study, which describes the first protozoan GPAT gene, reveals an important role for the endoplasmic reticulum in the initial step of *Plasmodium* membrane biogenesis.

Plasmodium species are obligate intraerythrocytic protozoan parasites that undergo a number of developmental stages in the vertebrate host. In humans, they annually cause clinical

* This work was supported in part by the University of Connecticut Health Center Fund (to C. B. M.), the Robert Leet and Clara Guthrie Patterson Trust (to C. B. M. and R. Z.), the United States Army Medical Research and Material Command (to C. B. M.), and General Clinical Research Center Grant M01RR06192 from the National Institutes of Health (to the University of Connecticut Health Center, Farmington). The costs of publication of this article were defrayed in part by the payment of page charges. This article must therefore be hereby marked “advertisement” in accordance with 18 U.S.C. Section 1734 solely to indicate this fact.

¶ These authors contributed equally to this work.

|| Supported by National Institutes of Health Grant DK56598.

\$ To whom correspondence should be addressed: Center for Microbial Pathogenesis, University of Connecticut Health Center, 263 Farmington Ave., MC3710, Farmington, CT 06030-3710. Tel.: 860-679-3544; Fax: 860-679-8130; E-mail: choukri@up.uhc.edu.

illness in 300–500 million people with 1.5–2.7 million deaths, mainly caused by *Plasmodium falciparum* (1). Drug resistance is widespread, and the need for more efficacious and less toxic agents that exploit pathways and targets unique to the parasite is acute.

In the 48 h after invasion of human red blood cells, *P. falciparum* grows to many times its original size and then divides to produce 16–32 daughter parasites. This high rate of growth and multiplication requires synthesis of new membranes. Accordingly, the phospholipid content of malaria-infected erythrocytes increases by up to 5-fold during parasite maturation, with 85% of the newly synthesized phospholipids being either phosphatidylcholine or phosphatidylethanolamine (2). Parasite infection is also accompanied by a marked increase in neutral lipid species like fatty acids, diacylglycerol (DAG)¹ and triacylglycerol (TAG) (3). This synthesis of parasite phospholipids and neutral lipids relies upon transport of choline, inositol, and fatty acids from host plasma (2, 4–10) and *de novo* synthesis of fatty acids by type II fatty acid-synthesizing enzymes (11). The finished malaria genome sequence revealed the presence in *P. falciparum* of type II fatty acid and phospholipid genes (12, 13). Whereas all of the known and predicted enzymes of the type II fatty acid-synthesizing enzyme pathway contain a signal peptide and a targeting sequence for apicoplast (14, 15), a plastid-like organelle in *Apicomplexa* parasites, most known and predicted enzymes for the synthesis of phosphatidylcholine, phosphatidylethanolamine, phosphatidylserine, and phosphatidylinositol lack these signals, suggesting that the synthesis of the malarial phospholipids does not occur in the apicoplast and that this process takes place in other cellular organelles, the identity of which is not yet known.

Because of their importance for parasite development, the pathways of synthesis of phospholipids have long been considered attractive targets for chemotherapy. Accordingly, quaternary ammonium compounds, analogs of choline, have been shown to interfere with phospholipid metabolism, to inhibit parasite growth *in vitro*, and to clear malaria infection in mice and monkeys (16). In eukaryotes, the initial step of phospholipid synthesis involves acylation of glycerol 3-phosphate at the *sn*-1 position by glycerol-3-phosphate acyltransferases (GPAT) to form lysophosphatidic acid (17–21). Lysophosphatidic acid acyltransferases then catalyze the acylation of lysophosphatidic acid at the *sn*-2 position to generate phosphatidic acid (19, 20). Phosphatidate phosphatase and CDP-DAG synthase en-

¹ The abbreviations used are: DAG, diacylglycerol; DHAPAT, dihydroxyacetone phosphate acyltransferase; FITC, fluorescein isothiocyanate; GPAT, glycerol-3-phosphate acyltransferase; PBS, phosphate-buffered saline; *PfGAT*_{CO}, codon-optimized *PfGAT*; TAG, triacylglycerol.

TABLE I
S. cerevisiae strains analyzed in this study

Strain	Genotype	Source
BY4741 (ScCHO1)	<i>MATα his3Δ1 leu2Δ0 met15Δ0 ura3Δ0</i>	Research Genetics
gat1Δ (ScCHO113)	<i>MATα his3Δ1 leu2Δ0 met15Δ0 ura3Δ0 gat1::KANr</i>	Research Genetics
ScCHO99	<i>MATα his3Δ1 leu2Δ0 met15Δ0 ura3Δ0 gat1::KANr [pYES2.1 GAL1::PfGAT URA3]</i>	This study
ScCHO102	<i>MATα his3Δ1 leu2Δ0 met15Δ0 ura3Δ0 gat1::KANr [pYES2.1 GAL1::PfGAT_{co} URA3]</i>	This study
ScCHO93	<i>MATα his3Δ1 leu2Δ0 met15Δ0 ura3Δ0 gat1::KANr [pYES2.1 GAL1 URA3]</i>	This study
CMY228	<i>MATα his3-11,15 leu2-3,112 trp1-1 ade2-1 can1-100 gat1Δ::TRP1 gat2Δ::HIS3 ura3-1 [pGAL1::GAT1 URA3]</i>	Ref. 27
SeCHO88	<i>MATα his3-11,15 leu2-3,112 trp1-1 ade2-1 can1-100 gat1Δ::TRP1 gat2Δ::HIS3 ura3-1 [pGAL1::GAT1 URA3] [pBEVY-L ADH1::PfGAT_{co} LEU2]</i>	This study
SeCHO90	<i>MATα his3-11,15 leu2-3,112 trp1-1 ade2-1 can1-100 gat1Δ::TRP1 gat2Δ::HIS3 ura3-1 [pGAL1::GAT1 URA3] [pBEVY-L ADH1 LEU2]</i>	This study
SeCHO104	<i>MATα his3-11,15 leu2-3,112 trp1-1 ade2-1 can1-100 gat1Δ::TRP1 gat2Δ::HIS3 ura3-1 [pBEVY-L ADH1::PfGAT_{co} LEU2]</i>	This study

zymes convert the phosphatidic acid formed into DAG and CDP-DAG, respectively. DAG subsequently enters the *de novo* CDP-choline and CDP-ethanolamine Kennedy pathways for synthesis of phosphatidylcholine and phosphatidylethanolamine, respectively. CDP-DAG enters the CDP-DAG pathway for synthesis of phosphatidylserine and phosphatidylinositol (22–24). DAG also serves as a substrate to DAG acyltransferases for the synthesis of TAGs (25, 26).

Here we describe the identification and characterization in *P. falciparum* of the gene, *PfGAT*, encoding GPAT activity. We show that the encoded protein, PfGatp, is a yeast-like GPAT enzyme localized in the endoplasmic reticulum membrane and exists as a large multimeric protein complex. PfGatp activity is required for survival of yeast cells lacking GPAT activity because of the loss of the two GPAT-encoding genes *GAT1* and *GAT2* (27, 28). The identification of *PfGAT* will set the stage for a better understanding of glycerolipid biosynthesis in *P. falciparum* and could lead to better therapeutic strategies to inhibit this process and block parasite proliferation.

EXPERIMENTAL PROCEDURES

Parasite Culture—All reagents were from Sigma unless otherwise specified. *P. falciparum* clones were grown using the method developed by Trager and Jensen (29). Serum was replaced with 0.5% Albumax (Invitrogen) in the culture medium.

Plasmid Construction—Codon-optimized *PfGAT_{co}* was synthesized using the forward and reverse primers shown in Fig. 5 and those described below. *PfGAT_{co}* was first assembled and amplified as four small fragments that were subsequently used as templates to amplify the whole gene. Assembly reactions were performed using Platinum *Taq* High Fidelity enzyme (Invitrogen), with 4 μM final concentration for each primer. The program for assembly is the following: 2 min at 94 °C, 25 cycles of 30 s at 94 °C, 30 s at 55 °C, and 1 min at 68 °C, and terminated by a final elongation at 68 °C for 3 min. The resulting products were purified and used as templates for amplification using Platinum *Taq* High Fidelity enzyme and the following PCR program: 2 min at 94 °C, 20–25 cycles of 30 s at 94 °C, 30 s at 63 °C, and 45 s at 68 °C, and terminated by a final elongation at 68 °C for 2 min. The full-length *PfGAT_{co}* was cloned into XmaI and KpnI sites of the *pBEVY-L ADH1 LEU2* plasmid thus yielding the vector *pBEVY-L ADH1::PfGAT_{co} LEU2*. For construction of the plasmid *pYES2.1 GAL1::PfGAT URA3*, *PfGAT* was PCR-amplified using genomic DNA from the *P. falciparum* 3D7 clone and the primers OCHO101 (CGCG-GATCCATGCCAGATTCTTACTTTAATAAGATGG) and ScPfGat-F' (TAAGATCTCTTCTTATATTCTAATTG) and subsequently cloned into the *pYES2.1/V5-His-TOPO* vector (Invitrogen). Similarly the *pYES2.1 GAL1::PfGAT_{co} URA3* was generated by PCR amplification of *PfGAT_{co}* using *pBEVY-L ADH1::PfGAT_{co} LEU2* as a template and the primers PfScGat1 primer 1 (CCCCCCCAGGATGCCAGATTCTACTTC-CTAACATCAGATGGCTGTGAAGGTTATCGTTAA) and ScPfGat-F' (T-AAGATCTCTTCTTATATTCTAATTG) followed by cloning into the *pYES2.1/V5-His-TOPO* vector. The sequence contiguity of *PfGAT* and *PfGAT_{co}* was confirmed by DNA sequencing.

Yeast Strains and Growth Conditions—The *Saccharomyces cerevisiae* strains used in this study are described in Table I. Yeast strains were grown in rich medium (2% Bacto-peptone and 1% yeast extract) containing either 2% dextrose (YPD) or 2% galactose (YPG), or in

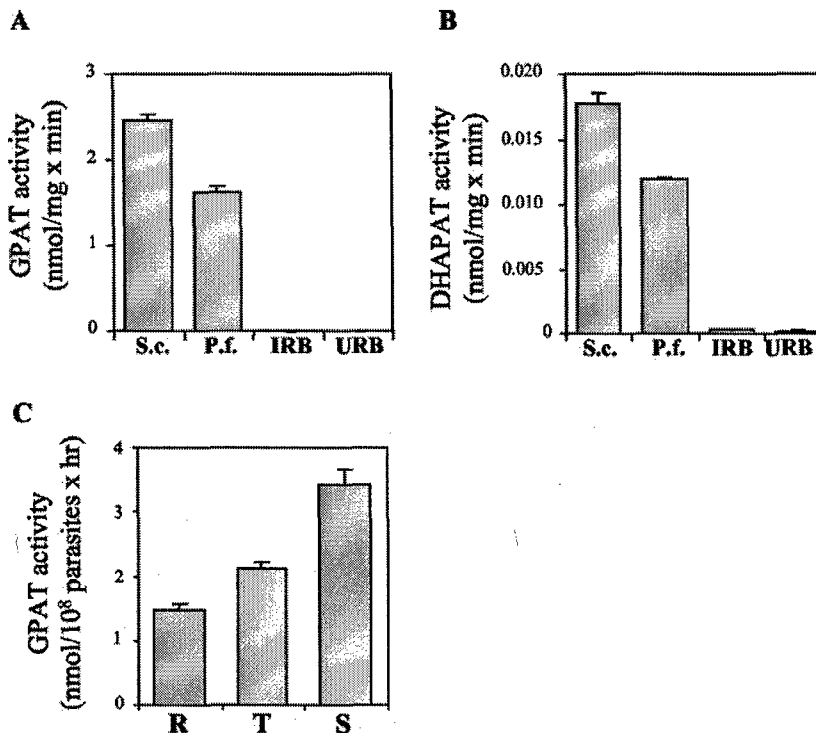
minimal medium (1.7% yeast nitrogen base, 0.5% ammonium sulfate, 2% dextrose, or 2% galactose). Supplements were added as required to maintain cell growth. SeCHO104 that lacks the *pGAL1::GAT1 URA3* plasmid was generated by growing CMY228+ (*pBEVY-L ADH1::PfGAT_{co} LEU2*) (SeCHO88) on glucose-based minimal medium containing 0.1% 5-fluorotic acid and 12 μg/ml uracil. The genotype of this strain was confirmed by PCR analysis using *HN1-1*, *PfGAT_{co}*, and *GAT1*-specific primers ScHN1080–1098 (CATTGCTTGTACACTTCCCCAC-GGTAC), PfScGat1 primer 1 (CCCCCCGGGATGCCAGATTCTACTT-CCTAATCAGATGGCTGTGAAGGTTATCGTTAA), ScPfGat primer 10' (GACTTCTGTCTGATTGATCTTAGGTATAATCTGAATGGTAC-ACCGTTCA), ScGAT1-749 (ATACGAAGGGCTGTAGG), and ScGAT1-1697 (TCAACACCGATTTCACCG).

Purification of PfGatp, Antiserum Production and Purification, and Protein Immunoblotting—The 3'-end of *PfGAT* open reading frame was PCR amplified using the oligonucleotides Ct-X-PfGAT-5' (CCGCTCG-AGATGGAAAGAAAAACACAT) and Ct-B-PfGAT-3' (CGCGGAT-CCTCAGTAAAGGTTTCGACAACC). The resulting PCR product was digested with XhoI and BamHI restriction enzymes and cloned into the XhoI and BamHI sites of the expression vector *pET-15b* (Novagen), thus creating *pET-15b-PfGAT-His₆-78* plasmid. This plasmid was expressed in BL21-CodonPlus-RIL *Escherichia coli* strain (Stratagene). A 200-ml culture of *E. coli* was grown to an *A*₆₀₀ of 0.6 in Luria broth at 37 °C. The cells were induced with 0.4 mM isopropyl β-D-thiogalactoside and incubated for an additional 6 h at 37 °C. Cells were collected by centrifugation at 2,000 × *g* for 15 min at 4 °C and lysed. Histidine-tagged protein was purified by Ni²⁺ chromatography at 4 °C (Qiagen) under denaturing conditions. Purified recombinant Ct-PfGatp was used to immunize rabbits, which was performed by Cocalico Biologicals, Inc.

To generate an antigen for screening and purification of PfGatp-specific antibodies, the *pET-15b-PfGAT-His₆-78* plasmid was digested with XhoI and HindIII restriction enzymes, and the 0.6-kb fragment containing the 3'-end of *PfGAT* was cloned into the SalI and HindIII sites of the expression vector *pMalC2-X* (New England Biolabs), thus creating *pMalC-PfGat-MBP-78* plasmid. This plasmid synthesizes the PfGatp C-terminal fragment as a fusion protein to the N-terminal portion of the *E. coli* maltose-binding protein. *pET-15b-PfGat-MBP-78* plasmid was expressed in BL21-CodonPlus-RIL *E. coli* strain. The purification of the PfGatp-MBP-78 fusion protein was performed using maltose affinity chromatography according to the manufacturer's instructions (New England Biolabs). The crude serum obtained from Cocalico Biologicals was affinity-purified over an Affi-15 gel (Bio-Rad) matrix to which PfGatp-MBP-78 fusion protein was bound covalently. For immunoblots, parasite lysates were resuspended in SDS-PAGE sample buffer, and the proteins were separated by electrophoresis on 12% SDS-polyacrylamide gels and transferred to nitrocellulose membranes. Preincubation, antibody incubations, and washes were conducted in 10 mM Tris-Cl, pH 8, 150 mM sodium chloride, and 0.05% Tween 20 with 5% skim milk. Preimmune and purified antibodies were used at 1:100 dilution. A chemiluminescence kit (ECL, Amersham Biosciences) was used to detect the immunological reaction.

For expression and purification of His₆-tagged PfGatp in *S. cerevisiae*, transformants expressing *pYES2.1 GAL1 URA3*, *pYES2.1 GAL1::PfGAT URA3* or *pYES2.1 GAL1::PfGAT_{co} URA3* (SeCHO93, ScCHO99, and ScCHO102, respectively) were grown on minimal medium containing galactose to mid-log phase. Cell extracts were prepared as described previously (28) except that protease inhibitor mixture (Roche Diagnostics GmbH) and 1% Triton X-100 were added. Six mg of cell extract was mixed with 4 volumes of buffer A (50 mM NaH₂PO₄, 200 mM NaCl, 10

FIG. 1. GPAT and DHAPAT activities in *P. falciparum*. Hemolysates from uninfected (URB) and infected (IRB) erythrocytes and parasite extracts (*P.f.*) were prepared as described under "Experimental Procedures" and analyzed for the presence of GPAT (A) or DHAPAT (B) activities. As a positive control for GPAT and DHAPAT activities, extracts from wild-type *S. cerevisiae* (S.c.) were used. Assays were performed at 37 °C for 60 min using C16:0-CoA as a fatty acyl-CoA donor. C, GPAT activity in extracts prepared from synchronous cultures of ring (R), trophozoite (T), and schizont (S) stage parasites. Each point represents an average of duplicate experiments \pm S.D.



mm imidazole, 0.2% Triton X-100, pH 8). Histidine-tagged proteins were purified by Ni²⁺ chromatography, washed with 20 volumes of buffer A, and eluted in the presence of 50 mM NaH₂PO₄, 200 mM NaCl, 250 mM imidazole, and 0.2% Triton X-100, pH 8.

GPAT and Dihydroxyacetone Phosphate Acyltransferase (DHAPAT) Assays—Parasites from 3D7 asynchronous and synchronous cultures (2% hematocrit, 10% parasitemia) were isolated from infected erythrocytes by treatment with 0.07–0.1% saponin for 15 min at 0 °C followed by centrifugation at 2,061 × g for 15 min. The pellet was washed in PBS and resuspended in 500 μl of 50 mM Tris-HCl, pH 7.5, 10% glycerol, 1 mM dithiothreitol, 1 mM EDTA. After sonication followed by centrifugation at 1,500 × g, the supernatant was recovered and used for GPAT and DHAPAT assays. Yeast extracts were obtained as described previously (28). For the GPAT assay, 200 μg of protein extracts was added to 200 μl of GPAT buffer (75 mM Tris-HCl, pH 7.5, 1 mM dithiothreitol, 2 mM MgCl₂, 45 μM fatty acyl-CoA, 1 mg/ml bovine serum albumin, and 0.4 mM [¹⁴C]glycerol 3-phosphate (2.5 μCi/μmol) and incubated at 37 °C for 1 h except as otherwise mentioned. The reaction was stopped by the addition of 600 μl of 1% HClO₄. The DHAPAT assay was performed as described by Athenstaedt *et al.* (30). For both activities, lipid extraction was performed by adding 3 ml of chloroform:methanol (1:2, v/v) to the mixture followed by adding 1 ml of chloroform and 1 ml of 1% HClO₄. After centrifugation at 1,250 × g for 5 min, the organic phase was recovered and washed with 2 ml of 1% HClO₄ followed by centrifugation at 1250 × g for 5 min. The chloroform phase was transferred to a scintillation vial, dried, and counted. Aqueous and organic phases were also analyzed by thin layer chromatography (TLC) using silica gel plates (Whatman). The hydrophilic phase of the first extraction was dried in a SpeedVac and resuspended in chloroform for loading on TLC. A solvent made of chloroform:methanol:water:acetic acid (70:30:4:2) was used to separate radiolabeled products and to confirm their identity. The main product detected in the organic phase of the GPAT assay was phosphatidic acid. No phosphatidic acid or lysophosphatidic acid could be detected in the aqueous phase. For the DHAPAT assay, low counts could be measured from the organic phase, and no radiolabeled acyl dihydroxyacetone phosphate could be measured in the water phase after TLC separation. Standards used were 1-oleoyl-sn-glycerol 3-phosphate and 1,2-dioleoyl-sn-glycerol 3-phosphate (Sigma).

Gel Filtration Assay—Infected red blood cells from 84 ml of *P. falciparum* asynchronous culture (2% hematocrit, 10% parasitemia) were treated with 0.15% saponin for 15 min at 0 °C. After centrifugation at 1,875 × g for 10 min the pellet was washed in PBS, resuspended in PBS containing a mixture of protease inhibitors, sonicated, incubated in 1% Triton X-100 for 30 min at 0 °C, and centrifuged at 16,300 × g for 15

min. The supernatant was concentrated and separated on a Superose 12 HR 10/30 column at a flow rate of 0.2 ml/min. Fractions of 1 ml were collected and trichloroacetic acid precipitated. The precipitates were resuspended in 20 μl of SDS-PAGE loading buffer, neutralized and separated by electrophoresis on 10% SDS-polyacrylamide gels, and analyzed by Western blotting, using affinity-purified anti-PfGatp antibodies.

Analysis of PfGatp Membrane Association—Infected red blood cells from a 36-ml asynchronous culture (2% hematocrit, 10% parasitemia) were treated with 0.07% saponin for 15 min at 0 °C. After centrifugation at 1,875 × g for 10 min, the pellet was washed in PBS and resuspended in PBS. After sonication, the extract was subjected to various treatments followed by a 10-min centrifugation at 100,000 × g. Treatments included a 30-min incubation at 0 °C with buffer alone, 1% Triton X-100, 1% Triton X-114, 1% n-decyl-β-D-maltoside (Anatrace), 0.5 M potassium acetate or 0.1 M Na₂CO₃ at pH 11. Supernatant and pellet fractions were separated by SDS-PAGE and immunoblotted with affinity-purified anti-PfGatp and anti-PNT1 antibodies (31). Bound antibodies were visualized by ECL.

Immunofluorescence Microscopy—Synchronous cultures of *P. falciparum*-infected erythrocytes were washed twice in PBS, placed onto coverslips, and dried at room temperature. Fixation, washes, and mounting were performed as described by Rager *et al.* (31). Coverslips were incubated simultaneously with affinity-purified anti-PfGatp antibodies (diluted 1:10) and either mouse monoclonal antibodies (Sigma) to the red blood cell Band 3 protein (diluted 1:500) or rat polyclonal antibodies (MR4) to the *P. falciparum* endoplasmic reticulum marker BiP (32) at 37 °C with gentle shaking for 1 h. The coverslips were washed and then incubated with anti-rabbit fluorescein isothiocyanate (FITC) conjugate and anti-mouse conjugated to Texas Red (Molecular Probes) or anti-rabbit rhodamine and anti-rat FITC-conjugated secondary antibodies for 1 h at 37 °C. Nuclei were stained by incubating the coverslips in PBS containing 3 μg/ml Hoechst stain (Molecular Probes) for 5 min at room temperature. Mitochondrial staining was performed by incubating infected red blood cells with 250 nM MitoTracker Red CMXRos (Molecular Probes) for 5 min prior to fixation and incubation with affinity-purified PfGatp antibodies (diluted 1:10). The coverslips were washed and then incubated with goat anti-rabbit conjugated to FITC (Molecular Probes) secondary antibodies for 1 h at 37 °C. Images were analyzed by high resolution fluorescence and confocal microscopy.

RESULTS

GPAT and DHAPAT Activities in *P. falciparum*—To examine the presence of GPAT and/or DHAPAT activities in *P. falciparum*

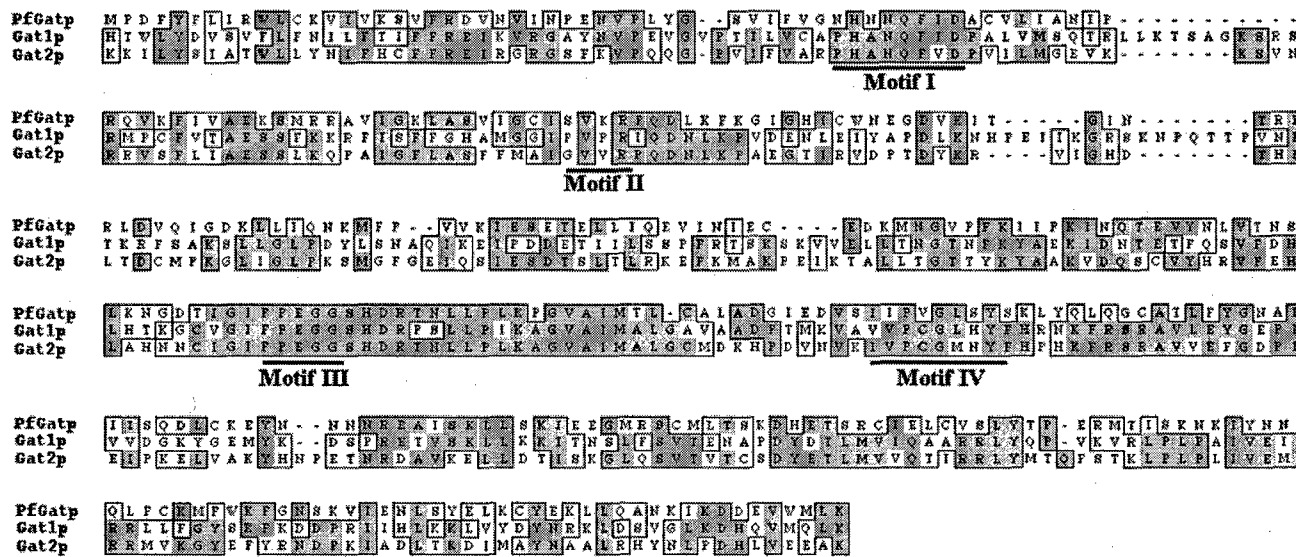
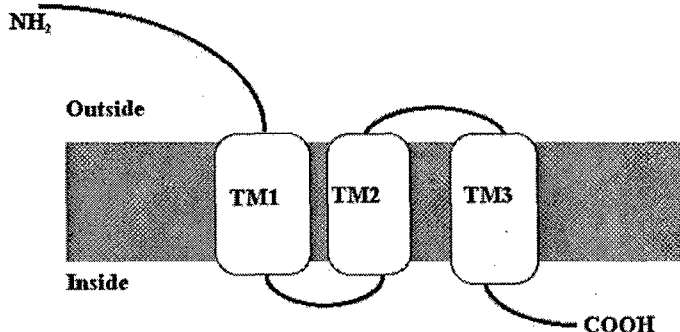
A**B**

FIG. 2. *A*, PfGatp sequence alignment. The alignment of PfGatp from 3D7 isolate with *S. cerevisiae* Gat1p and Gat2p is shown. *B*, PfGatp predicted topology. PfGatp topology was predicted by standard hydrophathy algorithms and includes a large extracellular domain (residues 1–382) and three transmembrane domains TM1, TM2, and TM3.

TABLE II
Glycerol-3-phosphate acyltransferase homology motifs

PfGatp, *P. falciparum* GPAT; Gat1p and Gat2p, GPAT proteins from *S. cerevisiae*; Hs.GAT, mitochondrial GPAT from *Homo sapiens*; Mm.GAT, mitochondrial GPAT from *Mus musculus*; Ec.GAT, GPAT from *Escherichia coli*; At.GAT, GPAT from *Arabidopsis thaliana*; Ps.GAT, GPAT from *Pisum sativum*.

Protein	Motif I	DBM ^a	Motif II	DBM	Motif III	DBM	Motif IV	Accession no.
PfGatp	HNNQFID	36	SVKR	102	FPEGG	29	SIIPVGLSY	AY007373
Gat1p	HANQFID	47	PVPR	120	FPEGG	31	VVPCCGLHY	P36148
Gat2p	HANQFVD	40	GVVR	109	FPEGG	31	IVPCGMNY	Z35773
Hs.GAT	HRSHID	38	FFIR	35	FLEG	30	LUPVGISY	NP065969
Mm.GAT	HRSHID	38	FFIR	35	FLEG	30	LVIPVGISY	AAH19201
Ec.GAT	HRSHMD	38	FFIR	29	FVEGG	30	TLIPIYIGY	AAA24395
At.GAT	HQSEAD	22	AGDR	57	WIAPSGG	36	IYPLA	Q43307
Ps.GAT	HQSEAD	22	AGDR	57	WIAPSGG	36	IYPLA	P30706

^a DBM, distance between motifs in number of amino acid residues.

rum-infected erythrocytes and to determine their origin (*i.e.* red blood cell or parasite), hemolysate and parasite fractions were prepared from red blood cells infected with an asynchronous culture of the 3D7 clone of *P. falciparum* and analyzed for their GPAT and DHAPAT activities using glycerol 3-phosphate and dihydroxyacetone phosphate substrates, respectively. Parasite extracts were able to catalyze the acylation of glycerol 3-phosphate substrate and dihydroxyacetone phosphate substrates (Fig. 1, *A* and *B*). However, the *P. falciparum* DHAPAT represented less than 1% of the GPAT activity (Fig. 1*B*). No GPAT or DHAPAT activities could be detected in red blood cell hemolysates from infected as well as control uninfected red

blood cells (Fig. 1, *A* and *B*). To determine the GPAT activity during *P. falciparum* intraerythrocytic development, extracts were prepared from a highly synchronous culture of 3D7-infected erythrocytes and analyzed for GPAT activity. Equal amounts of proteins from each developmental stage resulted in relatively similar acylation activities (not shown). However, determination of the total activity per developmental stage indicated a 1.4- and 2.8-fold increase in the acylation activity during trophozoite and schizont stages (1.267 nmol of glycerol 3-phosphate/10⁸ trophozoites and 2.052 nmol of glycerol 3-phosphate/10⁸ schizonts), respectively, compared with the ring stage (0.88 nmol of glycerol 3-phosphate/10⁸ rings) (Fig.

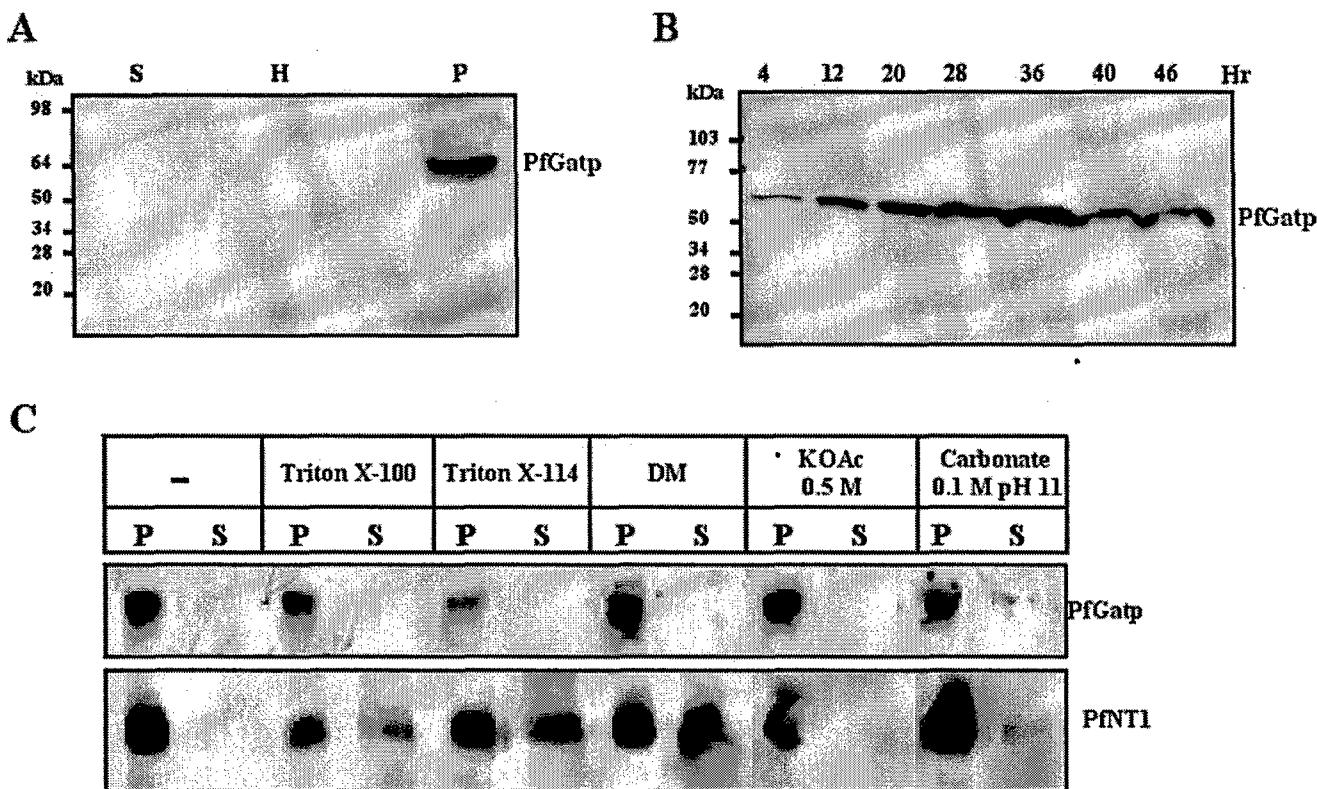


FIG. 3. PfGatp expression during *P. falciparum* intraerythrocytic life cycle. *A*, Western blot analysis was performed using protein extracts from supernatant (*S*), hemolysate (*H*), and parasite (*P*) fractions from an asynchronous culture of *P. falciparum* 3D7 clone. Proteins were separated by SDS-PAGE, transferred to a nitrocellulose membrane, and analyzed by immunoblot using affinity-purified PfGatp-antibodies as described under “Experimental Procedures.” *B*, Western blot analysis was performed using protein extracts prepared from a highly synchronous culture of *P. falciparum* 3D7 clone at different times after *P. falciparum* invasion of red blood cells. *C*, Western blot analysis was performed using soluble (*S*) and pellet fractions (*P*) of parasite extracts treated or not with 1% Triton X-100, 1% Triton X-114, 1% *n*-decyl- β -D-maltopyranoside (*DM*), 0.5 M potassium acetate or 0.1 M carbonate, pH 11, followed by 100,000 \times *g* ultracentrifugation. Immunoblot analysis was performed using anti-PfGatp and anti-PfNT1 antibodies.

1C). Consistent with data from asynchronous parasites, only residual DHAPAT activity (~0.15% of the cellular GPAT activity) could be detected from ring, trophozoite, and schizont extracts (data not shown). These results indicate that in *P. falciparum* the first step of glycerolipid biosynthesis is directed mostly toward the acylation of glycerol 3-phosphate substrate. As a control, yeast extracts were used, and both activities were detected (Fig. 1, *A* and *B*) in agreement with data published previously (20, 28, 33).

PfGatp Is a Yeast-like GPAT Protein—To identify the enzyme(s) responsible for the malarial GPAT activity, we searched for GPAT-like proteins in the *P. falciparum* genome data bases using known GPAT proteins as query. A gene that we named *PfGAT* was identified based on its homology with yeast GPAT enzymes. *PfGAT* was cloned from the *P. falciparum* 3D7 clone (The Netherlands) and was found to encode a polypeptide of 583 amino acids which exhibits ~28% identity and 49% similarity to *S. cerevisiae* Gat1p and Gat2p (Fig. 2A) and other putative GPAT enzymes from the fission yeast *Schizosaccharomyces pombe* and the filamentous yeast *Candida albicans* (not shown). In contrast, PfGatp shares little or no homology with bacterial, mammalian, and plant known and putative GPAT proteins. The four motifs known to play a crucial role in GPAT activity are present in PfGatp and are highly homologous to those found in yeast GPAT proteins (34). Interestingly, these motifs are different from the previously characterized or predicted human, mouse, bacterial, and plant GPAT enzymes (Table II). Furthermore, whereas PfGatp and its yeast homologs Gat1p and Gat2p have a long stretch of 102, 120, and 109 amino acid residues between motifs II and III, respectively,

this linker is much shorter in the human, mouse, bacterial, and plant known and putative GPAT enzymes with, respectively, 35, 35, 29, and 57 amino acid residues only (Table II). The derived amino acid sequence of PfGatp was analyzed to determine the hydrophobic character of the protein, using the TMHMM program (35). PfGatp is predicted to possess three hydrophobic membrane spanning domains with a long N-terminal stretch (1–382) exposed outside the membrane (Fig. 2B). This topology is similar to that predicted for the yeast Gat1p and Gat2p proteins (28).

PfGatp Is an Endoplasmic Reticulum Membrane Protein Expressed throughout the Intraerythrocytic Life Cycle—We have expressed and purified the C-terminal region of PfGatp and used it to immunize rabbits and produce polyclonal antibodies. These antibodies were affinity purified over a PfGatp maltose-binding protein affinity matrix and used in Western blot assays to monitor PfGatp temporal and spatial expression during the *P. falciparum* intraerythrocytic life cycle. Although no immunoreaction could be detected in the culture supernatant or the hemolysate fractions of uninfected or *P. falciparum*-infected erythrocytes, a single band with a molecular mass of 67 kDa was detected in the parasite fraction (Fig. 3A). This size is consistent with that predicted from the PfGatp translation product. Analysis of PfGatp expression during the intraerythrocytic life cycle of the parasite showed that it is expressed in all the stages (ring, trophozoite, and schizonts), but its level increases during the trophozoite stage (24–36 h) (Fig. 3B). As a positive control, expression of the *P. falciparum* elongation factor 1 β was regulated, with higher expression observed during the later stages of the parasite development (data not

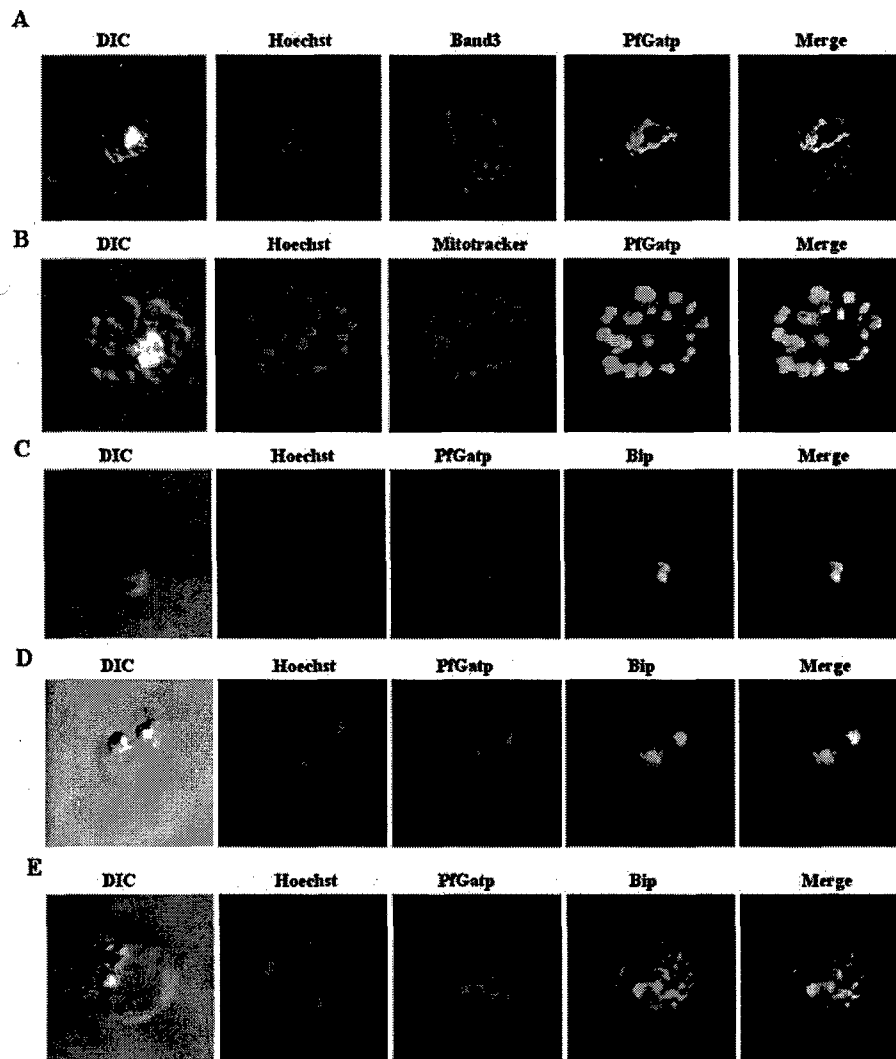


FIG. 4. Immunofluorescence microscopy of *P. falciparum*-infected red blood cells using PfGatp antibodies. *A*, double-labeling immunofluorescence of erythrocytes infected with *P. falciparum* at the schizont stage of the parasite intraerythrocytic development with PfGatp- and Band 3-specific antibodies. In green, PfGatp conjugated to the FITC-conjugated goat anti-rabbit secondary antibody. In red, Band 3 conjugated to the Texas Red-conjugated anti-mouse secondary antibody. *B*, double-labeling immunofluorescence of erythrocytes infected with *P. falciparum* at the schizont stage of the parasite intraerythrocytic development with PfGatp-specific antibodies and MitoTracker. In green, PfGatp conjugated to the FITC-conjugated anti-rabbit secondary antibody. In red, MitoTracker. DNA was counterstained with Hoechst. *C–E*, double-labeling immunofluorescence of erythrocytes infected with *P. falciparum* at the ring (*C*), trophozoite (*D*), and schizont (*E*) stages of the intraerythrocytic development with PfGatp- and BiP-specific antibodies. In red, PfGatp conjugated to the rhodamine-conjugated anti-rabbit secondary antibody. In green, BiP conjugated to the FITC-conjugated anti-rat secondary antibody. DNA was counterstained with Hoechst (blue). Yellow represents regions of overlap between red and green.

shown), as we have reported previously (31, 36). To determine whether PfGatp is an integral or peripheral membrane protein, parasite lysates prepared from *P. falciparum*-infected erythrocytes were treated with various detergents and salts. Membrane and soluble fractions were then separated by ultracentrifugation. In the absence of salts and detergents, PfGatp was associated with the membrane fraction (Fig. 3C). Treatment with salts or detergents had little or no effect on PfGatp cellular distribution (Fig. 3C). As a control, the nucleoside transporter, PfNT1, an integral membrane protein of the plasma membrane of the parasite (31, 37), partitioned in the soluble fraction in the presence of detergents but remained associated with the membrane fraction in the presence of salts (Fig. 3C). Together, these data suggest that PfGatp is an integral membrane protein that is associated with a detergent-resistant fraction.

GPAT activities characterized in different organisms have been shown to exist in the endoplasmic reticulum, lipid particles, peroxisomes, and mitochondria (38). To examine PfGatp localization during *P. falciparum* intraerythrocytic development, immunofluorescence analyses were performed using affinity-purified PfGatp antibodies and specific markers of red cell membrane (Band 3) and parasite organelles (BiP and MitoTracker). Fluorescence signals specific for PfGatp were detected in all three intraerythrocytic developmental stages (rings, trophozoites, and schizonts) and were limited to the parasite with no PfGatp staining detected in the erythrocyte

membrane or cytoplasm (Fig. 4). To localize PfGatp within the parasite further, we performed colocalization studies with the mitochondrial and endoplasmic reticulum markers, Mito-Tracker and BiP, respectively (39) (Fig. 4, *B–E*). The PfGatp signal was proximal and only partly overlapping with Mito-Tracker (Fig. 4B), whereas the signals of PfGatp and BiP completely overlapped in all the three stages (Fig. 4, *C–E*). Collectively, these data suggest that PfGatp is a component of the endoplasmic reticulum. This staining was proximal to the nucleus as revealed by Hoechst labeling (Fig. 4, *A–E*). Similar results were obtained using confocal microscopy (data not shown).

Yeast Complementation and PfGatp-mediated GPAT Activity—For functional analysis of PfGatp, we have used yeast as a model system to characterize the protein at the biochemical and genetic levels. In *S. cerevisiae*, two genes, *GAT1* and *GAT2*, encode GPAT activities (27, 28). Single disruption of *GAT1* or *GAT2* causes no discernible growth defects; however, disruption of both genes is lethal (27, 28). To overcome expression problems caused by the high A+T content of *PfGAT*, we used a PCR-based approach to synthesize a codon-optimized version of *PfGAT*, *PfGAT_{CO}*, thus changing its A+T composition from 73.4% to 65.5% (Fig. 5). Although immunoblot analysis revealed no expression of PfGatp from the original *PfGAT* gene in yeast, a major induction of PfGatp expression from *PfGAT_{CO}* could be detected (Fig. 6A). To determine whether expression of PfGatp in the *gat1Δgat2Δ* mutant could replace the yeast

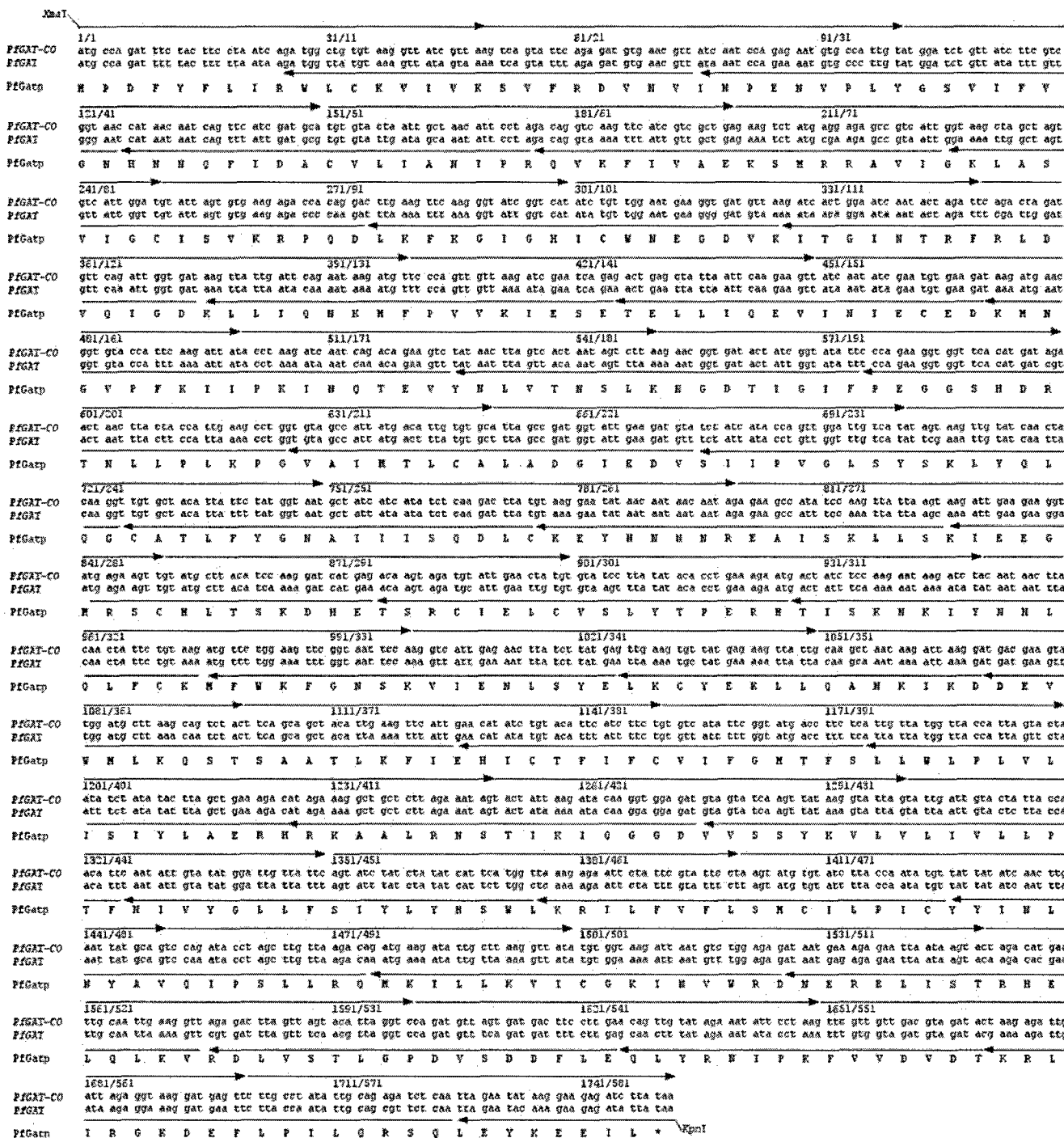


FIG. 5. Codon optimization of the *PfGAT* gene. Nucleotide and protein sequences of *PfGAT* and *PfGAT*_{CO} are shown. Arrows indicate the oligonucleotides used for assembly and amplification of *PfGAT*_{CO} as described under “Experimental Procedures.”

Gat1p GPAT activity, *PfGAT*_{CO} was expressed under the regulatory control of the *ADH1* constitutive promoter (*pBEVY-L ADH1::PfGAT*_{CO} *LEU2* plasmid) in the yeast strain CMY228, which is deleted for both *GAT1* and *GAT2* and contains the plasmid *pGAL1::GAT1 URA3*, which harbors the yeast *GAT1* gene under the regulatory control of the inducible *GAL1* promoter (27). The CMY228 strain is not viable on medium containing glucose and grows only on galactose (27). CMY228 cells expressing *PfGAT*_{CO} were able to grow on glucose (Fig. 6B), whereas CMY228 control cells expressing the empty vector *pBEVY-L ADH1 LEU2* (40) resulted in clones that were unable to grow on glucose (Fig. 6B). Furthermore, because the endogenous *pGAL1::GAT1 URA3* plasmid contains the *URA3* posi-

tive/negative marker, we applied a negative selection using 5-fluorotic acid to eliminate this plasmid. The strain ScCHO104, which harbors the plasmid *pBEVY-L ADH1::Pf-GAT_{CO} LEU2* and therefore relies solely on PfGatp expression for survival, was obtained and confirmed further for the loss of the endogenous *pGAL1::GAT1 URA3* plasmid (Fig. 6C). These studies thus provide genetic evidence that PfGatp plays the same cellular function as the yeast Gat1p and Gat2p. Protein extracts from ScCHO104 strain were prepared and used to characterize further the PfGatp-mediated GPAT activity in the presence of glycerol 3-phosphate and dihydroxyacetone phosphate substrates. Similar to our results in *P. falciparum*, PfGatp activity was specific for glycerol 3-phosphate substrate.

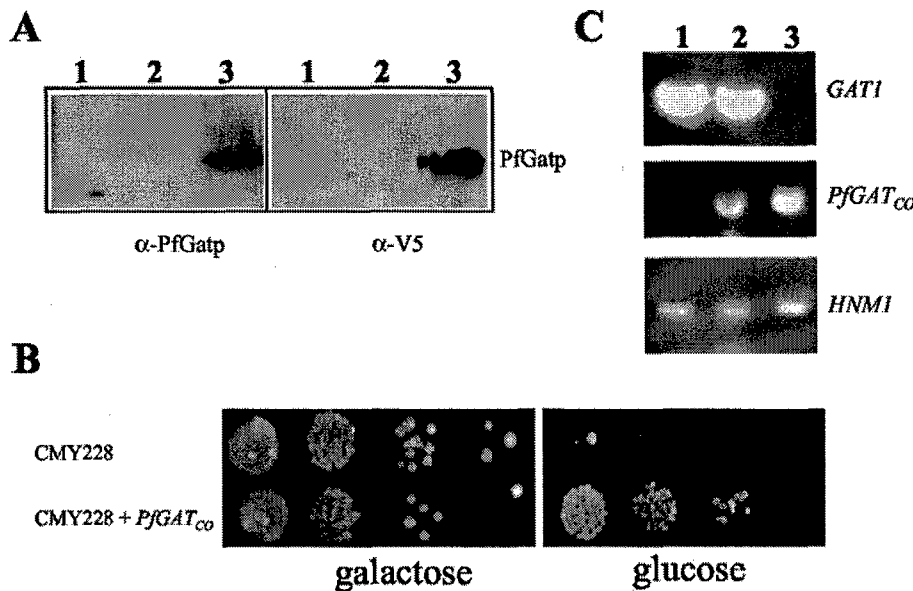


FIG. 6. *PfGAT* expression and functional complementation in yeast. *A*, Western blot analysis of expression of PfGatp from yeast cells expressing *pYES2.1 GAL1::PGAT URA3* (ScCHO93, lane 2) or *pYES2.1 GAL1::PfGAT_{co} URA3* (ScCHO102, lane 3) plasmids. The ScCHO93 harboring the empty vector *pYES2.1 GAL1 URA3* was used as a control (lane 1). Cell extract preparation followed by Ni²⁺ affinity chromatography was performed as described under "Experimental Procedures." Immunoblot analyses were performed using anti-PfGatp affinity-purified antibodies (1:100) and anti-V5 antibodies (1:5,000). *B*, *PfGAT*_{co} complementation of the conditional lethality of *S. cerevisiae* CMY228 grown on glucose. CMY228 cells harboring *pBEVY-L ADH1 LEU2* or *pBEVY-L ADH1::PfGAT_{co} LEU2* vector were grown to mid-log phase in galactose-containing minimal medium, washed twice in ice-cold water, and plated on YPD and YPG plates. Identical numbers of cells were serial 1:10 diluted and applied (starting with 3×10^5 cells). *C*, PCR analysis using primers specific for *S. cerevisiae* *GAT1* and *P. falciparum* *PfGAT*_{co} genes as described under "Experimental Procedures" and genomic DNA from CMY228 (lane 1), ScCH088 (CMY228 + (*pBEVY-L ADH1::PfGAT_{co} LEU2*), lane 2), and ScCHO104 (*gat1Δgat2Δ* + (*pBEVY-L ADH1::PfGAT_{co} LEU2*)), lane 3) strains as templates. The choline transporter gene, *HNM1*, was used as an internal positive control.

The PfGatp GPAT activity measured at 37 °C was linear during the first 6 min, after which it reached a plateau (Fig. 7A). No significant activity could be detected at 0 °C (Fig. 7A). We have measured the kinetic parameters of the GPAT activity using increasing concentrations of glycerol 3-phosphate substrate. PfGatp displayed an apparent affinity (K_m) for glycerol 3-phosphate of 2.55 ± 0.58 mM and a maximum velocity (V_{max}) of 55.1 ± 7.2 nmol × mg⁻¹ × min⁻¹ (Fig. 7B). The substrate specificity of PfGatp was measured using unsaturated and saturated fatty acyl-CoA substrates with different chain lengths (C12:0, C14:0, C16:0, C16:1, C18:0, C18:1, and C20:0). PfGatp displayed a major preference for palmitoyl-CoA (C16:0) and palmitoleoyl-CoA (C16:1), low preference for C14:0, C18:0, C18:1, and C12:0 substrates, and no specificity for C20:0 (Fig. 7C). Unlike its GPAT activity, PfGatp-mediated DHAPAT was found to be very low and represented only 0.5–2.5% of its GPAT activity (Fig. 7D).

***PfGatp* Exists as a Large Multimeric Protein Complex in the Endoplasmic Reticulum Membrane**—To examine whether the native PfGatp exists as a monomer or is part of protein complex, native proteins were separated under native conditions and analyzed by Western blot using anti-PfGatp-specific antibodies. Native PfGatp migrated as a high molecular mass polypeptide of an estimated >450 kDa (Fig. 8A). Cross-linking studies using increasing concentrations of the alkylating agent ethylene glycol bis(succinimidylsuccinate) followed by SDS-PAGE analysis showed a shift of PfGatp from a monomeric form to higher molecular masses, some of which could not enter the stacking gel (data not shown). To gain further insight into the approximate size of the native PfGatp, a gel filtration analysis of the native enzyme was performed and revealed the presence of PfGatp at the peak of migration of thyroglobulin (650 kDa) (Fig. 8B). As a control, the fractions collected by gel filtration were analyzed by Western blot using antibodies against *P. falciparum* elongation factor 1α and showed, as

expected, the presence of this protein both as a monomer (free PEEF-1α) and as a large protein complex (EF-1 complex) as described previously (Fig. 8, C and D) (36).

DISCUSSION

During its asexual 48-h development and multiplication cycle within human erythrocytes *P. falciparum* produces between 16 and 32 new merozoites that subsequently invade new red blood cells. This rapid multiplication of the parasite within human erythrocytes is accompanied by a marked increase in phosphatidylcholine, phosphatidylethanolamine, phosphatidylserine, phosphatidylinositol, fatty acids, DAG, and TAG content (3). This increased metabolic need of *P. falciparum* to generate new membranes has stimulated efforts to identify compounds that can interfere with parasite membrane biogenesis and block malaria proliferation. Analysis of the available *P. falciparum* genomic sequences points to the presence of the genes of the major pathways for synthesis of glycerolipids (12). The few of those genes that have been characterized thus far show major structural and catalytic differences from their human counterparts, thus opening future avenues for lipid-based therapeutic strategies to fight malaria.

Here, we have characterized the initial step of glycerolipid synthesis in *Plasmodium*-infected erythrocytes. We found that *P. falciparum* catalyzes the acylation of glycerol 3-phosphate into 1-acylglycerol 3-phosphate, which is the main precursor for phosphatidic acid and subsequently for the phospholipid precursors DAG and CDP-DAG. *P. falciparum* also catalyzes the acylation of dihydroxyacetone phosphate, although less efficiently compared with the GPAT substrate. This low DHAPAT activity suggests that malaria parasites may not require specialized DHAPAT enzymes and may not synthesize ether lipids. This idea is supported further by the lack in the finished genomic sequence of *P. falciparum* of homologs of

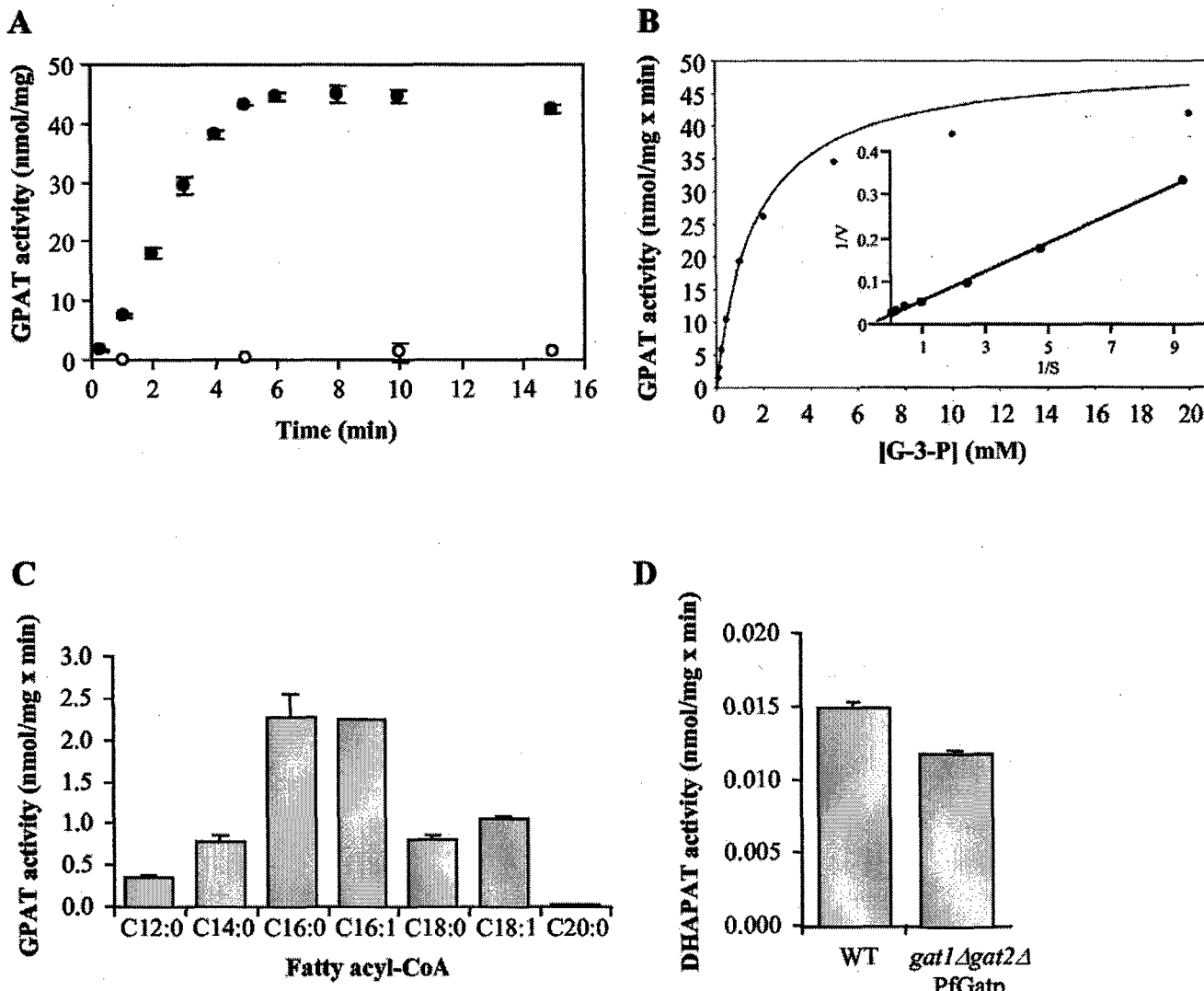


Fig. 7. Biochemical characterization of PfGatp activity. *A*, PfGatp time-dependent GPAT activity. ScCHO104 (*gat1Δgat2Δ+(pBEVY-LADH1::PfGAT_{CO} LEU2)*) strain was grown on glucose-based rich medium (YPD) and harvested at $A_{600} = 1.5$. Protein extracts were prepared and assayed for GPAT activity as described under “Experimental Procedures.” The assay was performed using 200 μ g of proteins, 0.4 mM glycerol 3-phosphate, C16:1-CoA, and incubated for the indicated times at 37 °C (black circles) or 0 °C (white circles). Each point represents an average of duplicate experiments \pm S.D. *B*, PfGatp-mediated GPAT kinetics. PfGatp activity was measured at 37 °C for 2.5 min in the presence of C16:1-CoA and the indicated concentrations of glycerol 3-phosphate. The curve was fitted to the Michaelis-Menten equation $V = V_{max} \times S/(K_m + S)$. The Lineweaver-Burk representation of the saturation curve is shown as an inset. *C*, PfGatp substrate specificity. The GPAT activity mediated by PfGatp was assayed as described under “Experimental Procedures” using fatty acid substrates with different chain lengths and incubated for 10 min at 37 °C. *D*, PfGatp DHAPAT activity. The DHAPAT assay was performed as described under “Experimental Procedures” for 10 min at 37 °C using extracts derived from wild-type (WT; ScCHO1) and ScCHO104 (*gat1Δgat2Δ* PfGatp) strains and C16:1-CoA as an acyl donor.

DHAPAT and alkyldihydroxyacetone phosphate synthase genes, which are important for ether lipid synthesis.

Our studies revealed that the *P. falciparum* *PfGAT* gene encodes a GPAT enzyme. To our knowledge, this is the first GPAT gene to be identified in protozoa. Affinity-purified polyclonal antibodies against PfGatp indicated that this protein is expressed throughout the asexual life cycle of the parasite but induced mainly during the trophozoite stage during which an active synthesis of phospholipids takes place, likely to provide membranes for the newly formed parasites. A similar regulation pattern was observed for the *PfGAT* transcript using large scale microarray analyses (41, 42). Our characterization of the native PfGatp demonstrated that it is an integral membrane protein of the endoplasmic reticulum and suggests that this organelle plays an important role in phospholipid biosynthesis in *P. falciparum*. Furthermore, we found that native PfGatp exists as a high molecular mass protein. We do not know at this stage whether this high molecular complex is composed solely

of PfGatp or whether this enzyme associates with other parasite proteins.

Analysis of the sequence of PfGatp protein suggests that it is a yeast-like GPAT enzyme. The four motifs known to be important for GPAT catalysis are present in PfGatp and are highly similar in residue composition as well as in their spatial distribution to those of the yeast GPAT proteins, Gat1p and Gat2p. Interestingly, these motifs are highly divergent from those of mammalian and bacterial GPAT enzymes. Motifs II and III in PfGatp are separated by 102 amino acid residues, whereas the human and mouse GPATs have only 35 residues between these two motifs. The fact that yeast possesses two genes *GAT1* and *GAT2* that catalyze the GPAT activity and that disruption of both genes is lethal has made it possible for us to functionally characterize *PfGAT* at the genetic and the biochemical levels using yeast as a surrogate system. The finished sequence of the *P. falciparum* nuclear genome indicated that its overall A+T composition is 80.6% and rises to ~90% in

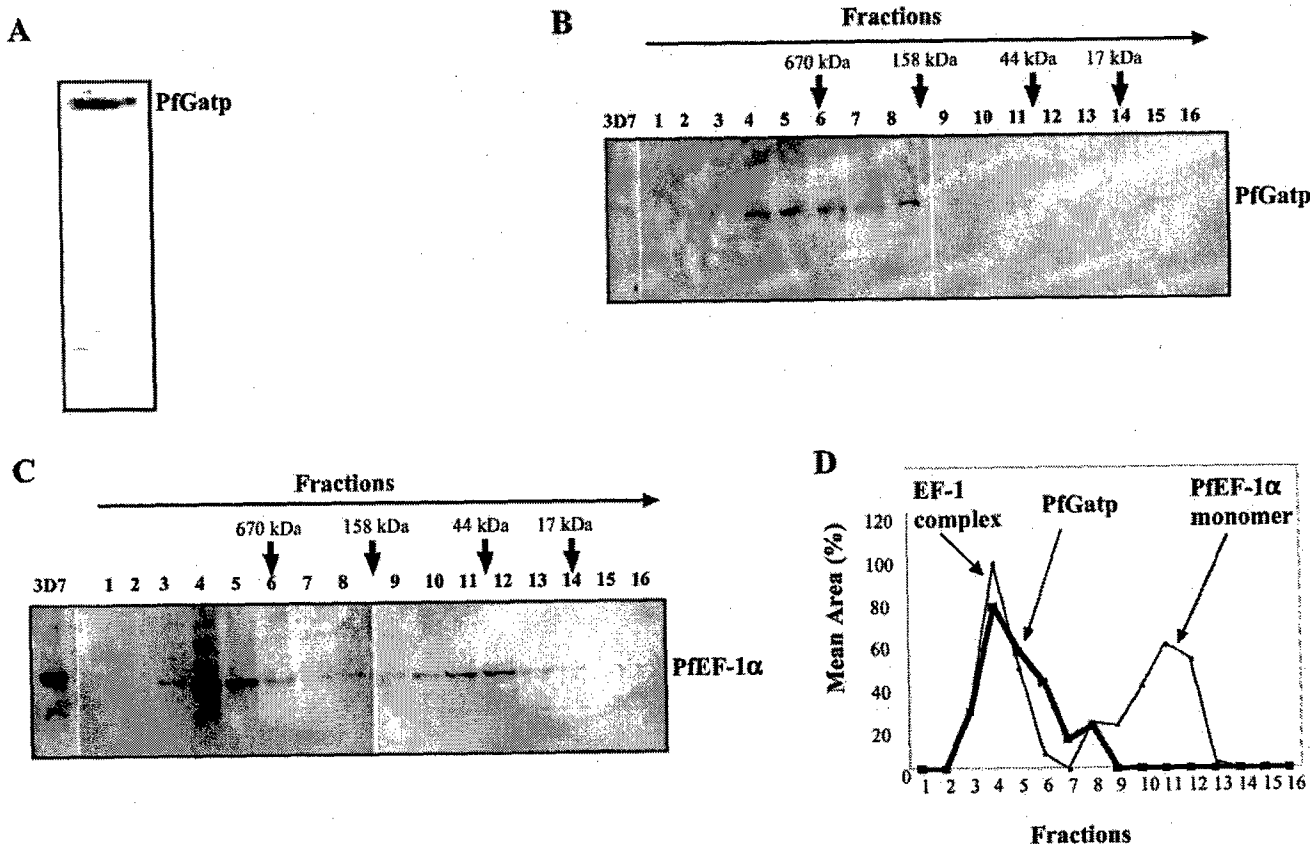


FIG. 8. PfGatp multimerization. *A*, analysis of PfGatp migration profile on a 5% native gel by immunoblot assay. *B* and *C*, analysis of PfGatp multimerization by gel filtration assay. *P. falciparum* extracts were separated by gel filtration on a Superose 12 column and analyzed by SDS-PAGE and Western blot, using PfGatp- (*B*) and PfEF-1 α - (*C*) specific antibodies. *D*, relative amounts of PfGatp (heavy line) and PfEF-1 α (thin line) present in each fraction obtained from *B* and *C*.

introns and intergenic regions, making it the most A+T-rich genome sequenced to date (12). This unusual property of *P. falciparum* genes has hampered efforts to perform straightforward expression and complementation analyses in heterologous systems. Because of low expression levels in yeast, initial attempts to express *PfGAT* gene in *gat1* Δ or *gat2* Δ single knock-outs to measure activity or in the double knock-out *gat1* Δ *gat2* Δ to complement its lethal phenotype were not successful. To overcome this problem, we synthesized a codon-optimized version, *PfGAT*_{CO}. This resulted in an increase in the G+C composition of *PfGAT* from 26.6 to 34.5% and a dramatic increase in the expression of PfGatp in yeast. Furthermore, expression of *PfGAT*_{CO} in the double knock-out *gat1* Δ *gat2* Δ mutant could complement its lethal phenotype. In accordance with our results in *P. falciparum*, PfGatp was found to be specific for glycerol 3-phosphate and showed a very low activity toward dihydroxyacetone phosphate substrate. Kinetic studies revealed that PfGatp is a low affinity GPAT enzyme that displays high substrate specificity. PfGatp activity was higher when the acyl-CoA substrates, C16:0 and C16:1, were used. Interestingly, C16:0 has been shown to be transported by the parasite from host plasma and is essential for *P. falciparum* growth and survival (43).

In summary, the work reported here supports the conclusion that *PfGAT* encodes an unusual yeast-like GPAT enzyme of *P. falciparum* expressed throughout the asexual life cycle (ring, trophozoite, and schizont stages) of the parasite within the host red blood cells. The identification of PfGatp is a critical step toward understanding membrane biogenesis in this parasite. The finished genome sequence of *P. falciparum* has also revealed a second gene, *PfPLSB*, encoding a polypeptide that

shares homology with plant GPAT enzymes. Future studies are needed to determine whether the encoded protein catalyzes the acylation of glycerol 3-phosphate and/or dihydroxyacetone phosphate. Our attempts to target *PfGAT* gene for disruption have resulted in integration events to different loci in the genome but not to *PfGAT* locus, suggesting that *PfGAT* might be essential for parasite survival and that PfGatp and PfPLSB functions might not be redundant. Future complementation studies in *P. falciparum* to confirm the essential role of *PfGAT* are warranted and could provide useful information for the rational design of compounds that could specifically inhibit PfGatp activity and block parasite membrane biogenesis and multiplication.

Acknowledgments—We are grateful to Jill Zimmermann, General Clinical Research Center, for excellent technical assistance. We are grateful to Daniel E. Goldberg and Ilya Y. Gluzman at Washington University School of Medicine and Justin D. Radolf and Stephen Wikle at the University of Connecticut Health Center for helpful suggestions. We thank Vanina Zaremba and Christopher R. McMaster at Dalhousie University, Canada for providing the CMY228 strain.

REFERENCES

- WHO (2000) *WHO Tech. Rep. Ser.* **892**, i-v, 1-74
- Holz, G. G. (1977) *Bull. WHO* **55**, 237-248
- Vial, H. J., and Ancelin, M. L. (1998) in *Malaria: Parasite Biology Pathogenesis and Protection* (Sherman, I. W., ed) pp. 159-175, American Society for Microbiology, Washington, D. C.
- Sherman, I. W. (1979) *Microbiol. Rev.* **43**, 453-495
- Vial, H. J., Ancelin, M. L., Philippot, J. R., and Thuet, M. J. (1990) *Blood Cells* **16**, 531-561
- Vial, H. J., Angelin, M. L., Elabbadi, N., Calas, M., Cordinas, G., and Giral, L. (1992) *Mem. Inst. Oswaldo Cruz* **87**, (Suppl. 3) 251-261
- Ancelin, M. L., and Vial, H. J. (1986) *FEBS Lett.* **202**, 217-223
- Ancelin, M. L., and Vial, H. J. (1986) *Biochim. Biophys. Acta* **875**, 52-58
- Mitamura, T., and Palacpac, N. M. (2003) *Microbes Infect.* **5**, 545-552

10. Hanada, K., Palacpac, N. M., Magistrado, P. A., Kurokawa, K., Rai, G., Sakata, D., Hara, T., Horii, T., Nishijima, M., and Mitamura, T. (2002) *J. Exp. Med.* **195**, 23–34
11. Prigge, S. T., He, X., Gerena, L., Waters, N. C., and Reynolds, K. A. (2003) *Biochemistry* **42**, 1160–1169
12. Gardner, M. J., Hall, N., Fung, E., White, O., Berriman, M., Hyman, R. W., Carlton, J. M., Pain, A., Nelson, K. E., Bowman, S., Paulsen, I. T., James, K., Eisen, J. A., Rutherford, K., Salzberg, S. L., Craig, A., Kyes, S., Chan, M. S., Nene, V., Shallom, S. J., Suh, B., Peterson, J., Angiuoli, S., Pertea, M., Allen, J., Selengut, J., Haft, D., Mather, M. W., Vaidya, A. B., Martin, D. M., Fairlamb, A. H., Fraunholz, M. J., Roos, D. S., Ralph, S. A., McFadden, G. I., Cummings, L. M., Subramanian, G. M., Mungall, C., Venter, J. C., Carucci, D. J., Hoffman, S. L., Newbold, C., Davis, R. W., Fraser, C. M., and Barrell, B. (2002) *Nature* **419**, 498–511
13. Waller, R. F., Keele, P. J., Donald, R. G., Striepen, B., Handman, E., Lang-Unnasch, N., Cowman, A. F., Besra, G. S., Roos, D. S., and McFadden, G. I. (1998) *Proc. Natl. Acad. Sci. U. S. A.* **95**, 12352–12357
14. Foth, B. J., Ralph, S. A., Tonkin, C. J., Struck, N. S., Fraunholz, M., Roos, D. S., Cowman, A. F., and McFadden, G. I. (2003) *Science* **299**, 705–708
15. Foth, B. J., and McFadden, G. I. (2003) *Int. Rev. Cytol.* **224**, 57–110
16. Wengelnik, K., Vidal, V., Ancelin, M. L., Cathiard, A. M., Morgat, J. L., Kocken, C. H., Calas, M., Herrera, S., Thomas, A. W., and Vial, H. J. (2002) *Science* **295**, 1311–1314
17. Bell, R. M., and Coleman, R. A. (1980) *Annu. Rev. Biochem.* **49**, 459–487
18. Lehner, R., and Kuksis, A. (1996) *Prog. Lipid Res.* **35**, 169–201
19. Dircks, L., and Sul, H. S. (1999) *Prog. Lipid Res.* **38**, 461–479
20. Christiansen, K. (1978) *Biochim. Biophys. Acta* **530**, 78–90
21. Coleman, R. A., Lewin, T. M., and Muoio, D. M. (2000) *Annu. Rev. Nutr.* **20**, 77–103
22. Kelley, M. J., and Carman, G. M. (1987) *J. Biol. Chem.* **262**, 14563–14570
23. Toke, D. A., Bennett, W. L., Dillon, D. A., Wu, W. I., Chen, X., Ostrander, D. B., Oshiro, J., Cremesti, A., Voelker, D. R., Fischl, A. S., and Carman, G. M. (1998) *J. Biol. Chem.* **273**, 3278–3284
24. Toke, D. A., Bennett, W. L., Oshiro, J., Wu, W. I., Voelker, D. R., and Carman, G. M. (1998) *J. Biol. Chem.* **273**, 14331–14338
25. Sorger, D., and Daum, G. (2003) *Appl. Microbiol. Biotechnol.* **61**, 289–299
26. Sorger, D., and Daum, G. (2002) *J. Bacteriol.* **184**, 519–524
27. Zaremberg, V., and McMaster, C. R. (2002) *J. Biol. Chem.* **277**, 39035–39044
28. Zheng, Z., and Zou, J. (2001) *J. Biol. Chem.* **276**, 41710–41716
29. Trager, W., and Jensen, J. B. (1976) *Science* **193**, 673–675
30. Athenstaedt, K., Weys, S., Paltauf, F., and Daum, G. (1999) *J. Bacteriol.* **181**, 1458–1463
31. Rager, N., Mamoun, C. B., Carter, N. S., Goldberg, D. E., and Ullman, B. (2001) *J. Biol. Chem.* **276**, 41095–41099
32. Kumar, N., Koski, G., Harada, M., Aikawa, M., and Zheng, H. (1991) *Mol. Biochem. Parasitol.* **48**, 47–58
33. Tillman, T. S., and Bell, R. M. (1986) *J. Biol. Chem.* **261**, 9144–9149
34. Lewin, T. M., Wang, P., and Coleman, R. A. (1999) *Biochemistry* **38**, 5764–5771
35. Krogh, A., Larsson, B., von Heijne, G., and Sonnhammer, E. L. (2001) *J. Mol. Biol.* **305**, 567–580
36. Mamoun, C. B., and Goldberg, D. E. (2001) *Mol. Microbiol.* **39**, 973–981
37. Carter, N. S., Ben Mamoun, C., Liu, W., Silva, E. O., Landfear, S. M., Goldberg, D. E., and Ullman, B. (2000) *J. Biol. Chem.* **275**, 10683–10691
38. Athenstaedt, K., and Daum, G. (1999) *Eur. J. Biochem.* **266**, 1–16
39. Elmendorf, H. G., and Haldar, K. (1993) *EMBO J.* **12**, 4763–4773
40. Miller, C. A., III, Martinat, M. A., and Hyman, L. E. (1998) *Nucleic Acids Res.* **26**, 3577–3583
41. Bozdech, Z., Zhu, J., Joachimiak, M. P., Cohen, F. E., Pulliam, B., and DeRisi, J. L. (2003) *Genome Biol.* **4**, R9
42. Le Roch, K. G., Zhou, Y., Blair, P. L., Grainger, M., Moch, J. K., Haynes, J. D., De La Vega, P., Holder, A. A., Batalov, S., Carucci, D. J., and Winzeler, E. A. (2003) *Science* **301**, 1503–1508
43. Mitamura, T., Hanada, K., Ko-Mitamura, E. P., Nishijima, M., and Horii, T. (2000) *Parasitol. Int.* **49**, 219–229

APPENDIX 6

Reexamining the Role of Choline Transporter-Like (Ctlp) Proteins in Choline Transport

Rachel Zufferey,^{1,2} Teresa C. Santiago,^{1,3} Valerie Brachet,^{1,3}
and Choukri Ben Mamoun^{1,3,4}

(Accepted August 25, 2003)

In *Saccharomyces cerevisiae*, choline enters the cell via a single high-affinity transporter, Hnm1p. *hnm1Δ* cells lacking *HNM1* gene are viable. However, they are unable to transport choline suggesting that no additional active choline transporters are present in this organism. A complementation study of a choline auxotrophic mutant, *ctr1-ise* (*hnm1-ise*), using a cDNA library from *Torpedo marmorata* electric lobe identified a membrane protein named *Torpedo marmorata* choline transporter-like, tCtl1p. tCtl1p was proposed to mediate a high-affinity choline transport (O'Regan et al., 1999, Proc. Natl. Acad. Sci.). Homologs of tCtl1p have been identified in other organisms, including yeast (Pns1p, YOR161c) and are postulated to function as choline transporters. Here we provide several lines of evidence indicating that Ctlp proteins are not involved in choline transport. Loss of *PNS1* has no effect on choline transport and overexpression of either *PNS1* or *tCTL1* does not restore choline uptake activity of choline transport-defective mutants. The data presented here call into question the role of proteins of the CTL family in choline transport and suggest that the mechanism by which *tCTL1* complements *hnm1-ise* mutant is independent of its ability to transport choline.

KEY WORDS: Choline; transport; yeast; Torpedo; CTL.

INTRODUCTION

In *Saccharomyces cerevisiae*, synthesis of the major phospholipids, phosphatidylcholine, phosphatidylethanolamine and phosphatidylinositol involves distinct but co-regulated biosynthetic pathways: (i) the CDP-choline pathway, which uses choline as a precursor for the synthesis of phosphatidylcholine; (ii) the CDP-ethanolamine pathway which uses ethanolamine as a precursor for the

synthesis of phosphatidylethanolamine, (iii) the CDP-DAG-serine pathway which initiates from serine and CDP-DAG to form phosphatidylserine, which is then decarboxylated to form phosphatidylethanolamine, and (iv) the CDP-DAG-inositol pathway which synthesizes phosphatidylinositol from CDP-DAG and inositol. The CDP-DAG-serine and the CDP-ethanolamine pathways converge into phosphatidylethanolamine, which is subsequently methylated in a three-step AdoMet-dependent methylation to form phosphatidylcholine (1). This reaction is catalyzed by two methyl transferases encoded by *CHO2* (*PEM1*) and *OPI3* (*PEM2*) genes (2–5). The CDP-DAG-serine pathway is the major pathway leading to the formation of phosphatidylcholine in *S. cerevisiae* (1). Therefore, in this organism, neither choline nor the enzymes of the CDP-choline pathway are essential for survival. The CDP-choline pathway becomes essential when the genes encoding the enzymes in the CDP-DAG-serine pathway are altered or deleted.

¹ Center for Microbial Pathogenesis, University of Connecticut Health Center, 263 Farmington Avenue, Farmington, Connecticut.

² Department of Pathology, University of Connecticut Health Center, 263 Farmington Avenue, Farmington, Connecticut.

³ Department of Genetics and Developmental Biology, University of Connecticut Health Center, 263 Farmington Avenue, Farmington, Connecticut.

⁴ Address reprint requests to: Tel: 860-679-3544; Fax: 860-679-8130; E-mail: choukri@up.schhc.edu

The *HNM1* gene (originally called *CTR1*) of *S. cerevisiae* (for hyper-resistant to nitrogen mustard) encodes a high affinity (K_m 0.5–1 μM) choline transporter protein of 563 amino acid residues with twelve predicted transmembrane domains (6). Hnm1p is also the transporter of the bifunctional alkylating agent nitrogen mustard (7,8). Deletion of *HNM1* leads to a nitrogen mustard hyper-resistant phenotype, while its overexpression causes increased sensitivity (7,8). *HNM1* was first isolated in a complementation assay of a double mutant *hnm1-ise*¹ by its ability to restore growth in the presence of high concentrations of inositol and choline in the medium (6,9–11). The single *ise* mutant is a conditional choline auxotroph whose growth is inhibited by high concentrations of inositol. The growth defect is suppressed by the addition of choline. The inositol sensitivity of the double mutant *hnm1-ise* is not suppressed by the addition of choline because of a mutation *hnm1* in the *HNM1* gene (11). The molecular identity of *hnm1* mutation in the *hnm1-ise* mutant and its effect on choline uptake is not known. Transformation of *hnm1-ise* mutant with a *Torpedo* electric lobe cDNA library in a yeast shuttle vector allowed the identification of a gene named *tCTL1* (12). This gene encodes a protein of 646 amino acids predicted to possess 10 transmembrane domains.

Choline uptake studies in *hnm1-ise* mutant showed that tCtl1p mediates choline uptake with an apparent K_m of 1 μM (12). tCtl1p-mediated choline transport was inhibited by hemicholinium (12). These studies concluded that tCtl1p is a choline transporter (12). Antibodies raised against tCtl1p indicated that it exists as a 60 kDa protein localized to the plasma membrane and prominent throughout the central nervous system (CNS) and along the electric nerves (13). Three homologs of tCtl1p are found in human cells, hCtl1p/CDw92, hCtl2p and hCtl4p (12). hCtl1p and CDw92 are 99.1% identical (14). CDw92 was shown to be constitutively expressed in various cells of the hematopoietic system and has been postulated to be involved in regulation of immune functions (14). Other ortholog and homolog genes of *tCTL1* are also found in mouse, rat, *Caenorhabditis elegans*, *Plasmodium falciparum* and *Leishmania major* genomes but their function has not yet been determined. Transformation of *hnm1-ise* with a yeast multicopy library resulted in the identification of a second gene *SCT1* (also referred to as *GAT2*) (15). However, further analysis of *GAT2* revealed that it encodes a glycerol-3-phosphate acyltransferase which catalyzes

the first acylation step of glycerol-3-phosphate into 1-acylglycerol-3-phosphate (16,17). As no further analyses of tCtl1p in better transport systems, such as *Xenopus laevis* oocytes or *S. cerevisiae* *hnm1Δ* strain lacking *HNM1* gene, are available, and the finding that Gat2p, which does not transport choline can suppress *hnm1-ise* mutant defect, prompted us to thoroughly examine the role of Ctlp proteins in choline uptake.

Here we report the identification of a homolog of tCtl1p in *S. cerevisiae* that we named Pns1p. Disruption of the *PNS1* gene has no effect on choline transport and its overexpression as well as that of *tCTL1* in *hnm1Δ* strain does not restore choline uptake. We mapped the mutation in *HNM1* gene in *hnm1-ise* mutant and found that it results in a single amino acid substitution G-461-E (Hnm1p^{G-461-E}) that severely decreases its transport activity without changing its affinity for the substrate. Overexpression of *PNS1* or *tCTL1* in *hnm1Δ-HNM1^{G-461-E}* strain has no effect on the basal transport activity of Hnm1p^{G-461-E}.

EXPERIMENTAL PROCEDURE

Strains and Growth Conditions. *S. cerevisiae* strains (Table I) were grown on YPD (1% yeast extract, 2% dextrose, and 2% peptone) or synthetic complete medium (SD: 1.7% yeast nitrogen base, 5% ammonium sulfate and 2% dextrose) supplemented as required to maintain cell growth.

Plasmid Construction. For construction of the plasmids pVT102-U-*HNM1* and pVT102-U-*HNM1^{G-461-E}*, pVT102-L-*HNM1* and pVT102-L-*HNM1^{G-461-E}*, *HNM1* and *HNM1^{G-461-E}* were PCR amplified from wild-type and *hnm1-ise* genomic DNAs, respectively, using the oligonucleotides *X-HNM1* 5'-CCGCTCGAGATGAGTATTGGAAATGATAATGC-3' and *P-HNM1* 5'-CCGCTCGAGCTGCAGTCACCT-CTTTCCCCACGGTAC-3'. The resulting PCR products were digested with *Xba*I and *Pst*I restriction enzymes and cloned into the *Xba*I and *Pst*I sites of pVT102-U and pVT102-L (18). For construction of the plasmid pVT102-U-*PNS1*, *PNS1* from wild-type strain was PCR amplified from genomic DNA using the oligonucleotides *B-PNS1* 5'-CGCGGATCCAT-GCCATTGAATGAAAAATACGAGAGG-3' and *X-PNS1* 5'-CGCCG-CTCGAGTCTCTCACACATTCTGGTGACTCA-3'. The resulting PCR product was digested and inserted into *Bam*HI and *Xba*I sites of pVT102-U. The contiguity of the vectors was confirmed by DNA sequencing.

Inositol Efflux Assay. Wild-type (ScCHO2) and *pns1Δ* (ScCHO18) strains were cultured in 5 ml of complete synthetic medium (SD) supplemented as required to maintain cell growth at 30°C. The overnight cultures were diluted, allowed to grow to exponential phase at 30°C and re-diluted in 1 ml to achieve an OD_{600} of 0.1. 2 μL of [³H]-inositol (1 $\mu\text{Ci}/\mu\text{l}$; 20 Ci/mmol, ICN) were added and the cultures were incubated overnight at 30°C. Triplicate cultures were prepared for each strain. Cells were washed in SD and resuspended in 6 ml SD containing 10 mM inositol. Samples (1 ml) were collected 0, 2, 4, 6, and 8 hours after washing. At each time point cells were concentrated by centrifugation for 10 min at 12,000 g and the supernatant was collected (extracellular fraction). The cell pellet was resuspended in 0.5 ml of 5% trichloroacetic acid and incubated on ice for 20 min. After centrifugation for 10 min at 12,000 g, the supernatant was collected in a separate tube (water-soluble fraction) and the cell pellet was resuspended in 0.5 ml of 1 M Tris-HCl pH 8. After

¹ *HNM1*, was previously referred to as *CTR1*. To avoid any confusions with the copper transporter gene (*CTR1*) we have used *HNM1* throughout the text to refer to the gene *HNM1* as well as to the mutant *hnm1-ise* (previously called *ctr1-ise*).

Table I. *S. cerevisiae* Strains Analyzed in This Study

Strain	Genotype	Source
BY4741 (ScCHO1)	<i>Mata his3Δ1 leu2Δ0 met15Δ0 ura3Δ0</i>	Research Genetics
ScCHO2	<i>Mata/Mata his3Δ1/his3Δ1 leu2Δ0/leu2Δ0 met15Δ0/MET15 LYS2/lys2Δ0 ura3Δ0/ura3Δ0</i>	This study
ScCHO16	<i>Mata his3Δ1 leu2Δ0 met15Δ0 ura3Δ0 pns1::KANr</i>	Mark Johnston, Wash. U.
ScCHO18	<i>Mata/Mata his3Δ1/his3Δ1 leu2Δ0/leu2Δ0 met15Δ0/MET15 LYS2/lys2Δ0 ura3Δ0/ura3Δ0 pns1::KANr/pns1::KANr</i>	This study
ScCHO28	<i>Mata his3Δ1 leu2Δ0 met15Δ0 ura3Δ0 hnm1::KANr</i>	Research Genetics
ScCHO34	<i>Mata his3Δ1 leu2Δ0 met15Δ0 ura3Δ0 hnm1::KANr, pVT102-U-HNM1</i>	This study
ScCHO38	<i>Mata his3Δ1 leu2Δ0 met15Δ0 ura3Δ0 hnm1::KANr, pVT102-U-HNM1^{G-416-E}</i>	This study
ScCHO39	<i>Mata his3Δ1 leu2Δ0 met15Δ0 ura3Δ0 hnm1::KANr, pFL61</i>	This study
ScCHO40	<i>Mata his3Δ1 leu2Δ0 met15Δ0 ura3Δ0 hnm1::KANr, pFL61-tCTL1</i>	This study
ScCHO41	<i>Mata his3Δ1 leu2Δ0 met15Δ0 ura3Δ0 hnm1::KANr, pVT102-U</i>	This study
ScCHO42	<i>Mata his3Δ1 leu2Δ0 met15Δ0 ura3Δ0 hnm1::KANr, pVT102-U-PNS1</i>	This study
ScCHO43	<i>Mata his3Δ1 leu2Δ0 met15Δ0 ura3Δ0 hnm1::KANr, pVT102-L-HNM1^{G-416-E}, pFL61</i>	This study
ScCHO44	<i>Mata his3Δ1 leu2Δ0 met15Δ0 ura3Δ0 hnm1::KANr, pVT102-L-HNM1^{G-416-E}, pFL61-tCTL1</i>	This study
ScCHO54	<i>Mata his3Δ1 leu2Δ0 met15Δ0 ura3Δ0, pVT102-U</i>	This study
ScCHO63	<i>Mata his3Δ1 leu2Δ0 met15Δ0 ura3Δ0 pns1::KANr hnm1::URA3</i>	This study
hnm1-ise	<i>ctrl ise ura3Δ</i>	O'Regan et al., (12)

centrifugation, the supernatant was added to the tube containing the water-soluble fraction. Finally, the cell pellet was resuspended in 1 ml of 1 M Tris-HCl pH 8 (membrane fraction). A 150 μ l aliquot of each fraction was added to 3 ml of scintillation fluid and radioactivity was measured using a scintillation counter.

Choline Uptake. Yeast strains were grown in SD supplemented as required to maintain cell growth to an optical density of 0.55–0.65/ml at 600 nm. Cells were harvested by centrifugation at 3,200 \times g for 10 min at 4°C, washed twice in ice-cold water and resuspended in nitrogen-free medium (SD without ammonium sulfate). Each reaction was performed in a 1 ml final volume in the presence of 12 nM of [³H]-methylcholine (82 Ci/mmol, Amersham Pharmacia Biotech, Inc., USA). After 3.5 min incubation at 30°C with shaking, transport was immediately stopped by filtration through Whatman GF/C glass microfiber paper. The filters were washed three times with 5 ml ice-cold PBS, air-dried, and analyzed in a scintillation counter.

RESULTS

tCtl1p and Its Yeast Homolog Are Not Choline Transporters

The *Torpedo* electric lobe protein, tCtl1p, has been proposed to function as a high-affinity choline transporter in the yeast *hnm1-ise* mutant context (12). *S. cerevisiae* has only one choline transporter gene, *HNMT*, disruption of which results in a complete loss of choline transport activity. This makes *hnm1Δ* strain, lacking *HNMT*, a better genetic background to further characterize the role of tCtl1p and its homologs in choline transport. *hnm1Δ* strain was transformed with the empty vector pFL61 or pFL61-tCTL1 carrying *tCTL1* gene and the transformants were assessed for choline uptake using radiolabeled choline. No difference in choline uptake was detected between *hnm1Δ*, *hnm1Δ* + pFL61, and *hnm1Δ* + pFL61-tCTL1

strains (Fig. 1A). Choline transport assays were also performed at different pH and no differences could be detected (data not shown). Together, these data suggest

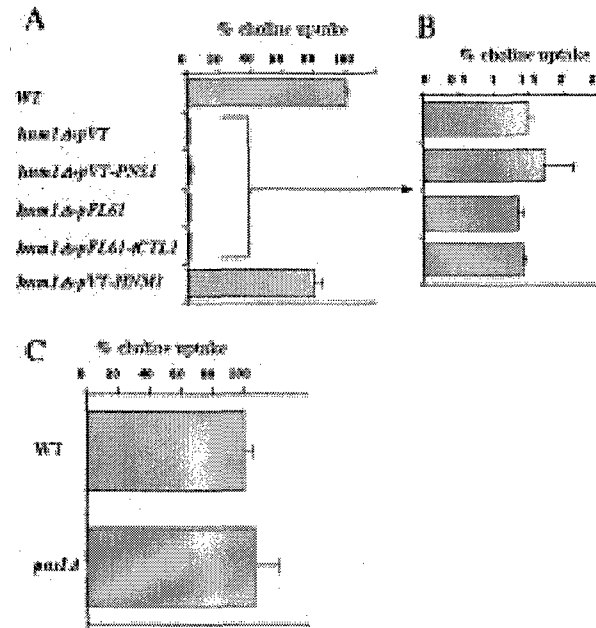


Fig. 1. Choline uptake assays. Transport activities were measured as described in material and methods. Assays were performed in duplicate. (A and B) Transport of [³H]-choline in wild-type (WT: ScCHO1), *hnm1Δ* + pVT strain (ScCHO41) harboring the empty vector pVT102-U, *hnm1Δ* + pVT-PNS1 strain (ScCHO42) harboring pVT102-U-PNS1 plasmid, *hnm1Δ* + pFL61 strain (ScCHO39) harboring the empty vector pFL61, *hnm1Δ* + pFL61-tCTL1 strain (ScCHO40) harboring pFL61-tCTL1 plasmid and *hnm1Δ* + pVT-HNM1 (ScCHO34) harboring the plasmid pVT102-U-HNM1. (C) Transport of [³H]-choline in wild-type (WT: ScCHO2) and *pns1Δ* (ScCHO18) strains.

that tCtl1p is not a choline transporter (Fig. 1A). We further found that *S. cerevisiae* possesses a gene that we named *PNS1* (pH Nine Sensitive), which is highly homologous to *tCTL1*. *PNS1* encodes a polypeptide of 539 amino acids that shares ~30% identity and ~50% similarity with *T. marmorata*, tCtl1p, *Rattus norvegicus*, rCtl1p and human hCtl1p and hCtl2p (Fig. 2A). Pns1p does not share any sequence homology with Hnm1p or other higher eukaryotic choline or organic cation transporters. The derived amino acid sequence of Pns1p was analyzed to determine the hydrophobic character of the protein, using the TMHMM program (19). Pns1p shares similar predicted topology with other Ctl proteins with 10 hydrophobic membrane-spanning domains (Fig. 2B) and a large extracellular loop between the first and second transmembrane domains.

To assess whether Pns1p could be involved in choline transport, its open reading frame was cloned under the regulatory control of the alcohol dehydrogenase (*ADH1*) gene promoter in a 2 μ -based plasmid (pVT102-U) for overexpression in *hnm1* Δ strain. Addition of radiolabeled choline to the transport medium

resulted in a high transport activity in the wild-type cells and no detectable levels in the *hnm1* Δ cells alone or harboring either pVT102-U empty vector or pVT102-U-PNS1 carrying the *PNS1* gene, suggesting that Pns1p is not a choline transporter (Fig. 1A and B). We have also compared choline uptake between wild-type and *pns1* Δ strains and no differences were detected (Fig. 1C). Furthermore, the choline transport defect of *hnm1* Δ mutant was similar to that of a double mutant *hnm1* Δ *pns1* Δ (Fig. 3A). Taken together, these biochemical data suggest that neither Pns1p nor tCtl1p proteins are choline transporters.

hnm1-ise Mutant Harbors a G-461-E Substitution in Hnm1p That Affects its V_{max} but not its K_m for Choline

An alternative interpretation of the *tCTL1* complementation of the *hnm1*-ise mutant and its two-fold-mediated increase of choline uptake is that tCtl1p acts to stabilize the Hnm1p mutated protein rather than transport choline. To further examine this hypothesis, we have cloned *HNMI*

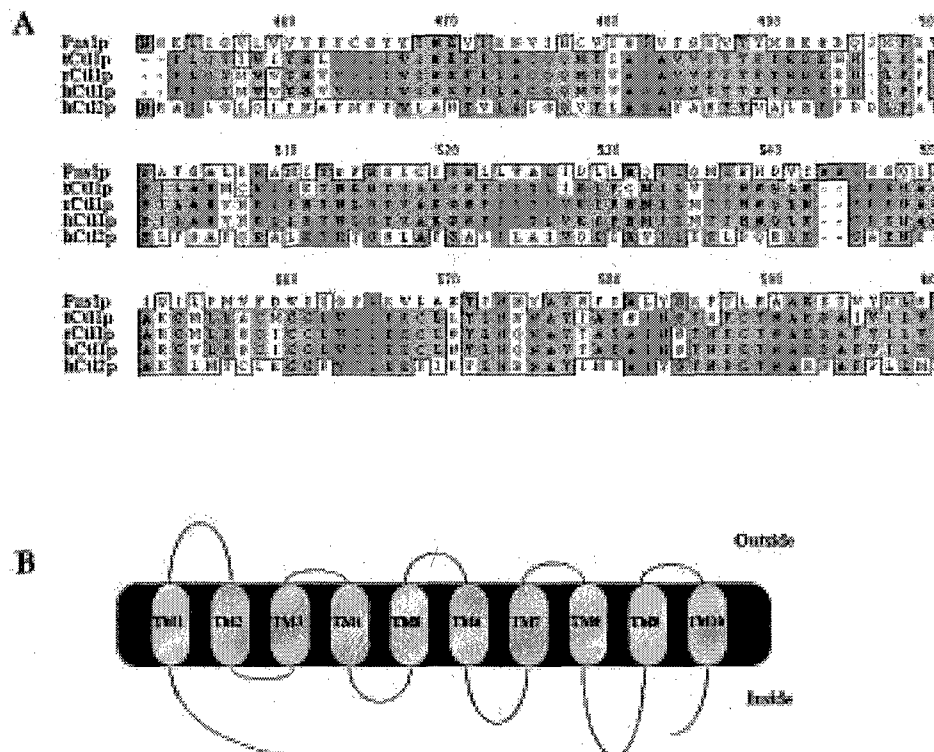


Fig. 2. (A) Pns1p sequence alignment. Alignment of the C-terminal regions of Pns1p (GenBank accession number Z35773) and its homologs from *T. marmorata* (tCtl1p: GenBank Accession Number CAB75556), *R. norvegicus* (rCtl1p: GenBank Accession Number AAB71605), human (hCtl1p and hCtl2p: GenBank Accession Numbers CAB75541 and NP_065161, respectively). Identical (gray) residues and similar (light) residues are outlined. **(B)** Pns1p predicted topology. Pns1p topology was predicted by standard hydropathy algorithms.

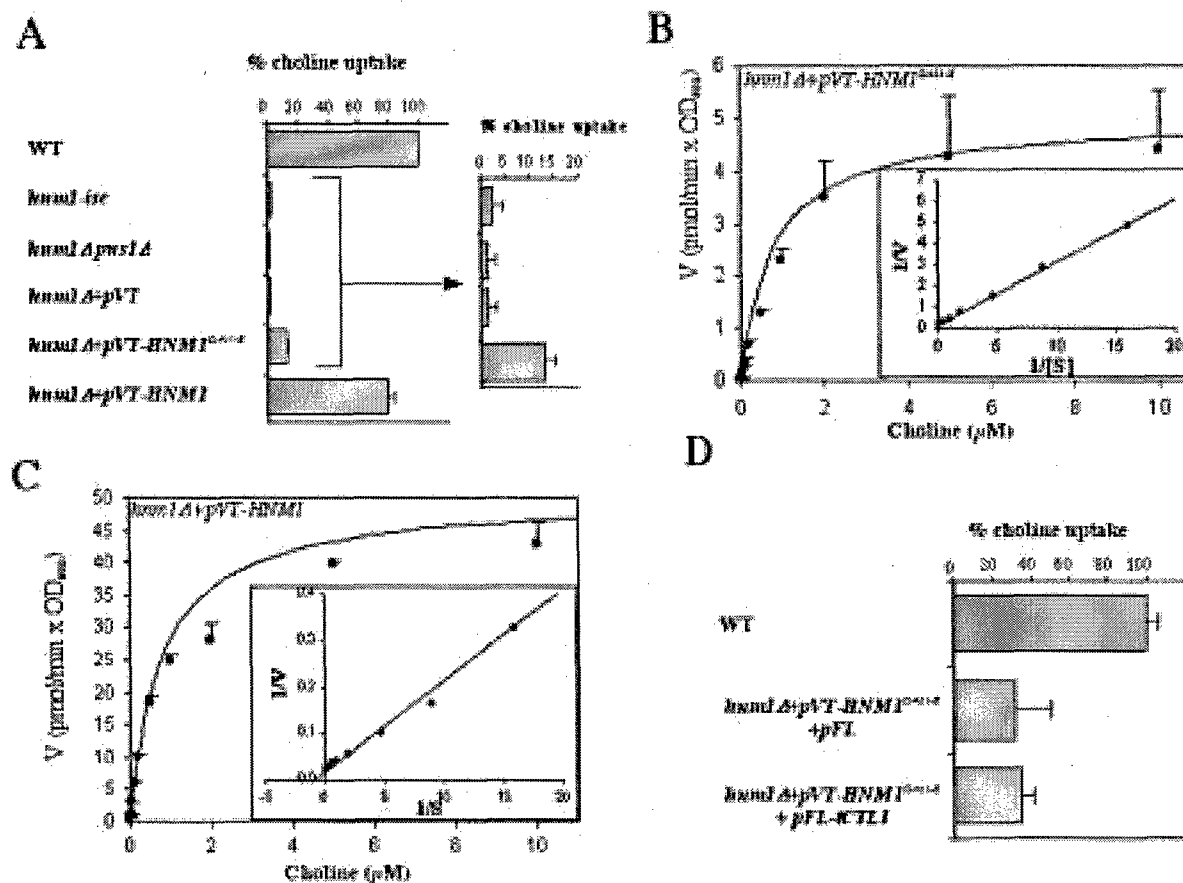


Fig. 3. Transport activity of *Hnm1p*^{G-461-E} mutant. **A**, Comparison of choline uptake between wild type (ScCHO1), *hnm1*-*ise*, *hnm1* Δ -*pns1* Δ double mutant (ScCHO63), *hnm1* Δ + *pVT* strain (ScCHO41) harboring the empty vector *pVT102-U*, *hnm1* Δ + *pVT-HNM1*^{G-461-E} strain (ScCHO38) harboring the plasmid *pVT102-U-HNM1*^{G-461-E} and *hnm1* Δ + *pVT-HNM1* strain (ScCHO34) harboring the plasmid *pVT102-U-HNM1*. **B** and **C**, Transport kinetics in *hnm1* Δ + *pVT-HNM1*^{G-461-E} strain (ScCHO38) (**B**) and *hnm1* Δ + *pVT-HNM1* (ScCHO34) (**C**). The saturation curve versus substrate concentration is fitted to the Michaelis-Menten equation. Double reciprocal plot is represented in the inset. Lineweaver-Burk plot representation allowed determination of a K_m of $\sim 1 \mu\text{M}$. **D**, Comparison of choline uptake between wild-type (ScCHO1), *hnm1* Δ + *pVT-HNM1*^{G-461-E} + *pFL* strain (ScCHO43) harboring the plasmids *pVT102-L-HNM1*^{G-461-E} and *pFL61*, and *hnm1* Δ + *pVT-HNM1*^{G-461-E} + *pFL-tCTL1* strain (ScCHO44) harboring the plasmids *pVT102-L-HNM1*^{G-461-E} and *pFL61-tCTL1*.

allele from *hnm1*-*ise* mutant, determined its sequence, characterized its transport kinetic properties and assessed the effect of tCtl1p as well as Pns1p on these properties. *HNM1* from the *hnm1*-*ise* mutant differed from the wild-type sequence by a single A > G transition at position 1382 of the *HNM1* open reading frame. Thus, amino acid 461 is a glutamic acid in the *hnm1*-*ise* mutant and a glycine in the wild-type strain. The glycine residue is also highly conserved in other Hnm1p homologs as well as other members of the amino acid permease family to which Hnm1p belongs. Comparison of choline transport activities of *hnm1* Δ and *hnm1*-*ise* mutants showed that the latter mutant is severely affected in choline uptake with only 2-fold increase in choline transport compared to *hnm1* Δ (Fig. 3A). *HNM1*^{G-461-E} allele was cloned into *pVT102-U* vector

and transformed into *hnm1* Δ for overexpression. The resulting strain *hnm1* Δ + *pVT-HNM1*^{G-461-E} was then examined for choline transport activity. Transport of choline was 10-fold higher in *hnm1* Δ + *pVT-HNM1*^{G-461-E} ($V_{max} \sim 9.75 \text{ pmol/min} \times \text{OD}_{600}$) (Fig. 3A and B) than in *hnm1* Δ strain, but this activity was only $\sim 20\%$ of that of the wild-type Hnm1p ($V_{max} \sim 52 \text{ pmol/min} \times \text{OD}_{600}$) (Fig. 3A-C). The apparent affinity of choline transport mediated by *Hnm1p*^{G-461-E} ($K_m = 0.9 \pm 0.25 \mu\text{M}$) (Fig. 3B) is similar to that of the wild-type Hnm1p ($K_m = 0.68 \pm 0.13 \mu\text{M}$) (Fig. 3C) as well as that reported for tCtl1p in *hnm1*-*ise* context, suggesting that G-461-E substitution results in a decrease of choline transport capacity without changing the affinity of the transporter for its substrate, and that the reported apparent affinity of tCtl1p is simply that of *HNM1*^{G-461-E} allele. To assess whether tCtl1p

or Pns1p could stabilize Hnm1p^{G-461-E}, *tCTL1* and *PNS1* genes were individually overexpressed in *hnm1Δ* + *pVT-HNMI*^{G-461-E} strain and the choline transport activity of Hnm1p^{G-461-E} was measured. As shown in Figure 3D, expression of tCtl1p or Pns1p (data not shown) had no effect on Hnm1p^{G-461-E} choline transport activity.

Pns1p and tCtl1p Are Not Involved in Inositol Efflux

Another alternative explanation for the complementation of *hnm1-ise* mutant by *tCTL1* is that overexpression of this gene results in lifting the inhibitory effect of inositol on the phosphatidylethanolamine methyltransferases. Phosphatidylcholine biosynthesis would thus generate from both the CDP-choline pathway and the three-step AdoMet-dependent methylation of phosphatidylethanolamine. One hypothesis is that Ctlp proteins are involved in inositol efflux. To assess the validity of this hypothesis, wild-type and *pns1Δ* strains were uniformly labeled with radiolabeled inositol, washed and resuspended in a medium containing excess of cold inositol. Released radiolabeled inositol was measured in the extracellular medium, in the cellular soluble and membrane fractions. No differences in inositol efflux were observed between these strains (Fig. 4), suggesting that Pns1p is not involved in inositol efflux.

DISCUSSION

This work was motivated by the observation that Pns1p is a homolog of the *Torpedo* electric lobe tCtl1p, a defining member of a large family of membrane proteins found in lower and higher eukaryotes that are pos-

tulated to function as choline transporters (12). Evidence for this function emerged from a complementation study of a yeast *hnm1-ise* mutant affected in choline uptake (harboring a mutation in *HNMI* gene) and highly sensitive to inositol, which makes its survival dependent on an active choline uptake when inositol is available (12). Choline transport assays in *hnm1-ise* *tCTL1* strain indicated that tCtl1p has a similar affinity for choline as the endogenous choline transporter Hnm1p (12). Our finding that yeast possesses a homolog of tCtl1p, Pns1p, prompted us to question the validity of the transport hypothesis. Our studies show that disruption of *PNS1* gene in wild-type or *hnm1Δ* strains has no effect on choline uptake. Furthermore overexpression of *PNS1* or *tCTL1* in *hnm1Δ*, lacking the only yeast choline transporter, did not restore choline uptake. Together, these data indicate that Pns1p, tCtl1p and probably all members of this family of membrane proteins are not choline transporters.

Because of this important finding, we have proposed alternative interpretations to the previously reported results of complementation of the yeast *hnm1-ise* mutant by *tCTL1* and the transport activity associated with its expression. The K_m value reported for tCtl1p and measured in *hnm1-ise* mutant background was similar to that of Hnm1p, suggesting that it might be that of the endogenous mutated Hnm1p. Therefore, one possible interpretation is that overexpression of tCtl1p caused stabilization of the mutated Hnm1p in *hnm1-ise* mutant, thus resulting in an increase in choline uptake. To assess the validity of this analysis we cloned the mutated *HNMI* allele from the *hnm1-ise* mutant and determined its sequence. We found that *HNMI* from the *hnm1-ise* mutant differed from the wild-type sequence by a single A > G transition at position 1382 of the *HNMI* open reading frame. Thus, amino acid 461 is a glutamic acid in the *hnm1-ise* mutant and a glycine in the wild-type strain. Comparison of choline transport activities of $\Delta hnm1$ and *hnm1-ise* mutants showed that *hnm1-ise* mutant is severely affected in choline uptake with only 2-fold increase in choline transport compared to *hnm1Δ*. Overexpression of *HNMI*^{G-461-E} allele in *hnm1Δ* resulted in 10-fold increase of choline uptake compared to *hnm1Δ*, but this activity was only ~20% of the wild-type. Expression of Pns1p or tCtl1p in *hnm1Δ* + *pVT-HNMI*^{G-461-E} had no effect on Hnm1p^{G-461-E} activity, suggesting that Pns1p and tCtl1p proteins do not act to stabilize the Hnm1p^{G-461-E} mutant.

Another alternative explanation for the complementation of the *hnm1-ise* mutant by *tCTL1* is that overexpression of this gene results in reversion of the inhibitory effect of inositol on the phosphatidylethanol-

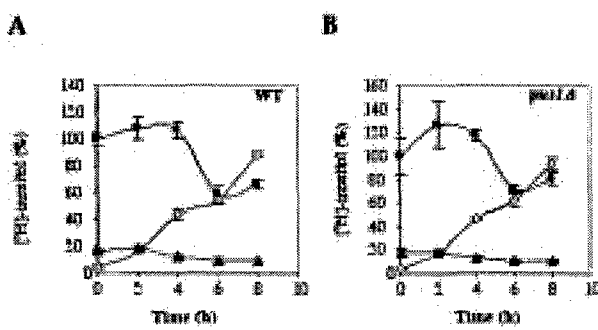


Fig. 4. Inositol efflux assays. Inositol efflux was measured in wild-type (ScCHO2) (A) and *pns1Δ* (ScCHO18) (B) strains as described in Experimental Procedure Section. Membrane fraction (triangles), soluble cytoplasmic fraction (squares), and extracellular fraction (open diamonds).

amine methyltransferases. Phosphatidylcholine biosynthesis would thus result from both the CDP-choline pathway and from the three-step AdoMet-dependent methylation of phosphatidylethanolamine. In such a scenario tCtl1p and Pns1p would be involved in inositol efflux. We compared wild-type and *pns1Δ* for inositol efflux and no differences could be detected, suggesting that these proteins are not involved in inositol efflux.

CONCLUSION

The reported data provide compelling evidence that Ctlp proteins are not involved in choline transport or inositol efflux. These data will set the stage for future studies to investigate the importance and cellular function of this family of membrane proteins.

ACKNOWLEDGMENT

This work was supported by the University of Connecticut Health Center Research Fund, The Robert Leet and Clara Guthrie Patterson Trust, and the U.S. Army Medical Research and Material Command. We thank Dr. Stephen K. Wikle for helpful comments during the course of this work. We thank Dr. O'Regan for the pFL61 and pFL61-tCTL1 plasmids and the *hnml-ise ura3* strain. We thank Dr. David Y. Thomas, National Research Council of Canada for the pVT102 vectors and Dr. Mark Johnston, Washington University School of Medicine for the ScCHO16 strain.

REFERENCES

- Carman, G. M. and Henry, S. A. 1999. Phospholipid biosynthesis in the yeast *Saccharomyces cerevisiae* and interrelationship with other metabolic processes. *Prog. Lipid Res.* 38:361–399.
- Kodaki, T. and Yamashita, S. 1987. Yeast phosphatidylethanolamine methylation pathway: Cloning and characterization of two distinct methyltransferase genes. *J. Biol. Chem.* 262:15428–15435.
- Kodaki, T. and Yamashita, S. 1989. Characterization of the methyltransferases in the yeast phosphatidylethanolamine methylation pathway by selective gene disruption. *Eur. J. Biochem.* 185: 243–251.
- Summers, E. F., Leffs, V. A., McGraw, P., and Henry, S. A. 1988. *Saccharomyces cerevisiae* cho2 mutants are deficient in phospholipid methylation and cross-pathway regulation of inositol synthesis. *Genetics* 120:909–922.
- McGraw, P. and Henry, S. A. 1989. Mutations in the *Saccharomyces cerevisiae* op13 gene: Effects on phospholipid methylation, growth and cross-pathway regulation of inositol synthesis. *Genetics* 122:317–330.
- Nikawa, J., Hosaka, K., Tsukagoshi, Y., and Yamashita, S. 1990. Primary structure of the yeast choline transport gene and regulation of its expression. *J. Biol. Chem.* 265:15996–16003.
- Li, Z. and Brendel, M. 1994. Sensitivity to nitrogen mustard in *Saccharomyces cerevisiae* is independently determined by regulated choline permease and DNA repair. *Mutat. Res.* 315:139–145.
- Li, Z. Y., Haase, E., and Brendel, M. Hyper-resistance to nitrogen mustard in *Saccharomyces cerevisiae* is caused by defective choline transport. *Curr. Genet.* 19:423–427.
- Nikawa, J. and Yamashita, S. 1983. 2-Hydroxyethylhydrazine as a potent inhibitor of phospholipid methylation in yeast. *Biochim. Biophys. Acta* 751:201–209.
- Nikawa, J., Tsukagoshi, Y., and Yamashita, S. 1986. Cloning of a gene encoding choline transport in *Saccharomyces cerevisiae*. *J. Bacteriol.* 166:328–330.
- Hosaka, K. and Yamashita, S. 1980. Choline transport in *Saccharomyces cerevisiae*. *J. Bacteriol.* 143:176–181.
- O'Regan, S., Traffort, E., Ruat, M., Cha, N., Compaore, D., and Meunier, F. M. 2000. An electric lobe suppressor for a yeast choline transport mutation belongs to a new family of transporter-like proteins. *Proc. Natl. Acad. Sci. USA* 97:1835–1840.
- Meunier, F. M. and O'Regan, S. 2002. Expression of CTL1 in myelinating structures of *Torpedo marmorata*. *Neuroreport* 13:1617–1620.
- Wille, S., Szekeres, A., Majdic, O., Prager, E., Staffler, G., Stockl, J., Kunthalert, D., Prieschl, E. E., Baumruker, T., Burtscher, H., Zlabinger, G. J., Knapp, W., and Stockinger, H. 2001. Characterization of CDw92 as a member of the choline transporter-like protein family regulated specifically on dendritic cells. *J. Immunol.* 167:5795–5804.
- Matsushita, M. and Nikawa, J. 1995. Isolation and characterization of a SCT1 gene which can suppress a choline-transport mutant of *Saccharomyces cerevisiae*. *J. Biochem. (Tokyo)* 117:447–451.
- Zheng, Z. and Zou, J. 2001. The initial step of the glycerolipid pathway: Identification of glycerol 3-phosphate/dihydroxyacetone phosphate dual substrate acyltransferases in *Saccharomyces cerevisiae*. *J. Biol. Chem.* 276:41710–41716.
- Zaremberg, V. and McMaster, C. R. 2002. Differential partitioning of lipids metabolized by separate yeast glycerol-3-phosphate acyltransferases reveals that phospholipase D generation of phosphatidic acid mediates sensitivity to choline-containing lysolipids and drugs. *J. Biol. Chem.* 277:39035–39044.
- Vernet, T., Dignard, D., and Thomas, D. Y. 1987. A family of yeast expression vectors containing the phage f1 intergenic region. *Gene* 52:225–233.
- Krogh, A., Larsson, B., von Heijne, G., and Sonnhammer, E. L. 2001. Predicting transmembrane protein topology with a hidden Markov model: Application to complete genomes. *J. Mol. Biol.* 305: 567–580.

Unraveling the Mode of Action of the Antimalarial Choline Analog G25 in *Plasmodium falciparum* and *Saccharomyces cerevisiae*

Rodolphe Roggero,^{1,2} Rachel Zufferey,^{2,3,4} Mihaela Minca,^{2,3} Eric Richier,¹ Michele Calas,¹ Henri Vial,¹ and Choukri Ben Mamoun^{2,3*}

Center for Microbial Pathogenesis,² Department of Genetics and Development Biology,³ and Department of Pathology,⁴ University of Connecticut Health Center, Farmington, Connecticut 06030, and Dynamique Moléculaire des Interactions Membranaires, CNRS UMR 5539, Université Montpellier II, 34095 Montpellier Cedex 05, France¹

Received 18 February 2004/Returned for modification 1 April 2004/Accepted 16 April 2004

Pharmacological studies have indicated that the choline analog G25 is a potent inhibitor of *Plasmodium falciparum* growth in vitro and in vivo. Although choline transport has been suggested to be the target of G25, the exact mode of action of this compound is not known. Here we show that, similar to its effects on *P. falciparum*, G25 prevents choline entry into *Saccharomyces cerevisiae* cells and inhibits *S. cerevisiae* growth. However, we show that the uptake of this compound is not mediated by the choline carrier Hnm1. An *hnm1Δ* yeast mutant, which lacks the only choline transporter gene *HNM1*, was not altered in the transport of a labeled analog of this compound. Eleven yeast mutants lacking genes involved in different steps of phospholipid biosynthesis were analyzed for their sensitivity to G25. Four mutants affected in the de novo cytidylphosphate-choline-dependent phosphatidylcholine biosynthetic pathway and, surprisingly, a mutant strain lacking the phosphatidylserine decarboxylase-encoding gene *PSD1* (but not *PSD2*) were found to be highly resistant to this compound. Based on these data for *S. cerevisiae*, labeling studies in *P. falciparum* were performed to examine the effect of G25 on the biosynthetic pathways of the major phospholipids phosphatidylcholine and phosphatidylethanolamine. Labeling studies in *P. falciparum* and in vitro studies with recombinant *P. falciparum* phosphatidylserine decarboxylase further supported the inhibition of both the de novo phosphatidylcholine metabolic pathway and the synthesis of phosphatidylethanolamine from phosphatidylserine. Together, our data indicate that G25 specifically targets the pathways for synthesis of the two major phospholipids, phosphatidylcholine and phosphatidylethanolamine, to exert its antimalarial activity.

Plasmodium falciparum, the causative agent of the most severe form of human malaria, is responsible for over 2 million deaths annually (49). The emergence of parasites resistant to the most commonly used antimalarials, such as chloroquine, mefloquine, and pyrimethamine, has hampered efforts to combat this disease, emphasizing the need to develop new compounds for malaria treatment and prophylaxis.

The rapid multiplication of *P. falciparum* in human erythrocytes requires active synthesis of new membranes. Therefore, developing drugs that target membrane biogenesis is an attractive strategy to fight malaria. The finding that quaternary ammonium choline analogs inhibit the synthesis of new membranes and block the growth of the parasite has stimulated efforts to develop this class of compounds for antimalarial chemotherapy (4–6, 11, 12). With a combinatorial chemistry approach to obtain compounds with greater specificity and potency against malaria, more than 420 choline analogs have been synthesized, and their structures were optimized with quantitative structural-activity criteria (11, 12, 44, 45). These compounds displayed a very close correlation between inhibition of parasite growth in vitro and specific inhibition of parasite membrane biogenesis (1, 47, 48).

One of these compounds, G25, inhibited *P. falciparum* growth in vitro and cleared malaria infection in monkeys infected with *P. falciparum* and *Plasmodium cynomolgi* at very low doses (48). A tritium-labeled bisquaternary ammonium salt analog of G25, VB5-T (50% inhibitory concentration [IC_{50}], ≈ 18 nM), was shown to accumulate several hundredfold in trophozoite-infected compared to uninfected red blood cells (48). Accumulation of this agent within the parasite is linear with concentrations up to 1,000-fold above the IC_{50} and appears to be irreversible (48). The antimalarial potency of G25 is similar to that of chloroquine, which kills the parasite at low nanomolar extracellular concentrations but accumulates within the parasite food vacuole to the millimolar range (39). Although choline analogs are highly effective against malaria and are entering clinical evaluation, the difficulties in the experimental manipulation of *P. falciparum* has hampered efforts to understand their mode of action and identify their cellular targets.

The amenability of the yeast *Saccharomyces cerevisiae* to genetic manipulation has made it an invaluable system to characterize the metabolic pathways involved in the synthesis of phospholipids, sterols and fatty acids. *S. cerevisiae* membranes consist largely of phosphatidylcholine (44%), phosphatidylethanolamine (18%), and phosphatidylinositol (19.5%) (25). These glycerolipids are thought to be essential for *S. cerevisiae* growth in medium that contains glucose or nonfermentable carbon sources (7, 10, 38, 41). As summarized in Fig. 1, their synthesis involves distinct but highly coregulated biosynthetic pathways: (i) the cytidylphosphate (CDP)-choline pathway,

* Corresponding author. Mailing address: Center for Microbial Pathogenesis, Department of Genetics and Development Biology, University of Connecticut Health Center, 263 Farmington Ave., Farmington, CT 06030. Phone: (860) 679-3544. Fax: (860) 679-8130. E-mail: choukri@up.uhc.edu.

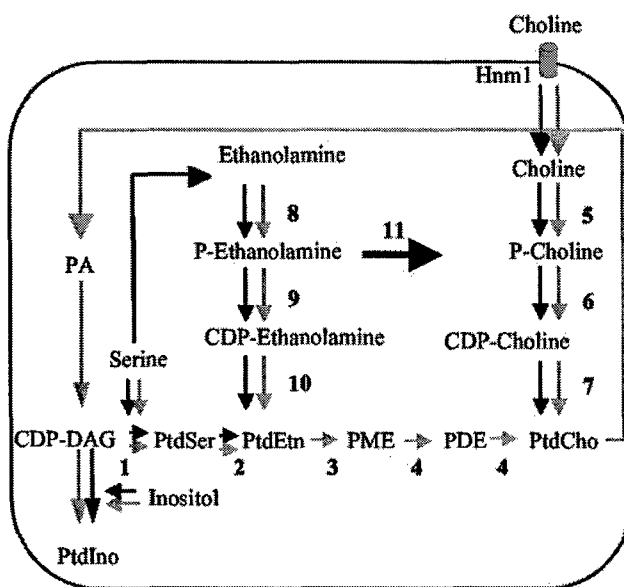


FIG. 1. Phospholipid metabolism in *S. cerevisiae* and *P. falciparum*. Pathways for the synthesis of the major phospholipids in *S. cerevisiae* (thin gray arrows) and *P. falciparum* (thick solid arrows) are shown: 1, phosphatidylserine synthase (*Pss1*); 2, phosphatidylserine decarboxylases (*Psd1* and *Psd2*); 3, phosphatidylethanolamine methyltransferase (*Pem1*); 4, phospholipid methyltransferase (*Pem2*); 5, choline kinase (*Cki1*); 6, phosphocholine cytidylyltransferase (*Pct1*); 7, choline phosphotransferase (*Cpt1*); 8, ethanolamine kinase (*Eki1*); 9, phosphoethanolamine cytidylyltransferase (*Ept1*); 10, ethanolamine phosphotransferase (*Ect1*); 11, phosphoethanolamine methyltransferase (*P. falciparum* *Pmt*). PA, phosphatidic acid; CDP-DAG, cytidyldiphosphate diacylglycerol; PtdSer, phosphatidylserine; PtdEtn, phosphatidylethanolamine; PME, phosphatidylmonomethylethanolamine; PDE, phosphatidylmethylethanolamine; PtdCho, phosphatidylcholine; PtdIno, phosphatidylinositol.

which uses choline as a precursor for the de novo synthesis of phosphatidylcholine (19, 21, 23, 27, 50); (ii) the CDP-ethanolamine pathway, which uses ethanolamine as a precursor for the de novo synthesis of phosphatidylethanolamine (20, 22, 26); (iii) the CDP-diacylglycerol (DAG) pathway, which utilizes serine and CDP-DAG to form phosphatidylserine, which is then decarboxylated to form phosphatidylethanolamine; and (iv) the phosphatidylinositol pathway, which synthesizes phosphatidylinositol from CDP-DAG and inositol (14, 28, 31, 34, 41–43).

The CDP-DAG and CDP-ethanolamine pathways converge into phosphatidylethanolamine, which is subsequently methylated in a three step *S*-adenosyl-L-methionine-dependent methylation to form phosphatidylcholine. This reaction is catalyzed by two methyltransferases encoded by the phosphatidylethanolamine *N*-methyltransferase *PEM1* and phospholipid *N*-methyltransferase *PEM2* genes. The CDP-DAG pathway is the major pathway leading to the formation of phosphatidylcholine in *S. cerevisiae* (13). Therefore, in this organism, neither choline nor the enzymes of the CDP-choline pathway are essential for survival. The CDP-choline pathway becomes essential when the genes encoding the enzymes in the CDP-DAG pathway are altered or deleted (29).

Biochemical studies in *P. falciparum* and the available genome sequences have made it possible to define the pathways for synthesis of the major phospholipids (18, 46) (Fig. 1). With

the exception of the choline transporter and the phospholipid methyltransferases, all the genes encoding enzymes of the CDP-choline, CDP-ethanolamine, and CDP-DAG pathways have been identified. The similarity between *P. falciparum* and *S. cerevisiae* in the biogenesis of the major phospholipids suggests that *S. cerevisiae* can be used as a surrogate system to characterize the function of *P. falciparum* phospholipid synthesizing genes and determine the mode of entry and cellular targets of antimalarial lipid inhibitors.

Here, we report that the antimalarial choline analog G25 inhibits the growth of *S. cerevisiae* in vitro and, in the same range of concentrations, is an effective inhibitor of choline transport in wild-type *S. cerevisiae*. Similar initial rate and overall uptake of a radiolabeled bisquaternary ammonium analog of G25 was measured in both wild-type and *hnm1Δ* cells lacking the only yeast choline transporter Hnm1. These results demonstrate that the choline carrier Hnm1 does not mediate the entry of bisquaternary ammonium compounds. Of 11 individual *S. cerevisiae* knockouts lacking genes involved in different steps of phosphatidylcholine biosynthesis, four mutants altered in the de novo CDP-choline pathway and one mutant lacking the phosphatidylserine decarboxylase-encoding gene *PSD1* were highly resistant to G25.

Labeling studies in *P. falciparum* demonstrated that G25 completely and specifically inhibits the de novo CDP-choline-dependent phosphatidylcholine biosynthetic pathway. Surprisingly, higher concentrations of this compound resulted in the inhibition of synthesis of phosphatidylethanolamine from phosphatidylserine but had no effect on any other step of the CDP-DAG pathway. Interestingly, we found that G25 inhibits the phosphatidylserine decarboxylase activity of purified recombinant *P. falciparum* *Psd1* in a way similar to the inhibition of the native enzyme. Together, our data indicate that G25 specifically targets the pathways for synthesis of the two major phospholipids, phosphatidylcholine and phosphatidylethanolamine, to exert its antimalarial activity. These novel findings constitute important information for quaternary ammonium compounds that are entering clinical studies and further support the use of *S. cerevisiae* as a surrogate system to identify the targets of antimalarial compounds.

MATERIALS AND METHODS

Chemicals. G25 (1,16-hexadecamethylenebis[N-methylpyrrolidinium] dibromide) (11), T16 (1,12-dodecanemethylene bis[4-methyl-5-ethylthiazolium] diiodide), and [³H]T16 were synthesized in house (Richier et al., unpublished data).

Strains and growth conditions. Wild-type BY4741 (*MAT**ahis3Δ1 leu2Δ0 met15Δ0 ura3Δ0*) and mutant (*hnm1Δ, psd1Δ, cki1Δ, pem1Δ, ept1Δ, cpt1Δ, eki1Δ, psd2Δ, pct1Δ, ect1Δ*, and *pem2Δ*) *S. cerevisiae* strains used in this study were purchased from Research Genetics (Invitrogen). These strains were grown on YPD (1% yeast extract, 2% dextrose, and 2% peptone) or synthetic complete medium (SD; 1.7% yeast nitrogen base, 5% ammonium sulfate, and 2% dextrose). The Nigerian strain of *P. falciparum* was propagated in human red blood cells at 4% hematocrit by the method of Trager and Jensen (40). Plate growth assays were performed by growing wild-type and mutant yeast strains in YPD to mid-log phase. Cultures were serially diluted 1:10 starting with a density of 3×10^7 cells/ml. The growth of cells was monitored by spotting 3 μ l of each dilution onto solid medium in the absence or presence of 5 μ M G25. Growth assays in liquid media were performed by inoculating wild-type and *hnm1Δ* cells to a density of 10^4 cells/ml in YPD supplemented with increasing concentrations of choline analogs. The optical density at 600 nm was measured when the control without choline analogs reached a density of 1.8×10^7 cells/ml.

Uptake assays. *S. cerevisiae* strains were grown in synthetic complete medium supplemented as required to maintain cell growth to an optical density at 600 nm

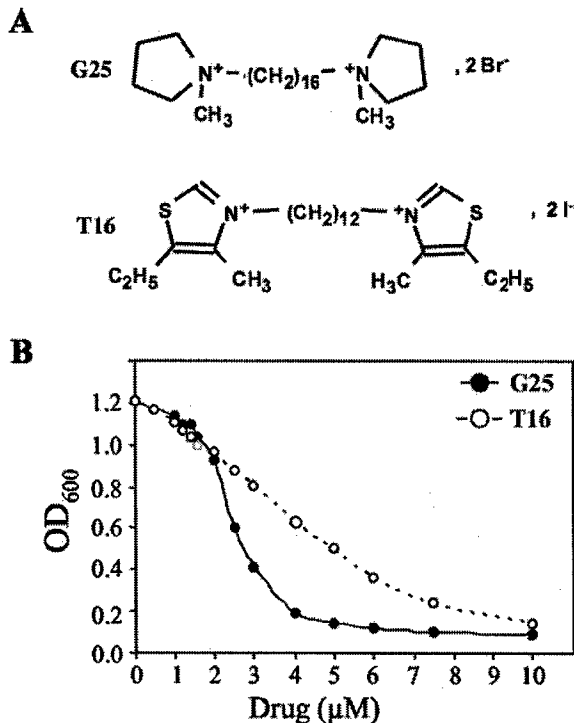


FIG. 2. Inhibition of *S. cerevisiae* growth by G25 and its analog T16. (A) Chemical structure of G25 (1,16-hexadecamethylenebis[N-methylpyrrolidinium] dibromide) and T16 (1,12-dodecanemethylene bis[4-methyl-5-ethylthiazolium] diiodide). (B) Liquid growth assays were performed in increasing concentrations of G25 and T16 as described in the text.

of 0.55 to 0.65. Cells were harvested by centrifugation at 3,200 × g for 10 min at 4°C, washed twice in cold phosphate-buffered saline and resuspended in nitrogen-free medium (SD without ammonium sulfate). Each reaction was performed in a 1-ml final volume in the presence of 12 nM [methyl-³H]choline (82 Ci/mmol; Amersham). After 3 min of incubation at 30°C with shaking, transport was immediately stopped by filtration through Whatman GF/C glass microfiber paper. The filters were washed three times with 5 ml of ice-cold phosphate-buffered saline, air dried, and analyzed in a scintillation counter.

For time course uptake, 3 × 10⁷ to 4 × 10⁷ cells were incubated at 30°C in 1 ml of nitrogen-free medium in the presence of 25 nM [³H]T16 (69 Ci/mmol) for 1, 2, 3, 4, 5, 7, 10, and 15 min, after which 5 ml of cold phosphate-buffered saline was added to stop the reaction. Kinetic parameters were determined after 4 min of incubation at 30°C in the presence of [³H]T16 at concentrations ranging from 25 nM to 75 μM (69 Ci to 23 mCi/mol). The samples were centrifuged at 4°C for 10 min at 1,200 × g, the supernatants were discarded, and the cells were then resuspended in 5 ml of cold phosphate-buffered saline. The reaction was terminated by filtering the cell suspension through GF/C membranes that had been treated with 15 ml of 0.05% polyethyleneimine. The filters were washed twice with 5 ml of cold phosphate-buffered saline, air dried, and analyzed in a scintillation counter. The cellular accumulation ratio was calculated as previously described for T16 and G25 (9, 48).

Labeling studies and phospholipid analysis in *P. falciparum*. Nigerian strains of *P. falciparum* were asexually cultured in the presence of basic medium (RPMI 1640 supplemented with 25 mM HEPES, pH 7.4) and 10% AB-positive human serum (40). Parasite synchronization was obtained with three successive 5% sorbitol treatments (30). Synchronized *P. falciparum*-infected erythrocytes (7 to 10% parasitemia, trophozoites) were incubated for 1 h at 37°C at 4% hematocrit in 2 ml (final volume) of basic medium in the absence or the presence of different concentrations of the compound G25. The appropriate radioactive precursor of lipid metabolism was then added, followed by a further 3 h of incubation. Radioactive precursors were used as follows: 30 μM [methyl-³H]choline (334 mCi/mmol), 2 μM [³H]ethanolamine (2 Ci/mmol), and 10 μM [³-¹⁴C]serine (57 mCi/mmol).

Following incubation with radiolabeled precursors, cells were concentrated by centrifugation at 1,200 × g for 5 min at 4°C and washed twice, the cellular lipids

were extracted by a mixture of chloroform and methanol (17), and the organic phase was evaporated under air. The dried material was dissolved in 100 μl of chloroform-methanol (9:1, vol/vol), and lipids were separated by thin-layer chromatography. Samples were applied to precoated silica gel plates (Merck, Darmstadt, Germany), which were developed in chloroform-methanol-acetic acid-0.1 M sodium borate (75:45:12:3, vol/vol/vol/vol). Phospholipids spots were revealed with iodine vapors and identified with appropriate standards. The silica gel of the lipid spots was scraped directly into scintillation vials containing 3 ml of liquid scintillation fluid and counted in a Beckman LS 5000 spectrophotometer. The amount of labeled precursors incorporated into cellular lipids was computed on the basis of radioactivity incorporated into lipids and the specific activity of the precursors in the incubation medium.

Phosphatidylserine decarboxylase assay. Recombinant *P. falciparum* phosphatidylserine decarboxylase was purified as described by Baunaure and colleagues (8). The assay mixture (0.3 ml) contained 0.1 M potassium phosphate buffer (pH 6.8), 0.06% (wt/vol) Triton X-100, 200 μM L-[dipalmitoyl]phosphatidyl[³-¹⁴C] serine (1.35 mCi/mmol; Amersham), and the enzyme fraction containing recombinant protein of *P. falciparum* (240 μg). After incubation at 37°C for 1 h, the reaction was terminated by the addition of 400 μl of chloroform. Chloroform-soluble materials were extracted, dried, and then dissolved in chloroform-methanol (9:1, vol/vol). Phospholipids were separated by thin-layer chromatography as described above. The radioactive phospholipids were localized and identified with appropriate standards, and radioactivity was quantified with a phosphoimager analyzer (Molecular Dynamics).

RESULTS

Antimalarial drug G25 inhibits the growth of *S. cerevisiae*. To examine the effect of the antimalarial choline analog G25 (1,16-hexadecamethylenebis[N-methylpyrrolidinium] dibromide) (Fig. 2A) on the growth of *S. cerevisiae* in vitro, wild-type strain BY4741 was inoculated at 10⁴ cells/ml in liquid medium in the presence of increasing concentrations of the compound and incubated at 30°C for 16 h. Growth inhibition was assessed by measuring the optical density at 600 nm and comparing it to that of the wild-type strain grown under the same conditions in the absence of the compound. G25 inhibited yeast growth with an IC₅₀ of 2.5 μM (Fig. 2B). This IC₅₀ value is in the range of the predicted intracellular concentration of G25 in *P. falciparum*

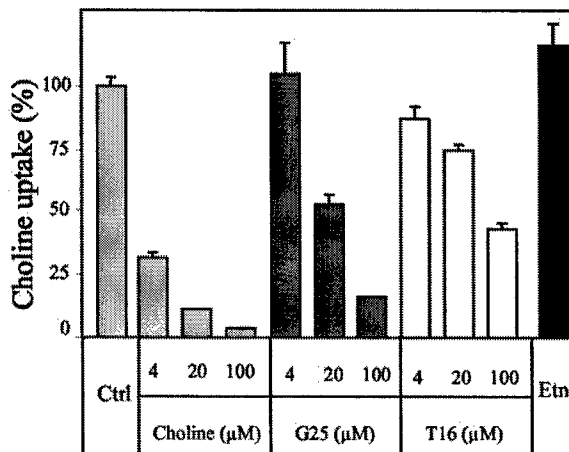


FIG. 3. Inhibition of choline uptake in *S. cerevisiae* by G25. Choline transport in the wild-type strain of *S. cerevisiae* was measured as described in Materials and Methods. The uptake of 1 μM [methyl-³H]choline in the presence of 100 μM ethanolamine (Etn) and a 4-, 20-, and 100-fold excess of unlabeled choline, G25, and T16 is shown as a percentage of the counts obtained in the control (Ctrl) without drugs, choline, or ethanolamine.

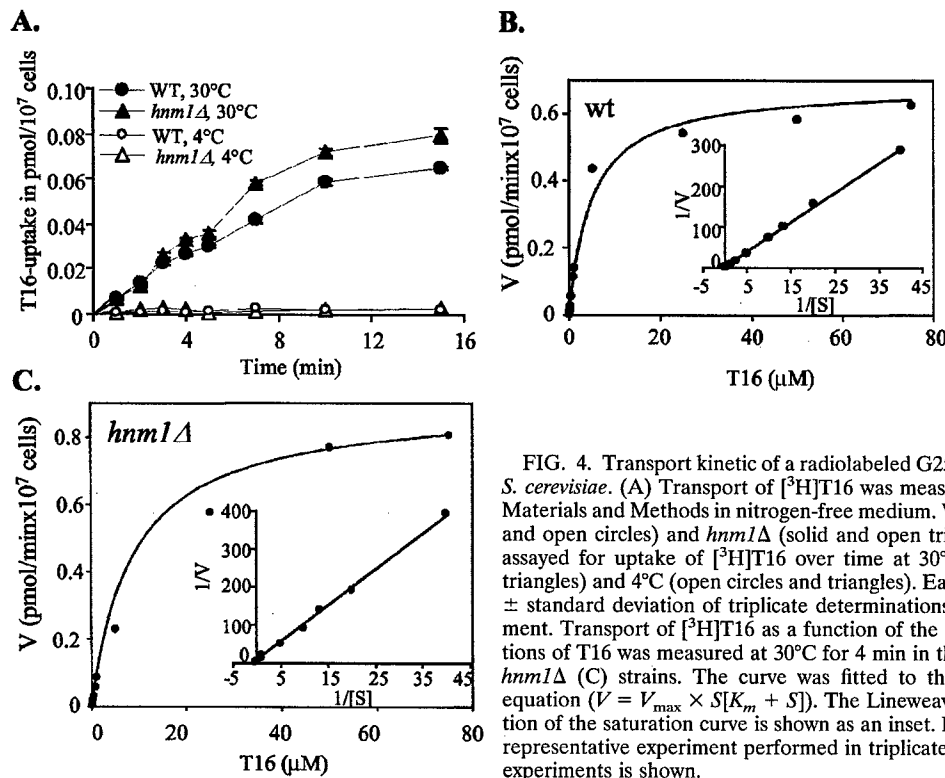


FIG. 4. Transport kinetic of a radiolabeled G25 analog, [³H]T16, in *S. cerevisiae*. (A) Transport of [³H]T16 was measured as described in Materials and Methods in nitrogen-free medium. Wild-type (WT, solid and open circles) and *hnm1* Δ (solid and open triangles) strains were assayed for uptake of [³H]T16 over time at 30°C (solid circles and triangles) and 4°C (open circles and triangles). Each value is the mean \pm standard deviation of triplicate determinations of a typical experiment. Transport of [³H]T16 as a function of the indicated concentrations of T16 was measured at 30°C for 4 min in the wild-type (B) and *hnm1* Δ (C) strains. The curve was fitted to the Michaelis-Menten equation ($V = V_{\max} \times S/[K_m + S]$). The Lineweaver-Burk representation of the saturation curve is shown as an inset. For A to C, only one representative experiment performed in triplicate of two independent experiments is shown.

rum due to the accumulative properties inside infected erythrocytes (48).

Uptake analysis and inhibition of choline transport by choline analogs in *S. cerevisiae*. Bisquaternary ammonium choline analogs have been shown to inhibit choline entry into *Plasmodium*-infected erythrocytes (1, 3). To determine whether these compounds block choline uptake in *S. cerevisiae*, we examined the transport of [methyl-³H]choline in the absence and presence of various concentrations of G25 and its structural analog T16 (1,12-dodecanemethylene bis[4-methyl-5-ethylthiazolium] diiodide) (Fig. 2A), predicted by quantitative structure-activity studies and confirmed experimentally to have potent in vitro antimalarial and antifungal inhibitory activities similar to those of G25 with IC₅₀ values of \approx 16 nM (9) and \approx 4 μM (Fig. 2B), respectively.

G25 inhibited choline uptake in a dose-dependent manner, with 50% inhibition of choline transport in 20-fold excess and 84% inhibition in 100-fold excess (Fig. 3). The G25 analog T16 also inhibited choline transport, albeit less efficiently than G25, with 26% inhibition of choline transport in 20-fold excess and 57% inhibition in 100-fold excess (Fig. 3). As a control, 20- and 100-fold excesses of unlabeled choline inhibited uptake of radiolabeled choline by 89 and 97%, respectively. Altogether, these data suggest that bisquaternary ammonium compounds are excellent inhibitors of choline uptake in *S. cerevisiae*.

To directly examine the transport of choline analogs in *S. cerevisiae*, we synthesized a tritium-labeled bisquaternary ammonium salt, [³H]T16, and examined its transport properties in wild-type cells at 4 and 30°C. No significant uptake of T16 in *S. cerevisiae* could be measured at 4°C (Fig. 4A). In contrast, [³H]T16 uptake could be measured at 30°C and was

linear during the first 12 min, after which it reached a plateau, suggesting that entry of bisquaternary ammonium compounds into yeast cells is carrier mediated (Fig. 4A). Unlike in *P. falciparum*-infected erythrocytes, where G25 and T16 have been shown to accumulate with cellular accumulation ratios of \approx 300 and \approx 500, respectively, after 3 h of incubation (9, 48), the cellular accumulation ratio of T16 in *S. cerevisiae* was estimated to be less than 7 (data not shown).

To determine the kinetic parameters of this transport, [³H]T16 uptake was measured after 4 min of incubation at 30°C as a function of its extracellular concentration. The Lineweaver-Burk representation of this transport resulted in an apparent K_m of 5.05 ± 0.26 μM for [³H]T16 and a maximum velocity V_{\max} of 0.98 ± 0.48 pmol/min per 10⁷ cells (Fig. 4B). As a control, uptake of [methyl-³H]choline in the wild-type strain was found to be carrier mediated, with a K_m of 0.53 ± 0.18 μM and a V_{\max} of 40 pmol/min/10⁷ cells (data not shown), as reported previously (33, 52).

To rule out the possible role of Hnm1 in the uptake of bisquaternary ammonium compounds by yeast cells, we measured the transport of [³H]T16 in an *hnm1* Δ mutant strain, which lacks the choline transporter gene *HNMI* (Fig. 4C), and compared it to that measured in the wild-type strain (Fig. 4B). As in the wild-type strain, T16 transport in the *hnm1* Δ strain was found to be carrier mediated, with a K_m of 7.45 ± 1.98 μM and a V_{\max} of 0.76 ± 0.21 pmol/min/10⁷ cells (Fig. 4C). Thus, no differences in T16 uptake could be detected between the *hnm1* Δ and wild-type strains. As expected, no choline transport could be detected in the *hnm1* Δ mutant (data not shown). Altogether, these data suggest that yeast cells utilize other

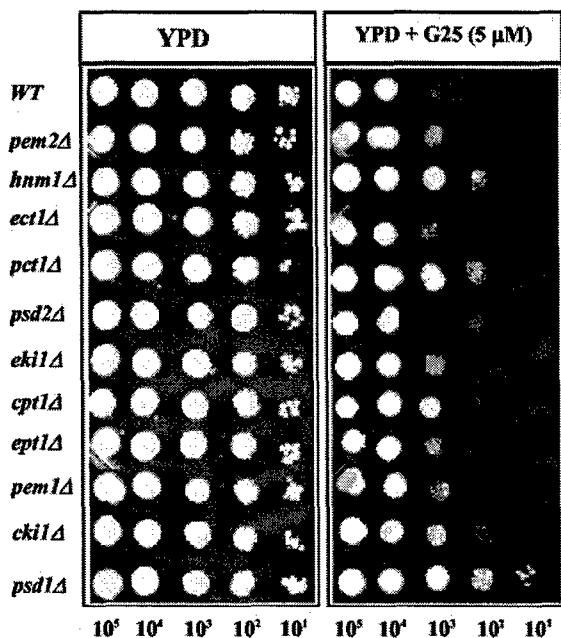


FIG. 5. Sensitivity to G25 of the wild type and mutants affected in different steps of phosphatidylcholine biosynthesis. Plate growth limiting-dilution assays were performed as described in Materials and Methods in the absence and presence of 5 μ M G25. The strains used are described in Materials and Methods. The genes deleted in these strains are detailed in Fig. 1.

transport systems for the uptake of bisquaternary ammonium compounds.

Sensitivity of mutants affected in phospholipid metabolism to choline analogs. Choline analogs are proposed to inhibit membrane biogenesis in *P. falciparum* (3, 11, 45). However, the steps in the phospholipid biosynthesis pathways that are specifically targeted by these compounds are not yet known. To assess whether the mode of action of G25 is linked to disruption of phospholipid metabolism, we used *S. cerevisiae* as a surrogate system to compare the sensitivity to G25 of the wild-type strain and 11 individual knockouts in the CDP-choline, CDP-ethanolamine, and CDP-DAG pathways. As shown in Fig. 5, substantial resistance to G25 was conferred by loss of the choline kinase (Cki1), choline phosphotransferase (Cpt1), phosphocholine cytidylyltransferase (Pct1), and choline carrier (Hnm1) activities of the CDP-choline pathway.

Surprisingly, the *psd1Δ* mutant strain, which lacks the *PSD1* gene encoding the phosphatidylserine decarboxylase activity that converts 95% of cellular phosphatidylserine into phosphatidylethanolamine in the mitochondria (42), was also found to be highly resistant to G25 (Fig. 5). No resistance was conferred by loss of the phosphatidylethanolamine methyltransferases Pem1 and Pem2 or the enzymes of the CDP-ethanolamine pathway. Furthermore, unlike the *psd1Δ* mutant strain, loss of the Golgi/vacuole phosphatidylserine decarboxylase Psd2, which synthesizes only 5% of the phosphatidylethanolamine pool, had no effect on G25 sensitivity. These data indicate that the sensitivity of *S. cerevisiae* to G25 requires a functional de novo CDP-choline pathway for synthesis of phosphatidylcholine from choline and a functional Psd1 activ-

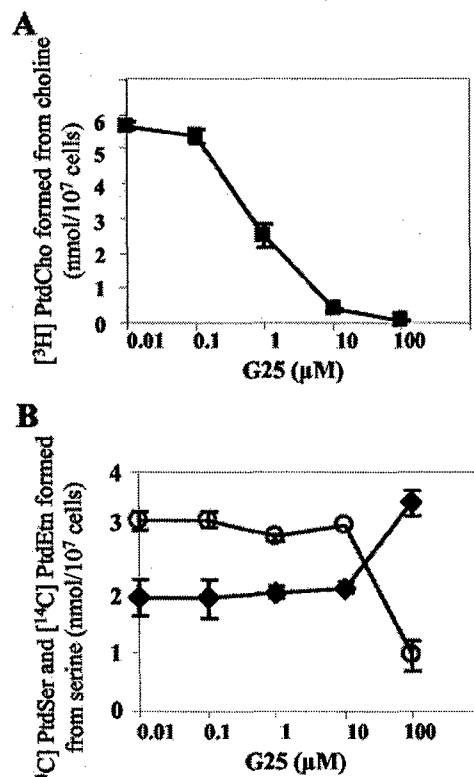


FIG. 6. Effect of G25 on phosphatidylethanolamine and phosphatidylcholine synthesis from phosphatidylserine and choline, respectively. From 5×10^7 to 6×10^7 synchronized *P. falciparum*-infected erythrocytes (7% trophozoite stage) were incubated at 4% hematocrit for 1 h in RPMI-based medium containing the indicated concentration of G25 before adding (A) 30 μ M [³H]choline (334 mCi/mmol) or (B) 10 μ M [¹⁴C]serine (57 mCi/mmol). After incubation at 37°C for 3 h, the cellular lipids were extracted and fractionated on thin-layer chromatography plates for quantification of radioactivity in phosphatidylserine (PtdSer, solid diamonds), phosphatidylcholine (PtdCho, solid squares), and phosphatidylethanolamine (PtdEtn, open circles). Each value is the mean \pm standard deviation of triplicate determinations of two independent experiments.

ity for phosphatidylethanolamine synthesis from phosphatidylserine.

G25 inhibits the CDP-choline pathway and phosphatidylethanolamine formation from phosphatidylserine in *P. falciparum*. The similarity between the *P. falciparum* and *S. cerevisiae* phospholipid metabolic pathways and the finding that deletion of numerous genes of phospholipid metabolism in *S. cerevisiae* resulted in major resistance to G25 suggested that this compound might directly inhibit phospholipid-synthesizing enzymes in *P. falciparum*. To investigate the possible inhibition by G25 of the de novo CDP-choline pathway in *P. falciparum*, we examined the incorporation of labeled choline into phosphatidylcholine in trophozoite-infected erythrocytes in the absence and presence of increasing concentrations of G25. This assay takes into account both the inhibitory effect of G25 on choline uptake and any additional inhibition by this compound of one or multiple enzymes of the CDP-choline pathway.

As shown in Fig. 6A, G25 induced a dose-dependent inhibition of the de novo synthesis of phosphatidylcholine. At con-

centrations higher than 0.1 μM , G25 caused a significant decrease of phosphatidylcholine biosynthesis, with 56% inhibition at 1 μM and nearly complete inhibition at 10 μM . In contrast, under similar conditions, G25 concentrations up 100 μM had no effect on the incorporation of radiolabeled ethanolamine into phosphatidylethanolamine (not shown). These results are consistent with our data for *S. cerevisiae*, which showed that deletion of *EKI*, *ECTI*, and *EPTI*, involved in the de novo synthesis of phosphatidylethanolamine from ethanolamine, did not confer resistance to G25 (Fig. 5).

We also investigated the possible inhibition of phosphatidylserine decarboxylase activity in *P. falciparum* by G25. *P. falciparum*-infected erythrocytes were labeled with radiolabeled serine, which is readily incorporated into phosphatidylserine, in the presence and absence of increasing concentrations of G25, and the effect of this compound on the parasite's endogenous phosphatidylserine decarboxylase activity was measured by following the formation of phosphatidylethanolamine from phosphatidylserine (Fig. 6B). Phosphatidylethanolamine was constantly formed from phosphatidylserine in the absence or presence of low concentrations of G25. Although the total incorporation of serine was not affected by G25, high concentrations of this compound resulted in a dramatic decrease in the endogenous phosphatidylserine decarboxylase activity, with a 77% decrease in the pool of phosphatidylethanolamine formed at 100 μM G25 (Fig. 6B). Concomitantly, at this concentration of G25, phosphatidylserine was increased in the same range, indicating that the phosphatidylserine decarboxylase activity was blocked (Fig. 6B).

G25 inhibits the activity of recombinant *P. falciparum* phosphatidylserine decarboxylase. To further investigate the inhibitory effect of G25 on the formation of phosphatidylethanolamine from phosphatidylserine, we performed *in vitro* assays with a recombinant phosphatidylserine decarboxylase enzyme Psd1 from *P. falciparum*, encoded by the single-copy gene *PSD1*. The enzymatic activity of the recombinant *P. falciparum* Psd1 protein was tested under optimal conditions as described in Materials and Methods in the absence and presence of increasing concentrations of G25. Whereas in the absence of G25 recombinant *P. falciparum* Psd1 efficiently converted phosphatidylserine into phosphatidylethanolamine, addition of G25 resulted in a steady decrease in the activity of the enzyme as the concentration of the compound increased (Fig. 7), suggesting a direct inhibition of *P. falciparum* Psd1 activity by G25.

DISCUSSION

Quaternary ammonium compound analogs of choline represent a new class of drugs with a promising therapeutic future for treatment of multidrug-resistant malaria (1–3, 11, 45, 48) and possibly other parasitic infections (51). Studies in *P. falciparum* have suggested that choline transport might be the primary target of these compounds (1, 4). However, the role of choline influx and phosphatidylcholine biosynthesis in parasite development and survival has not been detailed. Furthermore, the difficulty in genetically manipulating *P. falciparum* has severely hampered efforts to understand the exact mode of action of these compounds.

Here, we provide the first evidence that the antimalarial choline analog G25 inhibits the growth of *S. cerevisiae* and that

mutations in phospholipid metabolic genes affect the sensitivity of *S. cerevisiae* to this compound. The *S. cerevisiae* and malarial pathways of phospholipid biogenesis are similar enough that the targets of phospholipid inhibitors that we can find in *S. cerevisiae* are most likely to be relevant to *P. falciparum*. The IC₅₀ value measured in *S. cerevisiae* is 2.5 μM , whereas that measured in various *P. falciparum* strains ranged between 1 and 5.3 nM (11). Interestingly, whereas G25 and its analog T16 accumulate in *P. falciparum*-infected erythrocytes with cellular accumulation ratios of \approx 300 and \approx 500, respectively, after 3 h of incubation (9, 48), our results indicate a cellular accumulation ratio for T16 of less than 7 in *S. cerevisiae*. The differences in growth inhibition assays and drug cellular accumulation could thus account for the differences in IC₅₀s between the two organisms.

The sensitivity of *S. cerevisiae* to G25 and its structural analog T16 and the availability of a radioactive form of T16 led us to investigate the effect of these two compounds on the entry of choline into *S. cerevisiae* cells. Similar to previous studies in *P. falciparum*, our studies showed that G25 and T16 are very effective inhibitors of choline transport in *S. cerevisiae*, with 50% inhibition of choline uptake measured when G25 and T16 were present at 20- and 100-fold excess, respectively. Because choline is not essential for *S. cerevisiae* growth, and because the IC₅₀ values for G25 and T16 were not affected by the presence or absence of choline in the medium (data not shown), the ability of G25 to inhibit choline transport cannot alone account for its antifungal activity.

We showed that entry of the G25 analog T16 into wild-type and *hnm1* Δ yeast strains occurs through a temperature-dependent carrier-mediated process with similar kinetic characteristics, indicating a mode of entry of bisquaternary ammonium in *S. cerevisiae* distinct from that of the choline carrier. Deves and Krupka have shown that the lengthening of the alkyl chain in choline analogs makes them high-affinity inhibitors of choline transport but prevents their entry via the erythrocytic choline carrier (15). A similar mechanism might account for the ability of G25 and T16 to inhibit choline transport in *S. cerevisiae* and *P. falciparum* without being transported via the endogenous choline carriers. We suggest that in *S. cerevisiae* and most likely in *P. falciparum* as well, G25 is not transported via the choline transporter Hnm1 and that once inside the cell, this compound exerts its activity by interfering with specific cellular functions. Future studies will focus on determining the primary route of entry of this compound in *S. cerevisiae*.

Our data showed that *S. cerevisiae* mutants lacking specific phospholipid-synthesizing genes display substantial resistance to G25. Interestingly, loss of every gene of the de novo CDP-choline pathway, choline transporter (*HNM1*), choline kinase (*CKI1*), choline phosphotransferase (*CPT1*), and phosphocholine cytidylyltransferase (*PCT1*) resulted in resistance to this compound. Remarkably, a *psd1* Δ strain, which lacks *PSD1*, was also found to be highly resistant to G25. In *S. cerevisiae*, phosphatidylserine, which is synthesized in the endoplasmic reticulum and mitochondrion-associated membrane, is first transported to the inner mitochondrial membrane and Golgi/vacuole compartments, the sites of phosphatidylserine decarboxylase 1 (Psd1p) and 2 (Psd2), respectively. It is subsequently converted to phosphatidylethanolamine (41, 42). Psd1p is the major phosphatidylserine decarboxylase, converting 95% of the cel-

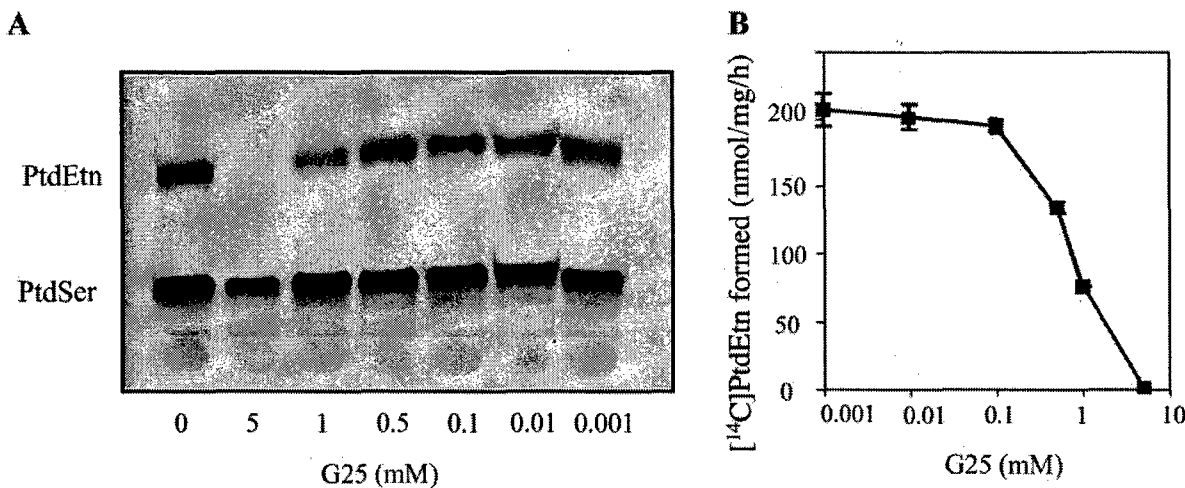


FIG. 7. Effect of G25 on the activity of purified recombinant *P. falciparum* Psd1 enzyme. *P. falciparum* Psd1 activity was determined as described in Materials and Methods by measuring the amount of [¹⁴C]phosphatidylethanolamine (PtdEtn) formed from phosphatidylserine (PtdSer). (A) Thin-layer chromatography analysis of *P. falciparum* Psd1-mediated conversion of phosphatidylserine into phosphatidylethanolamine in the absence and presence of increasing concentrations of G25. (B) Quantitative analysis of the thin-layer chromatography data shown in panel A. Values are means \pm standard deviation of triplicate determination of two independent experiments.

lular phosphatidylserine and producing most of the cellular phosphatidylethanolamine in the absence of an ethanolamine precursor (42). In addition to its role in *S. cerevisiae* membrane structure, phosphatidylethanolamine plays a central role in lysosome/vacuole autophagy by covalently conjugating to Apg8p (24) and also serves as a donor of ethanolamine phosphate to glycosylphosphatidylinositol anchors, whose synthesis is essential for yeast cell viability (16, 32). Because *P. falciparum* possesses homologues of the *S. cerevisiae* *PSD1*, *CKI1*, *CPT1*, and *PCT1* genes, we hypothesized that G25 might exert its antimalarial activity by blocking the synthesis of phosphatidylcholine from choline, and phosphatidylethanolamine from phosphatidylserine.

Labeling studies in *P. falciparum* with the phospholipid precursors choline and serine demonstrated that G25 inhibited both the incorporation of choline into phosphatidylcholine and phosphatidylserine decarboxylation in a dose-dependent manner. A concentration of only 1 μ M of this compound was sufficient to inhibit phosphatidylcholine synthesis from choline, and inhibition was complete at 10 μ M G25. Although this inhibition could be accounted for solely by the ability of choline analogs to inhibit choline entry into *Plasmodium*-infected erythrocytes (1), we cannot at this stage exclude additional inhibition by this compound of one or multiple enzymes of the CDP-choline pathway. Nonetheless, G25 concentrations up to 100 μ M had no effect on the de novo biosynthesis of phosphatidylethanolamine from ethanolamine in *P. falciparum*, suggesting that the effect of this compound on the de novo phosphatidylcholine biosynthetic pathway is very specific. Similarly, albeit at higher concentrations, G25 was able to affect the incorporation of serine into phosphatidylethanolamine via the CDP-DAG pathway by specifically inhibiting the decarboxylation step of phosphatidylserine into phosphatidylethanolamine. At a concentration of 100 μ M, G25 inhibited phosphatidylethanolamine formation from phosphatidylserine by 77%. Interestingly, at this concentration, G25 had no effect on the first step

of the CDP-DAG pathway catalyzed by the phosphatidylserine synthase.

Two possible hypotheses could account for the resistance of *S. cerevisiae* mutants to G25. First, G25 might not directly kill *S. cerevisiae* cells but rather be converted into toxic derivatives by Psd1 and other enzymes of the CDP-choline pathway. Deletion of the genes encoding those enzymes reduces the toxicity of the compound. Second, G25 might directly inhibit specific enzymes of the phospholipid metabolic pathways, and deletion of *PSD1* or any of the four genes of the CDP-choline pathway, although not essential for survival, results in changes in the composition and/or structure of the *S. cerevisiae* membranes, leading to low entry and/or effect of G25. In *S. cerevisiae*, phosphatidylcholine can be synthesized either via the CDP-choline pathway from choline transported via the choline transporter Hnm1 or via the transmethylation of phosphatidylethanolamine by two methyltransferases encoded by the *PEMI/CHO2* and *PEM2/OPI3* genes (13). The genes involved in these pathways are highly regulated by the availability of the phospholipid precursors inositol and choline (13, 37).

Yeast cells utilize the CDP-DAG pathway as the primary route of synthesis of phosphatidylcholine. The CDP-choline pathway, although not essential, is also active even in the absence of choline in the medium (13, 35). This suggests that although the two pathways can compensate for each other to allow survival, the composition of phosphatidylcholine synthesized by each pathway might be different under normal conditions. Considering the mechanism of catalysis of choline kinase, phosphocholine cytidyltransferase, CDP-choline phosphotransferase, and phosphatidylserine decarboxylase, it is difficult to envisage that G25 could be a substrate for those enzymes. Furthermore, studies in *P. falciparum* with a radioactive analog of G25, VB5-T, have shown that this compound was not metabolized and that it acts directly as an active compound (48). Our in vitro studies with recombinant *P. falciparum* Psd1 showed that G25 specifically inhibited the phospha-

tidylserine decarboxylation reaction catalyzed by this enzyme, providing further support for the second hypothesis.

The recent discovery in *P. falciparum* of a plant-like pathway for phosphatidylcholine biosynthesis involving methylation of phosphoethanolamine into phosphocholine by a phosphoethanolamine methyltransferase, Pmt (36), suggests that choline uptake might not be essential for parasite survival, whereas the later steps of the CDP-choline pathway catalyzed by the phosphocholine cytidyltransferase and CDP-choline phosphotransferase enzymes might be essential. Future genetic studies to determine the importance of the CDP-choline pathway in *P. falciparum* and future biochemical studies with recombinant *P. falciparum* choline kinase, phosphocholine cytidyltransferase, or CDP-choline phosphotransferase enzymes to directly determine their sensitivity to G25 are warranted.

In conclusion, our data unraveled two new mechanisms of action of G25 in *P. falciparum* and *S. cerevisiae*. G25 specifically inhibits the de novo synthesis of phosphatidylcholine from choline and the phosphatidylserine decarboxylase-dependent formation of phosphatidylethanolamine from phosphatidylserine. These novel findings constitute important information for quaternary ammonium compounds that are entering clinical studies. These studies further support the use of *S. cerevisiae* as a surrogate system to identify the targets of antimalarial compounds.

ACKNOWLEDGMENTS

This work was supported by the University of Connecticut Health Center Research Fund, the Robert Leet and Clara Guthrie Patterson Trust (to R.Z. and C.B.M.), the U.S. Army Medical Research and Material Command (to C.B.M.), the European Communities, QLK2-CT-2000-01166 (to H.V.), and the French Ministere de l'Education Nationale et Recherche Scientifique (to R.R.).

We thank Patrick Eldin and Francoise Baunaure for help with the phosphatidylserine decarboxylase assay. We are grateful to Stephen Wikle and Justin Radolf for advice and critical reading of the manuscript.

REFERENCES

- Ancelin, M. L., M. Calas, J. Bompard, G. Cordina, D. Martin, M. Ben Bari, T. Jei, P. Druilhe, and H. J. Vial. 1998. Antimalarial activity of 77 phospholipid polar head analogs: close correlation between inhibition of phospholipid metabolism and *in vitro* *Plasmodium falciparum* growth. *Blood* **91**:1426-1437.
- Ancelin, M. L., M. Calas, A. Bonhoure, S. Herbute, and H. J. Vial. 2003. *In vivo* antimalarial activities of mono- and bisquaternary ammonium salts interfering with *Plasmodium* phospholipid metabolism. *Antimicrob. Agents Chemother.* **47**:2598-2605.
- Ancelin, M. L., M. Calas, V. Vidal-Sailhan, S. Herbute, P. Ringwald, and H. J. Vial. 2003. Potent inhibitors of *Plasmodium* phospholipid metabolism with a broad spectrum of *in vitro* antimalarial activities. *Antimicrob. Agents Chemother.* **47**:2590-2597.
- Ancelin, M. L., and H. J. Vial. 1986. Quaternary ammonium compounds efficiently inhibit *Plasmodium falciparum* growth *in vitro* by impairment of choline transport. *Antimicrob. Agents Chemother.* **29**:814-820.
- Ancelin, M. L., H. J. Vial, M. Calas, L. Giral, G. Piquet, E. Rubi, A. Thomas, W. Peters, C. Slomiany, S. Herrera, and et al. 1994. Present development concerning antimalarial activity of phospholipid metabolism inhibitors with special reference to *in vivo* activity. *Mem Inst Oswaldo Cruz* **89 Suppl. 2**: 85-90.
- Ancelin, M. L., H. J. Vial, and J. R. Philippot. 1985. Inhibitors of choline transport into *Plasmodium*-infected erythrocytes are effective antiplasmodial compounds *in vitro*. *Biochem. Pharmacol.* **34**:4068-4071.
- Atkinson, K. D., B. Jensen, A. I. Kolat, E. M. Storm, S. A. Henry, and S. Fogel. 1980. Yeast mutants auxotrophic for choline or ethanolamine. *J. Bacteriol.* **141**:558-564.
- Baunaure, F., P. Eldin, A. M. Cathiard, and H. Vial. 2004. Characterization of a non-mitochondrial type I phosphatidylserine decarboxylase in *Plasmodium falciparum*. *Mol. Microbiol.* **51**:33-46.
- Biagini, G. A., E. Richier, P. G. Bray, M. Calas, H. Vial, and S. A. Ward. 2003. Heme binding contributes to antimalarial activity of bis-quaternary ammoniums. *Antimicrob. Agents Chemother.* **47**:2584-2589.
- Birner, R., M. Burgermeister, R. Schneiter, and G. Daum. 2001. Roles of phosphatidylethanolamine and of its several biosynthetic pathways in *Saccharomyces cerevisiae*. *Mol. Biol. Cell* **12**:997-1007.
- Calas, M., M. L. Ancelin, G. Cordina, P. Portefaix, G. Piquet, V. Vidal-Sailhan, and H. Vial. 2000. Antimalarial activity of compounds interfering with *Plasmodium falciparum* phospholipid metabolism: comparison between mono- and bisquaternary ammonium salts. *J. Med. Chem.* **43**:505-516.
- Calas, M., G. Cordina, J. Bompard, M. Ben Bari, T. Jei, M. L. Ancelin, and H. Vial. 1997. Antimalarial activity of molecules interfering with *Plasmodium falciparum* phospholipid metabolism. Structure-activity relationship analysis. *J. Med. Chem.* **40**:3557-3566.
- Carman, G. M., and S. A. Henry. 1999. Phospholipid biosynthesis in the yeast *Saccharomyces cerevisiae* and interrelationship with other metabolic processes. *Prog. Lipid Res.* **38**:361-399.
- Clancey, C. J., S. C. Chang, and W. Dowhan. 1993. Cloning of a gene (PSD1) encoding phosphatidylserine decarboxylase from *Saccharomyces cerevisiae* by complementation of an *Escherichia coli* mutant. *J. Biol. Chem.* **268**:24580-24590.
- Deves, R., and R. M. Krupka. 1979. The binding and translocation steps in transport as related to substrate structure. A study of the choline carrier of erythrocytes. *Biochim. Biophys. Acta* **557**:469-485.
- Englund, P. T. 1993. The structure and biosynthesis of glycosyl phosphatidylinositol protein anchors. *Annu. Rev. Biochem.* **62**:121-138.
- Folch, J., M. Lees, and G. H. S. Stanley. 1957. A simple method for the isolation and purification of total lipids from animal tissues. *J. Biol. Chem.* **226**:497-509.
- Gardner, M. J., N. Hall, E. Fung, O. White, M. Berriman, R. W. Hyman, J. M. Carlton, A. Pain, K. E. Nelson, S. Bowman, I. T. Paulsen, K. James, J. A. Eisen, K. Rutherford, S. L. Salzberg, A. Craig, S. Kyes, M. S. Chan, V. Nene, S. J. Shallom, B. Suh, J. Peterson, S. Angiuoli, M. Pertea, J. Allen, J. Selengut, D. Haft, M. W. Mather, A. B. Vaidya, D. M. Martin, A. H. Fairlamb, M. J. Fraunholz, D. S. Roos, S. A. Ralph, G. I. McFadden, L. M. Cummings, G. M. Subramanian, C. Mungall, J. C. Venter, D. J. Carucci, S. L. Hoffman, C. Newbold, R. W. Davis, C. M. Fraser, and B. Barrell. 2002. Genome sequence of the human malaria parasite *Plasmodium falciparum*. *Nature* **419**:498-511.
- Hjelmstad, R. H., and R. M. Bell. 1987. Mutants of *Saccharomyces cerevisiae* defective in sn-1,2-diacylglycerol cholinephosphotransferase. Isolation, characterization, and cloning of the *CPT1* gene. *J. Biol. Chem.* **262**:3909-3917.
- Hjelmstad, R. H., and R. M. Bell. 1991. sn-1,2-diacylglycerol choline- and ethanolaminephosphotransferases in *Saccharomyces cerevisiae*. Nucleotide sequence of the *EPT1* gene and comparison of the *CPT1* and *EPT1* gene products. *J. Biol. Chem.* **266**:5094-5103.
- Hjelmstad, R. H., and R. M. Bell. 1990. The sn-1,2-diacylglycerol cholinephosphotransferase of *Saccharomyces cerevisiae*. Nucleotide sequence, transcriptional mapping, and gene product analysis of the *CPT1* gene. *J. Biol. Chem.* **265**:1755-1764.
- Hjelmstad, R. H., and R. M. Bell. 1988. The sn-1,2-diacylglycerol ethanolaminephosphotransferase activity of *Saccharomyces cerevisiae*. Isolation of mutants and cloning of the *EPT1* gene. *J. Biol. Chem.* **263**:19748-19757.
- Hosaka, K., T. Kodaki, and S. Yamashita. 1989. Cloning and characterization of the yeast *CK1* gene encoding choline kinase and its expression in *Escherichia coli*. *J. Biol. Chem.* **264**:2053-2059.
- Ichimura, Y., T. Kirisako, T. Takao, Y. Satomi, Y. Shimonishi, N. Ishihara, N. Mizushima, I. Tanida, E. Kominami, M. Ohsumi, T. Noda, and Y. Ohsumi. 2000. A ubiquitin-like system mediates protein lipidation. *Nature* **408**:488-492.
- Jakovicic, S., G. S. Getz, M. Rabinowitz, H. Jakob, and H. Swift. 1971. Cardiolipin content of wild type and mutant yeasts in relation to mitochondrial function and development. *J. Cell Biol.* **48**:490-502.
- Kim, K., K. H. Kim, M. K. Storey, D. R. Voelker, and G. M. Carman. 1999. Isolation and characterization of the *Saccharomyces cerevisiae* *EK11* gene encoding ethanolamine kinase. *J. Biol. Chem.* **274**:14857-14866.
- Kim, K. H., D. R. Voelker, M. T. Flocco, and G. M. Carman. 1998. Expression, purification, and characterization of choline kinase, product of the *CK1* gene from *Saccharomyces cerevisiae*. *J. Biol. Chem.* **273**:6844-6852.
- Kiyono, K., K. Miura, Y. Fukushima, T. Hikiji, M. Fukushima, I. Shibuya, and A. Ohta. 1987. Primary structure and product characterization of the *Saccharomyces cerevisiae* *CHO1* gene that encodes phosphatidylserine synthase. *J. Biochem. (Tokyo)* **102**:1089-1100.
- Kodaki, T., and S. Yamashita. 1989. Characterization of the methyltransferases in the yeast phosphatidylethanolamine methylation pathway by selective gene disruption. *Eur. J. Biochem.* **185**:243-251.
- Lambros, C., and J. P. Vanderberg. 1979. Synchronization of *Plasmodium falciparum* erythrocytic stages in culture. *J. Parasitol.* **65**:418-420.
- Letts, V. A., L. S. Klig, M. Bae-Lee, G. M. Carman, and S. A. Henry. 1983. Isolation of the yeast structural gene for the membrane-associated enzyme phosphatidylserine synthase. *Proc. Natl. Acad. Sci. USA* **80**:7279-7283.
- Menon, A. K., and V. L. Stevens. 1992. Phosphatidylethanolamine is the

- donor of the ethanolamine residue linking a glycosylphosphatidylinositol anchor to protein. *J. Biol. Chem.* **267**:15277–15280.
33. Nikawa, J., K. Hosaka, Y. Tsukagoshi, and S. Yamashita. 1990. Primary structure of the yeast choline transport gene and regulation of its expression. *J. Biol. Chem.* **265**:15996–16003.
 34. Nikawa, J., Y. Tsukagoshi, T. Kodaki, and S. Yamashita. 1987. Nucleotide sequence and characterization of the yeast *PSS* gene encoding phosphatidylserine synthase. *Eur. J. Biochem.* **167**:7–12.
 35. Patton-Vogt, J. L., P. Griac, A. Sreenivas, V. Bruno, S. Dowd, M. J. Swede, and S. A. Henry. 1997. Role of the yeast phosphatidylinositol/phosphatidylcholine transfer protein (Sec14p) in phosphatidylcholine turnover and *INO1* regulation. *J. Biol. Chem.* **272**:20873–20883.
 36. Pessi, G., G. Kociubinski, and C. B. Mamoun. 2004. A pathway for phosphatidylcholine biosynthesis in *Plasmodium falciparum* involving phosphoethanolamine methylation. *Proc. Natl. Acad. Sci. USA* **101**:6206–6211.
 37. Santiago, T. C., and C. B. Mamoun. 2003. Genome expression analysis in yeast reveals novel transcriptional regulation by inositol and choline and new regulatory functions for Opi1p, Ino2p, and Ino4p. *J. Biol. Chem.* **278**:38723–38730.
 38. Storey, M. K., K. L. Clay, T. Kutateladze, R. C. Murphy, M. Overduin, and D. R. Voelker. 2001. Phosphatidylethanolamine has an essential role in *Saccharomyces cerevisiae* that is independent of its ability to form hexagonal phase structures. *J. Biol. Chem.* **276**:48539–48548.
 39. Sullivan, D. J., Jr., I. Y. Gluzman, D. G. Russell, and D. E. Goldberg. 1996. On the molecular mechanism of chloroquine's antimalarial action. *Proc. Natl. Acad. Sci. USA* **93**:11865–11870.
 40. Trager, W., and J. B. Jensen. 1976. Human malaria parasites in continuous culture. *Science* **193**:673–675.
 41. Trotter, P. J., J. Pedretti, and D. R. Voelker. 1993. Phosphatidylserine decarboxylase from *Saccharomyces cerevisiae*. Isolation of mutants, cloning of the gene, and creation of a null allele. *J. Biol. Chem.* **268**:21416–21424.
 42. Trotter, P. J., J. Pedretti, R. Yates, and D. R. Voelker. 1995. Phosphatidylserine decarboxylase 2 of *Saccharomyces cerevisiae*. Cloning and mapping of the gene, heterologous expression, and creation of the null allele. *J. Biol. Chem.* **270**:6071–6080.
 43. Trotter, P. J., and D. R. Voelker. 1995. Identification of a non-mitochondrial phosphatidylserine decarboxylase activity (PSD2) in the yeast *Saccharomyces cerevisiae*. *J. Biol. Chem.* **270**:6062–6070.
 44. Vial, H. 1996. Recent developments and rationale towards new strategies for malarial chemotherapy. *Parasite* **3**:3–23.
 45. Vial, H., and M. Calas. 2001. Inhibitors of phospholipid metabolism, p. 347–365. Humana Press Inc., Totowa, NJ.
 46. Vial, H. J., and M. L. Ancelin. 1998. Malaria lipids, p. 159–175. In I. W. Sherman (ed.), *Malaria: parasite biology, pathogenesis, and protection*. American Society for Microbiology, Washington, D.C.
 47. Vial, H. J., and M. Calas. 2001. Inhibitors of phospholipid metabolism, p. 347–365. In P. Rosenthal (ed.), *Antimalarial Chemotherapy, mechanisms of action, modes of resistance, and new directions in drug development*. Humana Press, Totowa, NJ.
 48. Wengelnik, K., V. Vidal, M. L. Ancelin, A. M. Cathiard, J. L. Morgat, C. H. Kocken, M. Calas, S. Herrera, A. W. Thomas, and H. J. Vial. 2002. A class of potent antimalarials and their specific accumulation in infected erythrocytes. *Science* **295**:1311–1314.
 49. World Health Organization. 2000. World Health Organization Expert Committee on Malaria. *World Health Org. Tech. Rep. Ser.* **892**:i–v, 1–74.
 50. Yamashita, S., and K. Hosaka. 1997. Choline kinase from yeast. *Biochim. Biophys. Acta* **1348**:63–69.
 51. Zufferey, R., and C. B. Mamoun. 2002. Choline transport in *Leishmania major* promastigotes and its inhibition by choline and phosphocholine analogs. *Mol. Biochem. Parasitol.* **125**:127–134.
 52. Zufferey, R., T. C. Santiago, V. Brachet, and C. Ben Mamoun. 2004. Reexamining the role of choline transporter-like (CTL) proteins in choline transport. *Neurochem. Res.* **29**:461–467.